UNIVERSITE DE NEUCHATEL FACULTE DES SCIENCES

Self-organizing properties of dendrimers and potential applications

Thèse
présentée à l'Institut de Chimie de la Faculté des Sciences
de l'Université de Neuchâtel
pour l'obtention du titre de Docteur ès Sciences

Myriam LOSSON

Chimiste diplômée de l'Université des Sciences de Nancy/Metz

Acceptée sur proposition du Jury

Prof. R. Descheneaux	Université de Neuchâtel, co-directeur de thèse
Dr. R. Pugin	CSEM Neuchâtel, co-directeur de thèse
Prof. T.Ward	Université de Neuchâtel, Rapporteur
Dr. J-L Gallani	GMO Strasbourg, Rapporteur

24 Octobre 2005

Université de Neuchâtel

IMPRIMATUR POUR LA THESE

Self-organizing properties of dendrimers and potential applications

Myriam LOSSON

UNIVERSITE DE NEUCHATEL

FACULTE DES SCIENCES

La Faculté des sciences de l'Université de Neuchâtel,
sur le rapport des membres du jury

MM. R. Deschenaux (co-directeur de thèse),
T. Ward,
R. Pugin (co-directeur de thèse, CSEM, Neuchâtel)
et J.-L. Gallani (Strasbourg F)

autorise l'impression de la présente thèse.

Neuchâtel, le 16 novembre 2005

Le doyen :

J.-P. Derendinger

Remerciements

Au terme de cette aventure, je tiens à remercier chaleureusement le CSEM ainsi que l'ensemble de mes collègues pour m'avoir permis d'effectuer mon doctorat dans un environnement scientifique et humain exceptionnel.

Je tiens à remercier tout particulièrement mon superviseur de thèse Raphaël Pugin pour m'avoir fait confiance tout au long de mon doctorat, pour son fort engagement et pour nos échanges scientifiques fructueux.

Je tiens aussi à remercier le Professeur Robert Deschenaux pour m'avoir accueillie comme doctorante « à temps partiel » dans son laboratoire et pour s'être engagé dans la collaboration CSEM/Université afin de créer un lien scientifique entre ces deux institutions.

Je tiens à remercier le Professeur Thomas Ward et le Docteur Jean-Louis Gallani pour avoir accepté de faire partie de mon jury de thèse.

Un grand merci à notre enthousiaste consultant Rolf Steiger. Je lui suis très reconnaissante car sans ses conseils très avisés et sa bonne humeur, une partie du travail de thèse n'aurait certainement pas eu la même saveur.

Je remercie l'ensemble des collègues externes avec lesquels j'ai pu collaborer pendant toute ma formation ainsi que les infrastructures mises à ma disposition. Il s'agit tout d'abord du laboratoire du Professeur W. Meier à Bâle, où Corinne Vebert m'a formée aux techniques de diffraction de la lumière. J'ai aussi eu l'occasion de m'initier à la cryo-TEM au sein du groupe de recherche du Professeur Jacques Dubochet à Lausanne, et je remercie Marc Adrian pour sa disponibilité, ses conseils avisés permettant la progression efficace de mon projet de recherche. Le « Groupe des matériaux organiques » à Strasbourg dirigé par le Dr. D.Guillon a été un lieu de séjour scientifique très agréable pour ses échanges intellectuels et relationnels ; un grand Merci à Jean-Louis spécialiste « de la monocouche »! Je remercie également le Professeur Thomas Bürgi à l'Université de Neuchâtel pour son aide précieuse lors des analyses FT-IRRAS effectuées au sein de son laboratoire. Je tiens à remercier tout particulièrement l'équipe du Professeur François Diederich, avec laquelle une collaboration étroite et fructueuse a pu s'établir. Merci à Derk Joester et Marine Guillot pour la synthèse de dendrimers, très intéressants pour de possibles applications en thérapie génique, ainsi que pour les bons moments partagés lors des conférences et des réunions de travail.

Une thèse est un véritable travail d'équipe et je remercie particulièrement toute l'équipe de la division « Nano Bio » (Harry, Silvia, Eric, Francis, Rolf, Freddy, Yvonne, Erika, Marta, Christian, Arno, Réal, Claude, Shiva, Nico, Rino, Martha, André, Véro Philippe, Stéphanie, Jérôme, Ana Maria, Raphaël, Sandrine, Tania, Emmanuel, Vladi, Ross, Maurizio, Guy, Cate, Kaspar, Hans, Sylvie, Hui et François) dans laquelle j'ai pu évoluer très positivement tout au long de ma formation. Merci à Cate, Nico, Shiva et Kaspar, les nouveaux docteurs ou docteurs à venir, avec lesquels j'ai pu partager à chaque instant des périodes de discussions scientifiques, de questionnement sur le travail de thèse, et finir autour d'une bonne bière ou d'un thé froid en fin de journée au Chauffage. Merci !

J'ai un grand merci à adresser à Vero, Sylvie et François pour leur disponibilité, gentillesse, humour et bien entendu, merci pour les Micamu ☺.

Merci à André pour m'avoir formée à la microscopie à force atomique et pour les bons gâteaux de Carole !

Je tiens à remercier les personnes qui ont participé à la correction du manuscrit. Merci à Shiva pour son influence philosophique, Yvonne pour sa sympathie et son soutien, Martha pour son LSITT ☺, Victor pour son intérêt à mon travail, Cate pour sa proximité malgré la distance géographique, Josep pour son Catalan parfait ☺ et Zabeth pour son aide en informatique.

Je voudrais aussi remercier l'ensemble des personnes qui ont rendu cette vie à Neuchâtel, exceptionnelle, riche d'expériences et si drôle (Silvia, Alexia, Shiva, Cate, Piero, Giuseppe, Sara, Giacomo, Daniel, Ariane, Sabine, Florent, Christophe, Madelyne, Nico, Nicolas (pseudo Nico de l'Uni), Olivier, Edith, Georges, Leszek Rolf, Mauri, Marta, Alexandra, Daniel, Myriem, Juju, Iovanna, Johanna, Anna, Mathias, Line, Aloma, Natacha, JP, Alain, Stéphane, Manu, Sandrine, Andreas, JB, Val, Alex, Gaby, Richard, Elly, Beat, Kaspar S, Suzanne, Kaspar C, Nathalie, Erika, Tine).

Merci tout particulièrement à mes parents et amis (Mathilde, Sébastien, Didine, Céline, Gérald, miss Crevette, Olivier, Marco, Rachel, Anne) résidant en France pour leur affection et bonne humeur tout au long de cette aventure Suisse☺.

Je finirai par :

Moltes gracies Pitu de les muntanyes. M'impresiona teva energia i el teu bonhumor. I finalement, moltes gràcies per la confiança que has posat en els mes projectes professionals i personals.

List of Abbreviations

PLED	Polymer light emitted diode
OLED	Organic light emitted diode
MO-layer	Matrix oriented layer
LB	Langmuir Blodgett
HOMO	Highest occupied molecular orbital
LUMO	Lowest occupied molecular orbital
H_2SO_4	Sulphuric acid
UV-Vis	Ultra-violet /visible light
PM-IRRAS	Polarization modulation infrared reflection absorption
HCl	Chlorhydric acid
PAMAM	Polyamidoamine
Ge	Germanium
Mw	Average molecular weight
λ	Wavelength
DNA	Deoxyribonucleic acid
PEI	Poly-ethylenimine
BAM	Brewster angle microscopy
AFM	Atomic force microscopy
Cryo-TEM	Cryogenic transmission electron microscopy
SPM	Scanning probe microscopy
HEK cells	Human embryonic kidney cells
GFP	Green fluorescent protein
CE	Charge excess
$CHCl_3$	Chloroform
RMS	Root means square
TFA	Trifluoroacetic acid
XRD	X-ray diffraction
Bp	Base pair
SAM	Self-assembled monolayer
Fwhm	Full width at half maximum
TE	Tris-EDTA

Résumé

La nanotechnologie est une science fondamentale et appliquée, à la frontière entre la physique, la chimie, l'ingénierie et les sciences de la vie. Basée sur une approche dite "bottom-up" cette thèse a permis, dans un premier temps, d'étudier la possibilité d'utiliser une matrice de dendrimères commerciaux (PAMAM) afin de promouvoir l'auto-organisation de cyanines en agrégats-J. Parallèlement à cette thématique, nous nous sommes aussi intéressés à l'étude des propriétés d'auto-assemblage de dendrimères amphiphiles synthétisés par le groupe du Professeur Diederich dans le cadre de la recherche de nouveaux vecteurs non-viraux en thérapie génique.

Dans la première partie de la thèse, nous avons proposé un nouveau procédé d'auto-organisation de cyanines en agrégats-J. Nous avons montré que cette méthode d'auto-organisation développée était plus simple, plus reproductible et plus robuste que celles habituellement utilisées. Deplus, cette méthode a pu facilement être appliquée à différents supports (or, verre,…) nous permettant d'obtenir une grande diversité de matériaux présentant de nouvelles propriétés optiques très intéressantes. Nous avons également montré que ce système dendrimers/agrégats-J pouvait être utilisé comme détecteur de molécules de paraquat grâce à un transfert d'électron entre un état excité de l'agrégat et la molécule à détecter.

Dans la seconde partie de la thèse, nous avons étudié les propriétés d'auto-assemblage de dendrimères amphiphiles à l'interface air/eau, en utilisant la technique Langmuir-Blodgett ainsi que la microscopie à l'angle de Brewster. Nous avons pu mettre en évidence l'influence du pH sur les interactions intermoléculaires et observer qualitativement les intéractions électrostatiques à l'interface air/eau entre une monocouche de TG1G1 et de l'ADN (plasmide). Les mesures effectuées en microscopie à force atomique ont confirmé la capacité des dendrimères TG1G1 à condenser de l'ADN sous forme de polyplexes bien définis. Suite à ces investigations, les expériences en cryo-microscopie électronique à transmission ont permis une meilleure évaluation de la structure des polyplexes TG1G1/ADN et TG2G1/ADN. Elles ont aussi permises de proposer un mécanisme possible de condensation de l'ADN, dépendant de la structure du dendrimère, dans des conditions de milieu tamponné.

Mots clés : Dendrimères, auto-assemblage, agrégats-J, transfection génique, microscopie, Langmuir.

Abstract

Nanotechnology is an interdisciplinary field merging on fundamental and applied research at the boundary between physical and chemical sciences, engineering and life sciences. Being based on a bottom-up approach this thesis has mainly studied the possibility of using commercial dendrimers in the arrangement of cyanine into J-Aggregates structures. Moreover, the potential of newly synthesized dendrimers self-assembled and to aid DNA-condensing for genetic therapy development has been evaluated.

In the thesis a new J-aggregation process on dendrimer templates has been proposed. This new process has demonstrated to be more reproducible, simple and robust than currently used methods. Moreover, the process could be easily adapted to different substrates (gold, glass, metal oxides). As a possible application, the dendrimer/J-aggregate layers have been used as sensors for the detection of Paraquat by electron transfer from the excited J-aggregate to Paraquat.

After promising biological investigations, the self-assembly properties of a new class of amphiphilic dendrimers were investigated at the air-water interface using Langmuir-Blodgett techniques and Brewster Angle Microscopy. The influence of pH on amphiphiles configurations and the electrostatic dendrimer/DNA interactions were qualitatively observed. Atomic Force Microscopy measurements confirmed the propensity of dendrimer TG1G1 to strongly condense DNA into well defined polyplexe. Additional cryogenic Transmission Electron Microscopy has also allowed better evaluation of the conformation of TG1G1/DNA and TG2G1/DNA plasmid polyplexes and of the DNA condensation mechanisms under buffer conditions. Therefore, when considering the biological applications, our results show a promising future to such dendritic molecules in the development of genetic therapy.

Keywords: Dendrimer, self-assembling, J-aggregate, gene transfection, microscopy, Langmuir.

Summary

Nanotechnology is an interdisciplinary field merging fundamental and applied research at the boundary between physical and chemical sciences, engineering and life sciences. Two ways of miniaturization are generally described: the top down approach (reducing the size of the smallest structures towards the nanoscale) and the bottom up approach (manipulating individual atoms and molecules in order to create self-assembled macromolecules with new properties). Being based on the bottom-up approach this thesis has mainly studied the possibility of using commercial dendrimers in the arrangement of cyanine into J-Aggregates structures. Moreover, the potential of newly synthesized dendrimers self-assembled and to aid DNA-condensing for genetic therapy development has been evaluated.

In the first part of this thesis a new approach to organize cyanine in J-aggregate structures was investigated. It is well known that this type of organization allows the formation and delocalisation of solitons. The soliton is an energetic *particle* that migrates without energy loss along the J-aggregate thanks to its brickstone-like architecture (Figure 1).

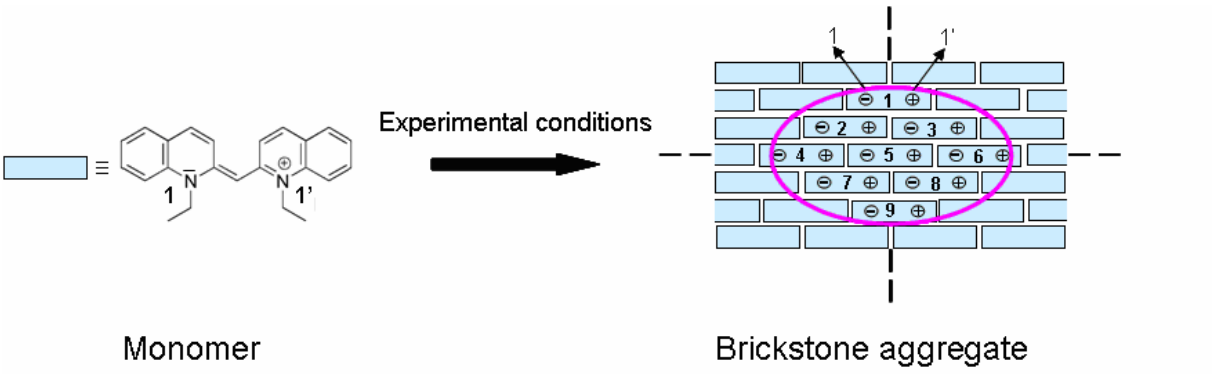

Figure 1 J-aggregation of a cyanine leading, after exposure to light to the formation of a soliton propagating along the brickstone architecture.

The interest on this particular molecular organisation is justified due to its interesting photophysical properties which may be useful in many devices such as electroluminescent screens, solar cells, non-linear optical elements and as sensitizers in photography or in biology.

One indication for the formation of such molecular organisation is a change in the absorption spectrum of the monomeric cyanine. In addition to the broad monomeric band, one observes the appearance of a new absorption band, that is significantly red-shifted (bathochromic effect) and strongly narrowed as compared to the monomeric one. Experiments in which J-aggregated cyanine dyes are self-organized with different degrees of perfection have been extensively studied on silver halide microcrystal surfaces, gelatine surfaces and polymers.

In all formation systems described so far, the J-aggregation process was slow, non reproducible and difficult to control. Our investigations were focused on a reproducible, simple, robust and controlled ways for the nucleation and growth of cyanines into J-aggregates. To the end, possible templates able to perform the formation of cyanine J-aggregates were identified.

A monolayer of polyamidoamine starbust (PAMAM), adsorbed on gold or glass substrate was used as a well defined template to influence the J-aggregation of cyanines, e.g, Myline1 (Figure 2). The charge density on the PAMAM periphery was well controlled. The Figure 3 shows the results we obtained after determination of parameters such as cyanine solubility, immersion time and dendrimer generation.

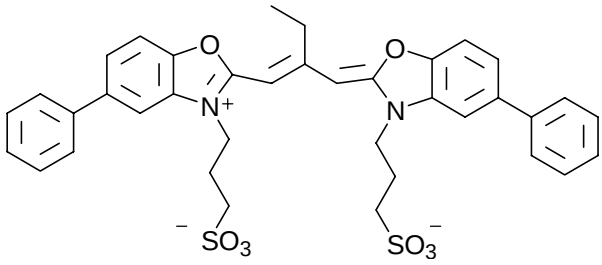

Figure 2 [5, 5'-diphenyl-dibenzoxazolo-N, N'-propylsulfonate] 9-ethyl trimethine cyanine (Myline1)

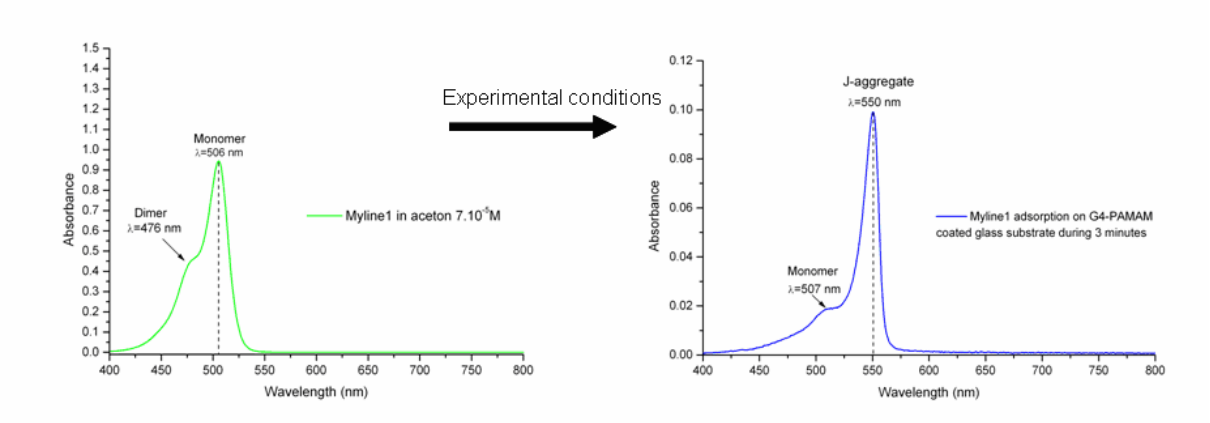

Figure 3 a) Absorption spectrum of Myline 1 in solution (acetone) b) Absorption of Myline 1 J-aggregate on PAMAM coated glass substrate after 3 minutes immersion into solution of Myline 1 in acetone.

The formation of a monolayer of J-aggregate on PAMAM coated substrates was observed. Moreover, the formation process was thermally stable, reproducible and well controlled. Experiments have shown that the presence of J-aggregate nuclei in the initial cyanine solution is useful for the formation of well-defined J-aggregates onto the G4-PAMAM monolayer.

According to the presented results, we assume that the J-aggregation process was realized by a two-step nucleation and growth mechanism.

Firstly, the nucleation was promoted in solution by dissolving the cyanine in an appropriate solvent (acetone, concentration of 7.10^{-5} to 7.10^{-4}M). The adsorption of a J-aggregate nucleus occurred at the functionalised dendrimeric monolayer.

Secondly, the growth of the adsorbed nucleus resulted from diffusion of cyanine monomers from solution to the dendrimer surface. A defect-free growth of this J-aggregate nucleus was favoured by the highly defined surface of a dendrimer nanoparticle, which itself was already highly ordered by adsorption on a gold surface presenting defects only in the nanometer range. During the process, we stated that the electrostatic charges of the PAMAM matrix periphery were of primary importance because of two reasons: firstly, the positively charged end-groups of PAMAM (after acidification) strongly interacted (attractive electrostatic forces) with the negatively

charged cyanines that were adsorbed. And secondly, the high density of functional groups on the PAMAM periphery may also promote nucleation as well as the mutual interaction between adsorbed cyanine molecules. This mutual interaction was necessary for the growth of the aggregates (controlled mobility/diffusion for molecular self-organization). The fact that the cyanine had to be negatively charged for J-aggregation at the positively charged dendrimer surface was corroborated by experiments with the cation of the same dye chromophore or the pseudo isocyanine functionalised with alkyl chains. In both cases no J-aggregation took place on protonated PAMAM.

The method proposed here is versatile since it allows us to tune the surface chemistry of substrates by changing the nature of the dendrimer. Moreover, the process could be easily adapted to different substrates (gold, glass, metal oxides). In order to improve the stability of the PAMAM layer, alternative methods exist allowing covalent linking (silanisation and EDC/chemistry). As a possible application, the dendrimer/J-aggregate layers were used as sensors for the detection of Paraquat by electron transfer from the excited J-aggregate to Paraquat.

The second part of the thesis was focused on the study of self-assembling properties of new amphiphilic dendrimers (Figure 4) designed by the group of the Professor Diederich (ETHZ) in the context of gene transfection. The goal was to determine a relationship between the chemical structure of these news dendrimers and their activity in cell transfection. In non-viral gene therapy, foreign genes are introduced into the nucleus of host cell, crossing different cell membranes on the way. Once the DNA is transfected and delivered into the nucleus, the gene can be expressed, leading to the production of new proteins giving a desired therapeutic effect. Because of strong electrostatic repulsions between DNA base pairs and the negatively charged cell surface, naked DNA can not be easily transfected into the cell. However, when strongly complexed with cationic transport vectors (e.g. lipids, polymers, dendrimers), DNA molecules have a lower charge density and a smaller effective hydrodynamic

radius. This facilitates the penetration of the resulting DNA/vector polyplexe into the cell.

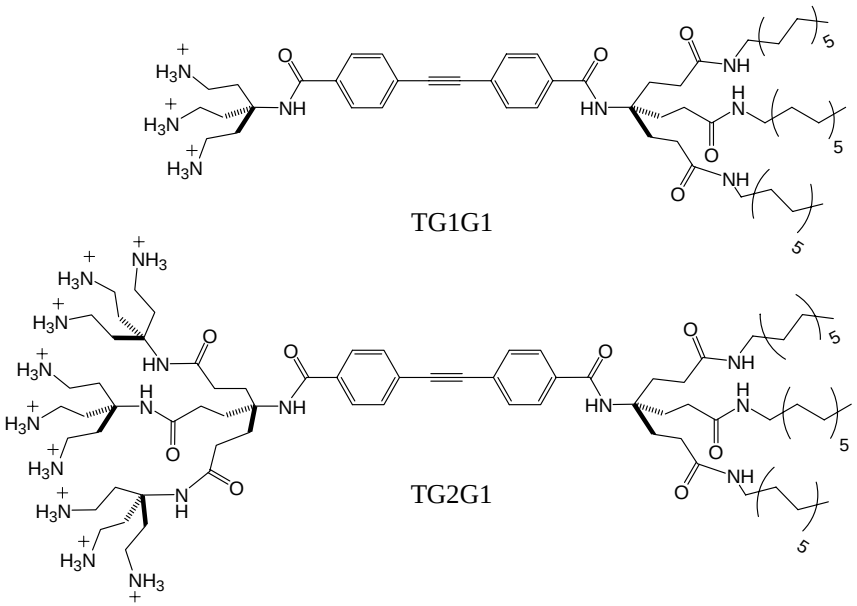

Figure 4 Developed structure of the amphiphilic dendrimers TG1G1 and TG2G1.

The preliminary *in vitro* experiments showed that the studied dendrimers were able to condense DNA and to allow its driving inside the transfected cell nucleus. The transfection efficiency (TE) of these new non viral vectors was compared to TE of already commercialised vectors (Figure 5). During the experiments, we observed a very strong influence of the lipophilic part of the dendrimer on the cell transfection efficiency in contrast to classical cationic dendrimers. As such lipophilic parts play a crucial role in the intermolecular self-assembling we focused our research on the understanding of this process.

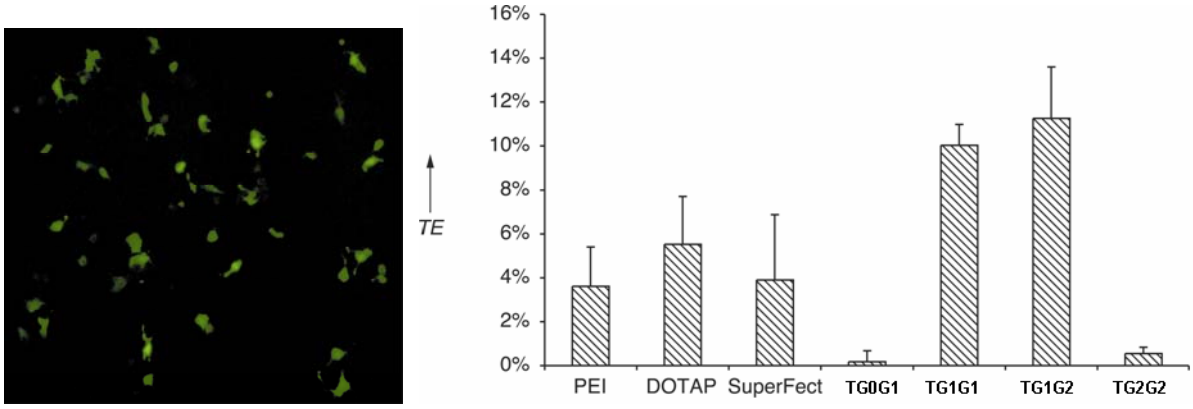

Figure 5 a) Fluorescence micrograph of HEK293cells transfected with a polyplex prepared from pGFP and TG1G1;b) Maximum TE of T0G1 to TG2G2 at optimum conditions are compared to reference commercial non viral vectors PEI, DOTAP and Superfect

The fundamental self-assembling properties of TG1G1 and TG2G1 at the interface air/water were studied by means of the Langmuir-Blodgett (LB) technique and the Brewster Angle Microscopy (BAM).

The techniques mentioned above allow the formation of an ordered monolayer and the evaluation of its morphology. In our experiments we observed a smaller minimal area per molecule for TG1G1 than for TG2G1. This difference is connected to a packing only by alkyl chains in the TG1G1 case while the polar head played also a role in the packing of TG2G1. In order to simulate the pH changes which occur in living cells, the influence of the pH subphase has also been investigated with the LB technique on the homogeneous monolayer formed with TG1G1. Based on variations of minimal area per molecule recorded for TG1G1, we could observe the propensity of TG1G1 monolayer to swell by addition below it of acidic solution. Even more, LB technique was used to evaluate the complexation of the DNA with self-assembled TG1G1 compounds. However, the results from this evaluation were not concluding enough.

Because of the limitations of the LB technique to evaluate the DNA condensation, we investigated the electrostatic interactions between amphiphilic dendrimer and plasmid DNA, by means of Atomic Force Microscopy (AFM) in Tapping Mode. Figure 6 shows the results from this microscopy technique. It is concluded that while individual pure plasmids are stretched over several hundreds of nanometers (Figure 6A),

dendrimer/plasmid DNA polyplexes present flattened spheroidal shape although uncondensed small portions of DNA are still observed (Figure 6C).

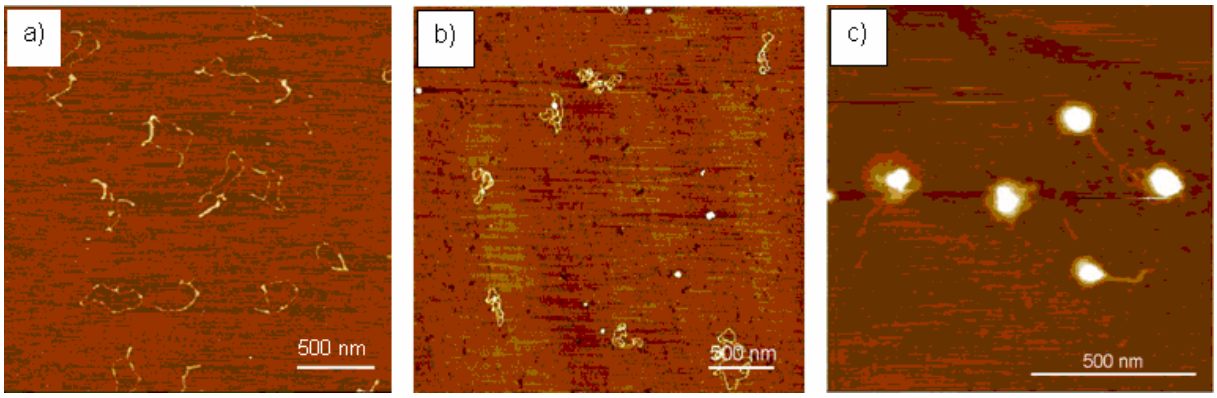

Figure 6 AFM images in tapping mode onto mica a) pure plasmid, b) first states of DNA coiling after addition of few droplet of an aqueous solution of TG1G1 c) TG1G1/DNA with a positive to negative charges ratio of 6 (CE=6) preformed in solution before mica coating

Futhermore, cryogenic-Transmission Electron Microscopy (cryo-TEM) were performed. The goal of the experiments was to provide both a clearer idea of the self-assembling dendrimer structure and the understanding of the DNA condensation mechanism.

Depending to the proper structure of TG1G1 (cylinder shape) and TG2G1 (conical shape) we could observe the formation of vesicles and micelles respectively in Tris-EDTA buffer. Afterwards, we mixed individual vesicles of TG1G1 with DNA plasmid under precise charge excess ratio (+ dendrimer/- DNA). We observed that vesicles were aggregated and that the thickness of the vesicle membrane was increased (Figure 7).

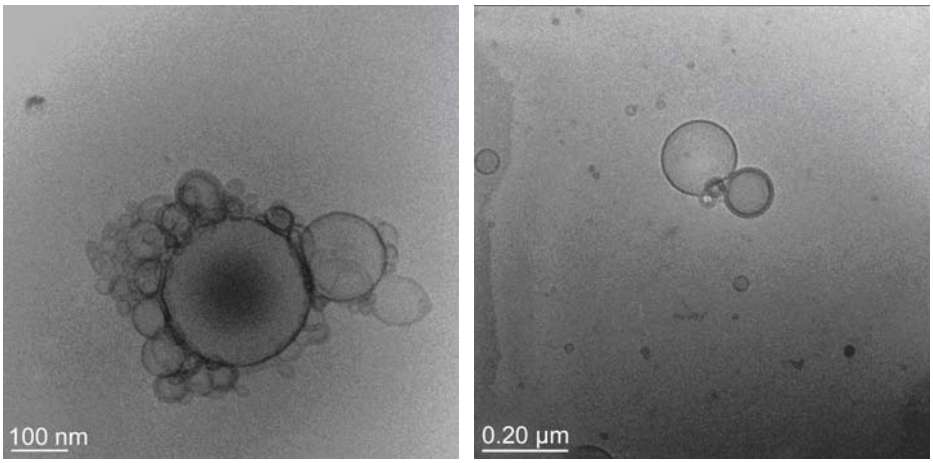

Figure 7 Cryo-electron microscopy images of TG1G1 /plasmid DNA polyplexes

The model suggested by Huebner to interpret his observation on DNA/cationic lipid complexes could be an explanation for the phenomena observed in our experiments (Figure 8).

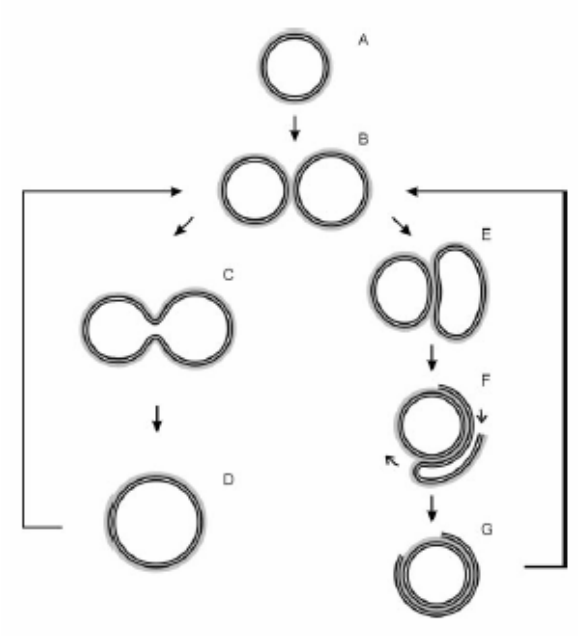

Figure 8 Reproduced from Huebner et al. DNA spins around a unilamellar vesicle (A).Two vesicles with one partially covered with DNA adsorb to each other (B). Fusion of 2 vesicles (C).The vesicle subsequently minimizes its membrane energy by adopting a near-spherical shape (D). Multilamellar structures form if one vesicle ruptures (E).Such a vesicle then rolls its bilayer over an host DNA/vesicle polyplex (F), forming one adsorbed bilayer with an open edge.(G) By such mechanism further layers could adsorb.

Therefore, cryo-TEM combined with the preliminary used techniques (LB and AFM) are able to give valuable information for a better understanding of plasmid DNA cell transfection. However, still some experiments on TG2G1 need to be performed in order to have a better idea on the structure activity relationship.

Additional investigations such as Small Angle X-ray Scattering (SAXS) would help to confirm structural parameters of Dendrimer/DNA aggregates. These complementary investigations should enable the establishment of relationships between dendrimer features and cell transfection efficiency for the design of new efficient gene delivery system.

These research investigations have therefore concluded that dendrimers are very good candidates for the self-assembly of cyanines into well defined J-aggregates: their possibilities in surface functionalisation open a wide range of innovation in material and biomaterial sciences. Futhermore, for biological applications, our results show a promising future to such dendritic molecules in the development of genetic therapy.

Keywords: Dendrimer, self-assembling, J-aggregate, gene transfection, microscopy, Langmuir.

Table of contents

Chapter 1

Introduction

1.1 Dendrimers

1.1.1 A novel class of hyperbranched macromolecules

The dendritic architecture is well represented in nature at the macro and microdimensions (e.g. tree architectures, leaves, neurons) and its observation has motivated investigations on the fractal theory as well as the design of new generations of molecules with similar structures. Dendrimers are an interesting class of three-dimensional macromolecules from 2 nm up to 10 nm. The name “dendrimer” derives from dendri (tree-branch-like) and meros (part of). They represent a novel class of structurally controlled and well defined macromolecules based on a branch-upon-branch structural motif. The branches radiate from a central core and are synthesized through a stepwise, repetitive reaction sequence that guarantees complete shells for each generation and leads to macromolecules that are monodisperse. This repetitive branching sequence gives rise to the novel architecture (Figure 1-1) shown below.

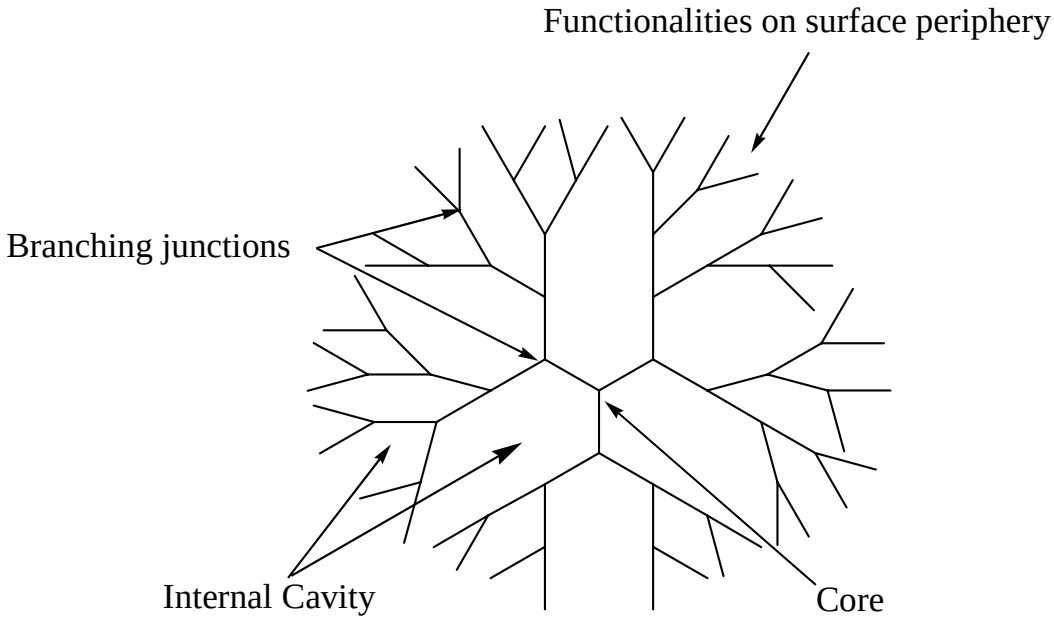

Figure 1-1 Dendritic structure

Characteristics of dendrimers include a high degree of structural symmetry and a well defined number of terminal functional groups that may be chemically different from the interior.

The synthetic procedures for dendrimer preparation permit complete control over the critical molecular design parameters, such as flexibility, size, shape, structure and surface/interior chemistry. In 1952, Flory was one of the first to present and discuss the benefits of hyperbranched structure synthesis in polymer science[1]. The first example of an iterative synthetic procedure towards well-defined branched structure (cascade synthesis) was reported by Vögtle[2] in 1978. Then, in 1985, Tomalia[3] and co-workers described the first highly controlled dendritic structure (called PAMAM for poly(amidoamine) dendrimer) with a globular shape due to symmetric branching . These starburst dendrimers are designed following a divergent synthesis (Figure 1-2) from a reactive core (e.g. amine or ethylenediamine) to reach progressively the dendrimer periphery. In this case the reiterative sequence consists of a double Michael addition of methyl acrylate to a primary amino group followed by amidation of the resulting carbomethoxy intermediate with an excess of ethylenediamine (or amine). This method allows the synthesis of high generations (up to ten) but with possible defects in the dendritic structure due to a progressive increase of steric hindrance at the periphery in high generation systems.

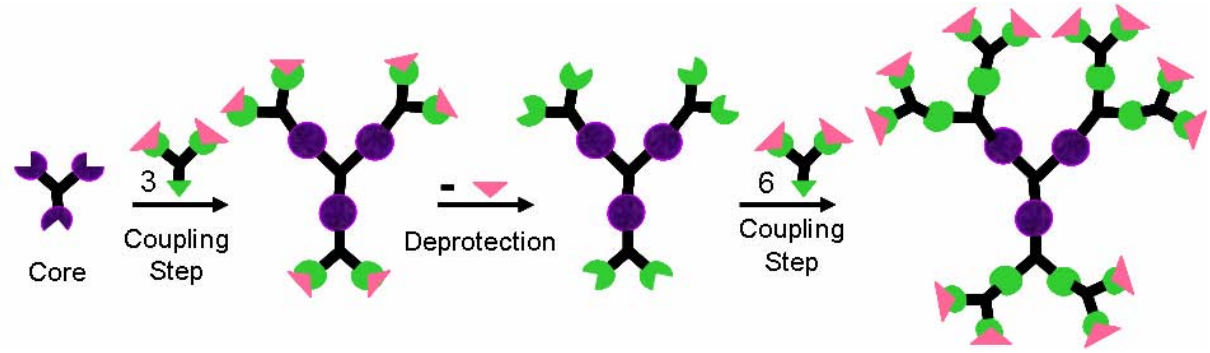

Figure 1-2 Divergent synthesis procedure

In the same period, Newkome and co-workers[4], referred to the formation of a tree-like structure called arborols. As for starburst dendrimers, the synthetic scheme started with a core, and attachment of multi-functional units was made. Particular properties were observed such as the formation of linear networks and micellar structures. Shortly thereafter, improvements on Vögtle's original synthesis were achieved by Meijer[5] and Mülhaupt[6] which enabled the production of poly(propylene imine) (PPI) dendrimers[7].

To avoid possible architectural defects occurring with the divergent method, a complementary growth strategy called convergent synthesis (Figure 1-3) was developed by Fréchet and Hawker[8]. This method consists in the priliminary synthesis of dendritic entities called dendrons. Afterwards, the dendrons' anchoring points are deprotected and covalently linked to the central core. This strategy provides better structural control and monodispersity of the dendrimer due to the possibility of purification at each growth step of the synthesis. Moreover, this synthetic approach allowed Fréchet and co-workers to synthesize dendrimers such as eg. globular amphiphiles molecules, by coupling lipophilic benzyl ether dendrons and hydrophilic carboxylate-functionalised dendrons[9].

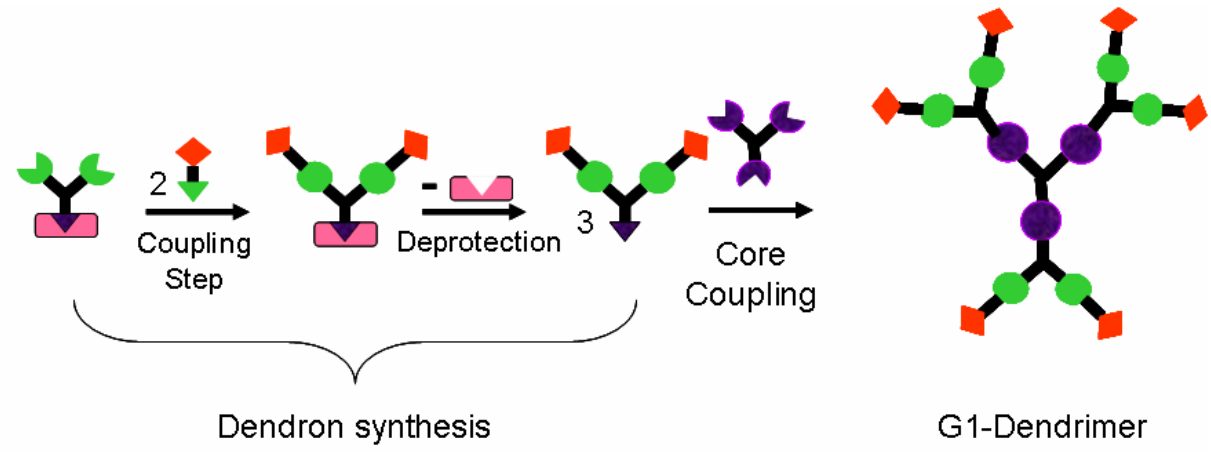

Figure 1-3 Convergent synthetic procedure

Nowadays, the combination of both divergent and convergent approaches allows the creation of a wide range of dendrimers specially designed for applications eg. in the fields of catalysis, drug delivery or sensors.

1.1.2 Versatile tailored dendrimers with defined properties

In nature many biological elements function and coordinate with each other in a programmed fashion e.g cell membranes, proteins and viruses. One of the key points for the functioning of such building blocks lies in molecular recognition and self-organization.

Figure 1-4 depicts some geometrical similarities between natural assemblies and synthetic dendrimers. On the one hand, such size similarity has motivated chemists to synthesize dendrimers as models for the better understanding of biomolecules self-assembly properties and activity. On the other hand, the modifications of core, shell and periphery of dendrimers may promote the recognition and complexation of biomolecules (proteins, DNA, …) during nanoscale events. As it will be illustrated in this work, research on dendrimers has found an extensive interest in biology, material science, surface engineering and drug delivery.

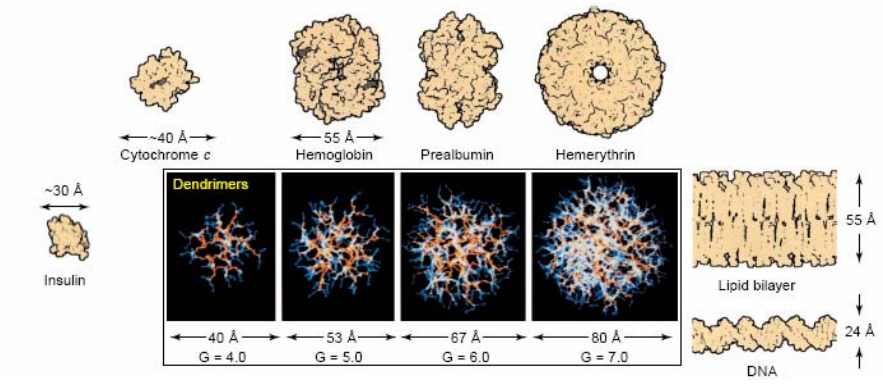

Figure 1-4 A dimensionally scaled comparison of a series of poly(amidoamine) (PAMAM) dendrimers with a variety of proteins, a typical lipid-bilayer membrane and DNA, indicating the closely matched size and contours of important proteins and bioassemblies (reproduced from literature[10])

1.1.2.1 Dendrimers in molecular recognition

In order to explore complexation possibilities which are offered by highly functionalised dendritic architectures, the modifications of core, internal cavity and specific terminal functions have been extensively studied.

1.1.2.2 Dendrimer: core modification

Many research groups[11-15] are interested to use dendrimers as models for mimicking the natural situations of metal-base catalytic centers in enzymes. In this context, Diederich and co-workers[16;17] synthesised novel metallodendrimers (Figure 1-5) for modelling the electron transfer induced in proteins such as cytochrome c.

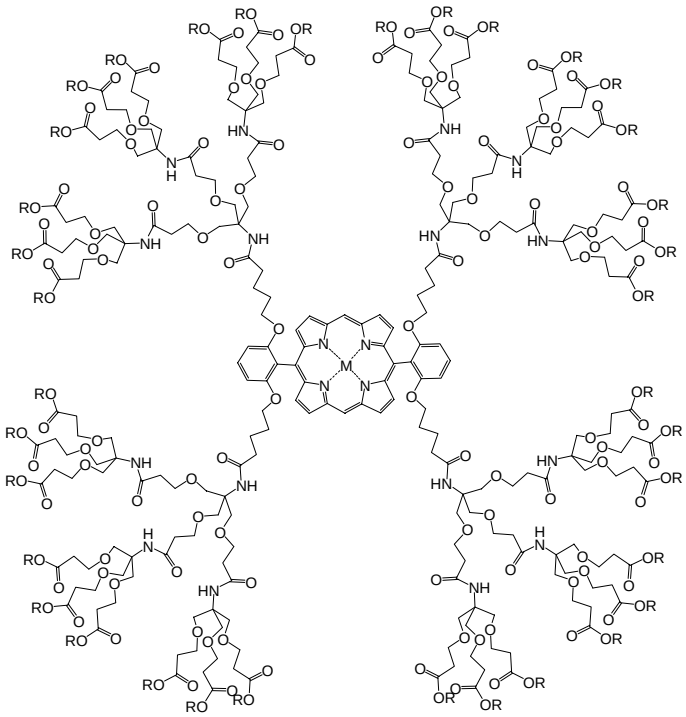

Figure 1-5 Example of dendritic metalloporphyrins

These dendrimers were used as models for studying oxygen storage processes. Cyclic voltammetry investigations have shown the dependence of the porphyrin redox potentials on the nature of the dendritic substituants.

1.1.2.2.1 The Internal cavity of dendritic molecules: an encapsulation interest

A specificity of dendrimer architectures when compared with linear polymers is the availability of internal cavities within their highly branched structure. The possibilities to encapsulate guest molecules in dendritic hosts were first pursued by Maciejewski in 1982. Then, further investigations were performed by Fréchet[18] who reported the "pyrene solubilization" in water after the encapsulation of the pyrene within the internal cavities of a water-soluble dendrimer. Meijer's group also pioneered the synthesis of a "dendritic box"[19;20]. The first host cavity designed by Meijer and co-workers was able to encapsulate dye molecules such as Bengal Rose and *p*-nitrobenzoic acid. After the hydrolysis of the protective groups on the dendrimer periphery, the selective release of encapsulated guests could also be demonstrated.

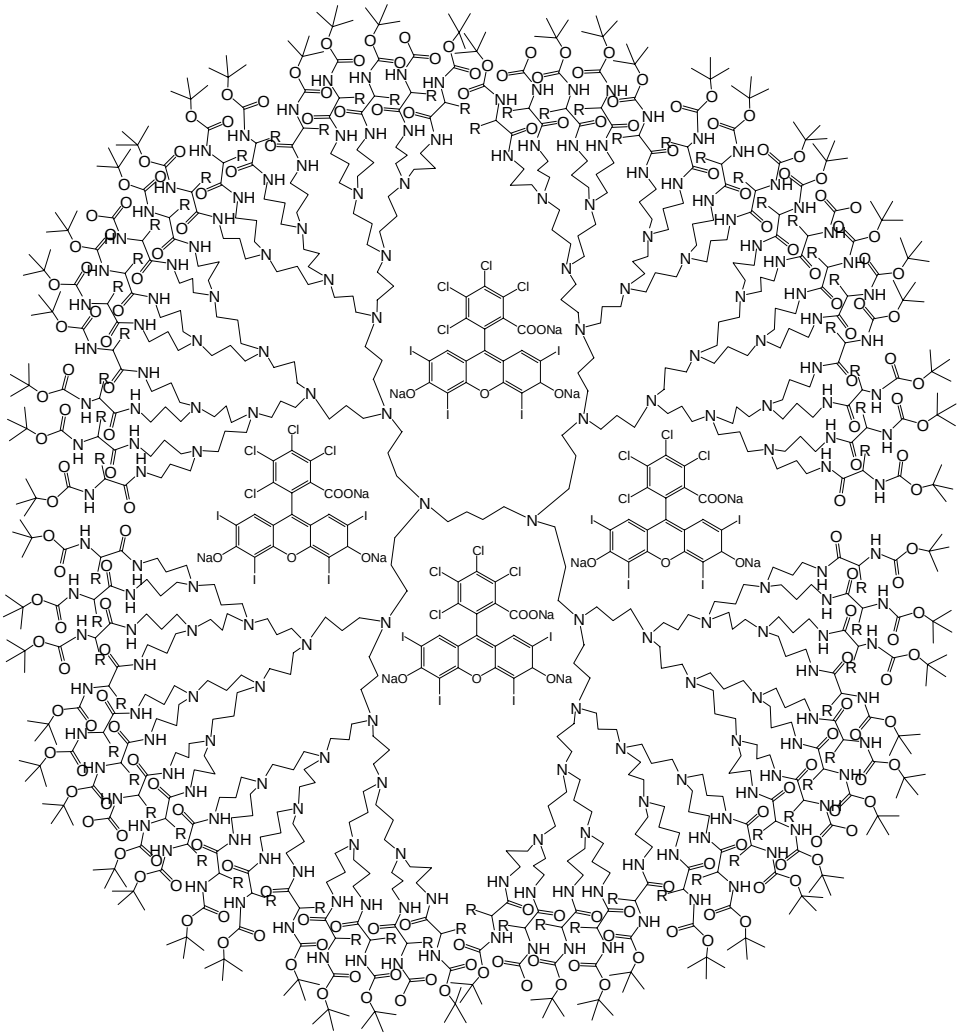

Figure 1-6 Meijer's dendritic box with encapsulated Bengal Rose molecules

In this case, while the hydrophobic internal cavity can accommodate a hydrophobic drug, the presence of peripheric hydrophilic functionalities facilitates solubility in polar solvents such as aqueous solutions. Such supramolecular architectures can thus form “magic bullets” used as drug delivery systems[21;22].

In addition, the complexation properties of dendrimer cavities have also been used in the field of organometallic chemistry to accommodate eg. small copper or boron clusters at precise depths within the dendrimer cascade structure[23-25].

1.1.2.2.2 Variation of external functionalisation

Dendrimers are generally characterized by the presence of a large number of terminal functional groups which decorates the dendrimeric outer surface with a high surface density. In this context, the ability of dendrimer to coordinate molecules such as catalysts, drug, clusters as well as larger nanoparticles has recently attracted much attention.

Dendrimers have been found to be ideal systems for catalytic studies[26;27]. Metallodendritic compounds are soluble, perfectly defined at the molecular level and can be recovered after catalytic reaction. Indeed, one major advantage of such molecules is that small catalytic units are covalently attached to the branches of large dendrimers. The catalysts can take part in homogeneous reactions and due to the large size of metallodendrimer catalysts can be easily recovered by precipitation or ultra-filtration processes using membranes. Additionally, and in contrast to core functionalised systems, catalysts coordinated on the dendrimeric periphery are directly available on the substrate during catalytic reaction.

On the other hand, the periphery-functionalised compounds contain multiple reaction sites and ligands thus providing extremely high local catalyst and ligand concentrations.

The first example of periphery functionalisation with inorganic end-groups has been published by Van Koten and co-workers in 1994[28]. Their system was based on a carbosilane dendrimer functionalised at the periphery by 12 Ni (II) complexes (Figure 1-7).

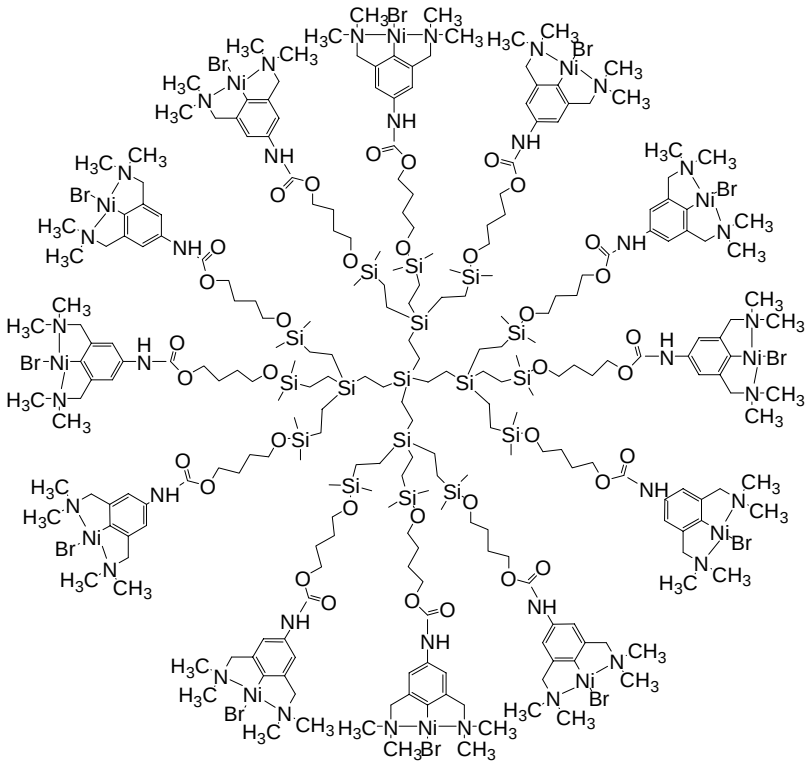

Figure 1-7 Cabosilane dendrimer (G1) functionalised at the periphery by 12 Ni (II) complexes

The ability of this molecule to behave as a catalyst (Kharasch addition of tetrachloromethane to methacrylate) has been evaluated. Despite a slightly lower activity, an excellent regioselectivity compared to the corresponding mononickel catalyst could be demonstrated.

Similarly, Majoral and co-workers have reported the preparation of phosphorus containing dendrimers (phosphorus in the core, within the cascade structure or at the surface) possessing up to 3072 terminal free phosphino end-groups (for generation 10)[29;30] . Then, using classical coordination chemistry reactions, this large number of chain-end functionalities allowed the surface to be densely covered with various metal fragments (G_x-$Ph_2P\rightarrow$MLn with MLn= $Fe(CO)_4$, $W(CO)_5$, Rh(acac)(CO) or RhCl(COD))[31-34] . More interesting was the complexation of 3072 AuCl moieties on the surface of a phosphine terminated-dendrimer (G_{10}-$Ph_2P\rightarrow$AuCl) which was imaged by High Resolution Transmission Electron Microscopy (HRTEM) in order to visualize the shape and the size of the gold-covered dendritic molecules[35;36].

Electrostatic complexation on the periphery of dendrimer was also intensively studied by Tomalia and co-workers[37] who published in 1996 their observations on organic dyes aggregation in the presence of PAMAM dendrimers. Detailed information on this topic is given in Chapter 3 which will describe the use of PAMAM coated surfaces for the preparation of highly defined cyanine J-aggregates.

In the field of bioengineering, biomineralization which can be defined as the synthesis of inorganic crystalline mineral-like material by living organisms is currently attracting increasing attention. Moreover, PAMAM dendrimers as a well-defined and controlled architecture can mimic proteins in order to provide insights into the possible mechanisms operating in biology[38]. In this context, Naka and co-workers[39-41], reported a controlled process of calcium carbonate crystallization (vaterite crystalline structure) induced by the presence of the carboxylate-terminated PAMAM dendrimers in the reactive mixture. To evaluate the influence of dendrimers on the crystallization process as well as on the resulting particle size, different concentrations and generations of dendrimers were tested. These investigations allowed them to demonstrate that an increase in dendrimer concentration induces the formation of smaller vaterite crystals. Using a high generation of dendrimer, the size of vaterite is decreased due to limitation of particle aggregation. They could also evaluate the importance of the generation in the nucleation step of the experiment and the importance of attractive electrostatic interactions between the negatively charged shell on the dendrimer periphery and cations present in the reactive mixture. Although this type of mineralization process is not yet completely understood, it clearly shows the potential of dendrimers for the synthesis of new bone materials.

Besides the utilization of dendrimers for the elaboration of new biomaterials, researchers also explore the structural properties diversity of dendrimers in order to create supramolecular structures for medical treatment related applications. In order to cure genetic diseases, Szoka *et al.*[42] were the first group to propose amine-terminated PAMAM as a positively charged nanoparticle for the complexation and transport of DNA through cell membranes. Compared to the well known non-viral vector poly-ethyleneimine (PEI), the structure of starburst PAMAM shows a higher density of amines on the molecule periphery. These outer amines enable efficient condensation

of nucleic acids, leaving the inner amine functions available for neutralization during endolysosomal acidification, thus enabling more efficient endosomal escape. To improve gene targeting and expression, Leong's group and others[43] designed new dendritic molecules by replacing, e.g., the PAMAM core by a trimesyl chemical group or introducing PEGylated dendrons. The potential of newly designed dendrimers to act as efficient non-viral vectors for gene delivery[44;45] will be intensively studied in Chapter 4.

1.1.2.3 Dendrimers and self-assembling properties

In nanoscience, the development of enabling technologies is currently strongly linked to the control of self-assembly processes. Self-assembly processes are simple, versatile and offer the possibility to generate "nanodevices" with a "relatively small synthetic input". Indeed self assembly relies on electrostatic interactions and on weak interactions such as Van der Waals, hydrophobic-hydrophobic interactions and H-bonding as well as recognition process which provide the driving force for assembling nanoscale building blocks in a controllable way. Smith and co-workers[46] reviewed dendrimers as a "nanoscale toolkit" due to their highly defined and controlled architectures. According to the complementarity of the different synthetic methods, individual dendrimers can be tailored with an almost infinite variety of arrangements. This impressive capacity provides a huge palette of nanoscale building blocks which may lead, through self-assembly processes, to new innovative applications in eg. biology and material science.

Concerning the development of liquid crystal systems, Smith and co-workers use the term of self-ordering in contrast to self-assembling mechanisms. This difference is due to the combination of individually weak interactions and ordering at long range scales. Self-ordering is driven by molecular shape, deformability, chirality and microphase separation.

Percec and co-workers demonstrated[47-49] the performance of structure– self-assembly property relationships. In 1998, Percec *et al.*[50] described two fashions of self-assembly (or self-ordering) driven by H-bonding exhibited by different dendrimer generations

having wedge- and cone-shaped geometrical structures. While dendrons with fewer tethered chains adopting a pie slice shape self-organize in a 2-dimensional hexagonal columnar lattice, dendrons with more end chains assume a conical shape and exhibit a cubic phase structure (Figure 1-8).

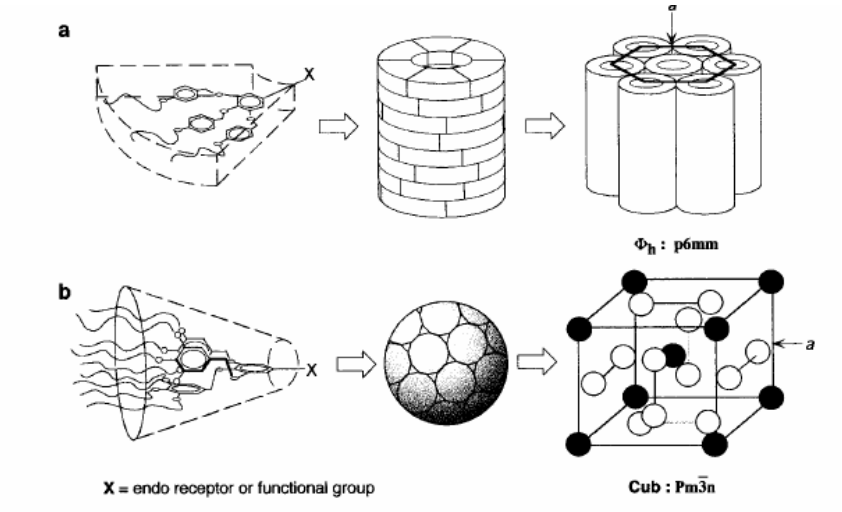

Figure 1-8 Percec's dendrons self-assembled in supramolecular architecture a) Hexagonal columnar phases b) Cubic phases (reproduced from literature [49])

In 2004, Percec and co-workers[51] have explored the self-assembly of peptide dendrons via hydrogen bonding. The use of such synthetic porous rod-like structures as drug delivery nanoscale channel systems could be demonstrated.

Recently Deschenaux and co-workers[52] have reported the synthesis of new dendritic molecules in which a liquid–crystal dendron is coupled to a ferrocene-fullerene donor-acceptor entity (Figure 1-9). The targeted compound displayed an enantiotropic smectic A phase, and organized into a partial bilayer structure.

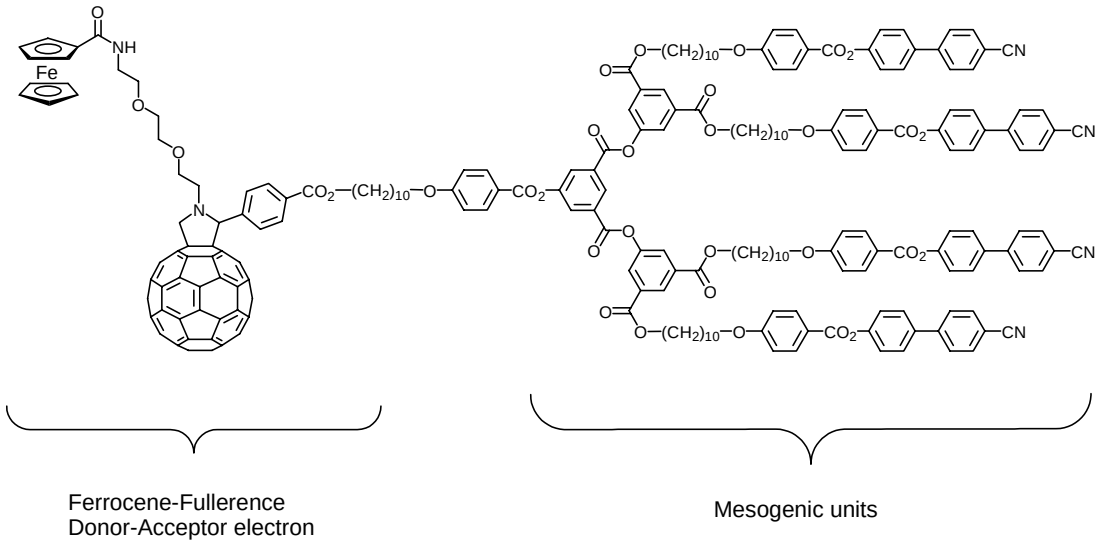

Figure 1-9 Fullerene (C_{60})-ferrocene liquid crystal dendrimers

The mesomorphic moiety allows molecules to self-assemble into a well defined supramolecular architecture resulting from π-π interactions and H-bonding.

Electrochemical investigations showed oxidation or reduction processes associated with ferrocene, linked via a poly (ethylenglycol) chain to the C_{60} and the dendritic moiety. Photoinduced electron transfer from ferrocene to fullerene was identified with lifetimes for the charge-separated state of 560 ns (THF) and 490 ns (benzonitrile).

As the two moieties do not interfere, this versatile dendritic structure allows further chemical modifications for the development of new materials. The various properties observed indicate that this liquid-crystalline dendrimer based on ferrocene and fullerene is a valuable candidate for the development of supramolecular switches for solar cell and display technologies.

1.1.2.4 Dendritic functionalised surfaces

As described above, the self-assembling properties in solution of specially designed dendrimers have already been extensively studied and applications such as eg. non-viral cell transfection, the construction of protein assemblies, new generations of highly performant solar cells and liquid crystal displays are already foreseen.

Additionally, the self-assembly of dendrimers into mono or multilayer thin films on solid substrates through weak interactions or covalent bonding is a key tool for the development of functional platforms, e.g. biosensing applications[53;54].

First investigations on self-assembling monolayers (SAMs) were performed by Whitesides and co-workers with thiol molecules on metal substrates. Recently they reviewed[55] thin-film formation mechanisms and highlighted the structure and characteristics of the SAMs as well as their resulting chemical and physical properties. By simple physisorption on gold, monocrystalline thiolated monolayers with thicknesses from 1 to 3 nm can be easily formed and used in, eg. active interface wetting studies, biomolecules immobilization and nanoparticles arrays formation. SAMs provide thus a convenient, flexible, and simple system which allows ones to tailor the interfacial properties of metals, metal oxides, and semiconductors. However, for some applications, SAMs prepared from linear alkyl chains based molecules present some significant disadvantages, for example, their limited functional group density and low stability due to their monopodal surface attachment.

To circumvent these drawbacks and with the aim to enhance the reactivity and adhesion properties of functionalised thin films, Crooks and co-workers have investigated the controlled formation of dendrimer self-assembled monolayers[56]. The resulting dendrimer monolayers have been characterized with FTIR-external reflection spectroscopy (FTIR-ERS) which has allowed the authors to demonstrate the attachment of the dendrimer to the surface. Moreover this characterization technique has confirmed the high stability of the dendrimer monolayer (no degradation after sonication and exposure to highly basic buffer) in contrast to simple primary alkylamines SAMs on gold which are not stable under the afore mentioned conditions. The enhanced stability is mainly explained by the large number of amine terminated group on the dendrimer periphery that chemisorbs to the Au-surface and by analogy to polydentate metal-ion chemistry stabilizes the amine/Au interactions.

In order to further improve the stability of the resulting dendrimeric thin film, the authors described also a procedure for covalently anchoring dendrimer onto the substrate[57;58]. The process consists to link (via the formation of amide chemical bond)

amine terminated PAMAMs to mercaptoundecanoic acid SAMs predeposited on gold. In this study the authors, demonstrated additionally that dendrimers-modified surfaces possess some unique structural and chemical characteristic that make them excellent candidates for highly sensitive and stable interfaces. Indeed, dendrimers combine a conformational variability on solid substrate following the dendrimer generation with a versatile chemistry at the periphery allowed by a particular tailoring in order to get a highly selective vapors organic sensor.

In order to better understand the structure of dendrimers adsorbed on a substrate, Mecke *et al*.[59] performed a series of atomistic molecular dynamics simulations. Model dendrimers which are here investigated sown to be highly flexible and capable of forming very flat structures in order to allow multiple interactions between their terminated groups and the substrate. The obtained results are in perfect agreement with experimental atomic force microscopy (AFM) investigations performed on individual adsorbed dendrimers molecules which demonstrate that dendrons are extremely deformed when they are in contact with the surface[60-62]. The flattening of the dendrimer structure has been demonstrated by Manfield *et al*.[63] by a study based on lattice Monte Carlo simulations of dendrimers under the influence of attractive forces to a plane. In addition to surface functionalisation and in order to create well-defined dendrimer surface patterns, microcontact printing and dip-pen nanolithography (DPN)[64-67] have been used as versatile techniques for the printing of dendrimer micro and nano features. A recent publication, Vancso *et al*.[68] present different routes for dendrimer surface patterning (Figure 1-10).

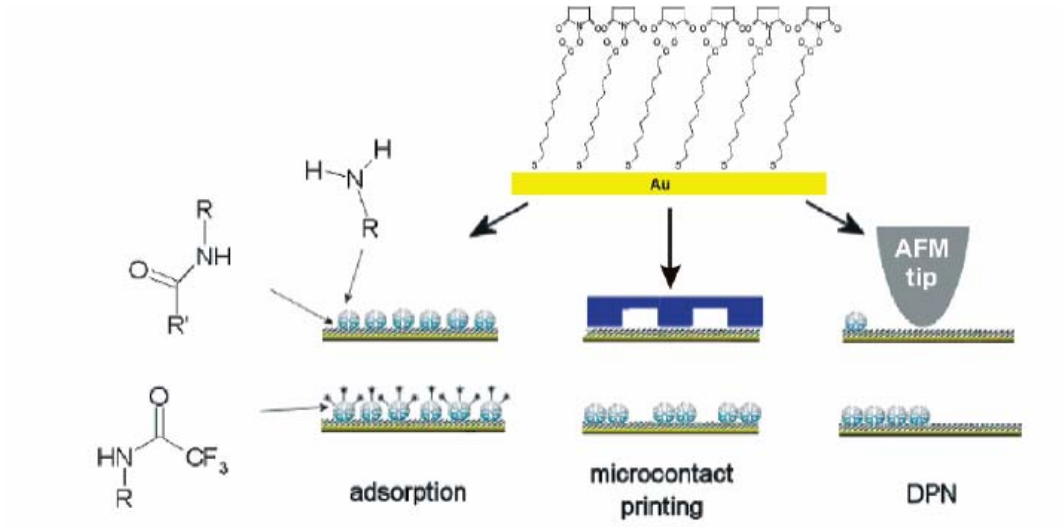

Figure 1-10 SAM's of thiol activated esters, functionalised by covalent coupling of PAMAM from solution (adsorption), microcontact printing and dip pen nanolithography (DPN) (reproduced from literature[69])

First thiols SAMs on Au were used as templates for the subsequent attachment of PAMAM molecules (Figure 1-10). Then, using microcontact techniques as well as a scanning probe microscopy based nanotool (DPN), they were able to pattern PAMAM molecules onto ester activated gold substrate with a resolution from micrometer to sub-100nm scale. Using such patterning methods the authors demonstrated the possibility to use patterned dendrimeric matrices, with a well defined thickness and functional group density as new interface for the fabrication of high density biochip.

The homogeneity and topography of such micro and nanopatterned surfaces were then characterizedwith XPS and AFM. By labelling with trifluoroacetic acid anhydre, the authors determine the number of amino end groups that may be derivatized via the complexation of biomolecules.

1.2 Context of the PhD thesis

CSEM investigations[70] on dendrimers have concerned the use of highly branched dendrimers for the functionalisation and microstructuring of surfaces. Monolayers prepared by the direct adsorption of several kinds of dendrimers onto different substrates have already attracted much attention[71-73]. First, they are highly stable in most cases since dendrimer are strongly adsorbed to the initial surface in contrast to

the monopodal attachment of linear alkyl-based self-assembled monolayers. Moreover, since such molecules contain a large number of peripheric reactive groups as well as a structure that is molecularly controllable (type of core, choice of branch point, and distance between successive branch junctions), they turned out to be very efficient in influencing the self-assembly properties of biomolecules[74] such as antibodies or plasmids.

In this context, our first experiments consisted of patterning surfaces with highly branched PAMAM dendrimers of the fourth generation (ethylenediamine core; 64 terminal-NH_2 groups). The ability of such dendrimeric patterned surfaces to be subsequently used as chemically sensitive interfaces for biomolecule complexation has also been investigated.

For patterning dendrimers on surfaces, the top-down microfluidic approach was first chosen to guide the self-assembly of PAMAM onto well defined areas. A PAMAM solution was allowed to flow through 2 μm and 20 μm wide periodic PDMS channels driven by capillary forces, on a photoactive Optodex® coated glass substrate (Figure 1-11).

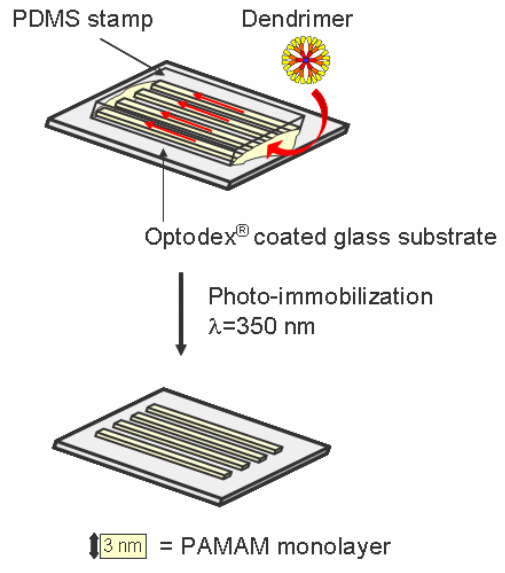

Figure 1-11 PAMAM solution sucked by capillary action through the channels of 2 μm and 20 μm periodic PDMS stamps.

After photo-immobilization of dendrimers, the surface was washed in order to remove non-covalently bound dendrimers and analyzed by Atomic Force Microscopy. The observation of 2 μm and 20 μm periodic dendrimer stripes (Figure 1-12) with heights from 3 to 4 nm was in agreement with the 4.5 nm theoretical diameter of G4-PAMAM and allowed us to confirm the monolayer character of adsorbed PAMAM dendrimers.

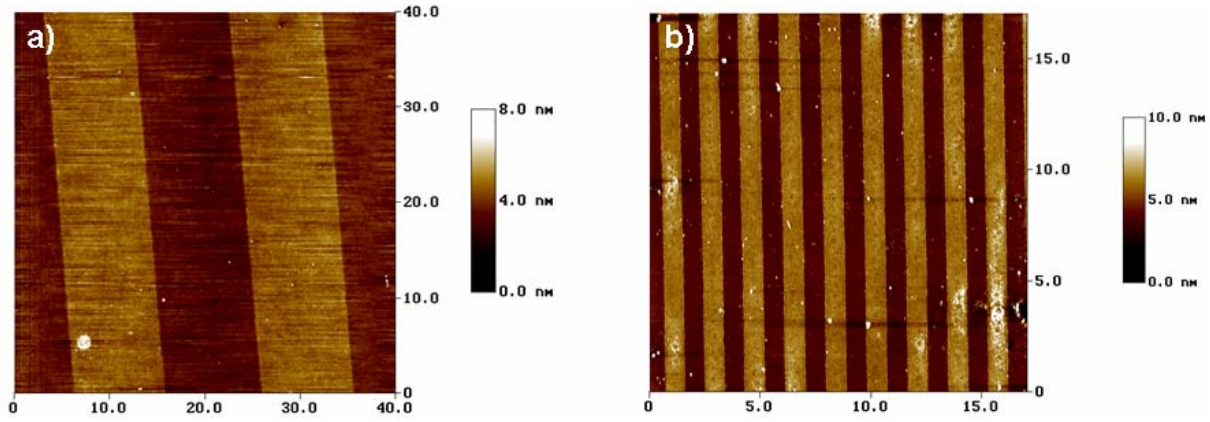

Figure 1-12 Tapping mode AFM images of dendrimeric patterned surface a) with 20 μm periodicity b) with 2 μm periodicity

The second step of this first study consisted in evaluating the reactivity of the free side of the adsorbed dendritic molecules. Amongst all possibilities, we first wished to investigate the ability of these pre-functionalised surfaces to coordinate biomolecules and semiconducting fluorescent nanoparticles.

Dendrimeric patterned surfaces were first tested by complexing fluorescent IgG antibodies via EDC chemistry. The functionalised substrates were simply dipped in a IgG/NHS/EDC solution (NHS: n-hydroxysuccinimide, EDC: N-(3-dimethylaminopropyl)-N'-ethyl carbodiimide, IgG: Guinea Pig Immunoglobulin), washed and analyzed by fluorescence microscopy (Figure 1-13).

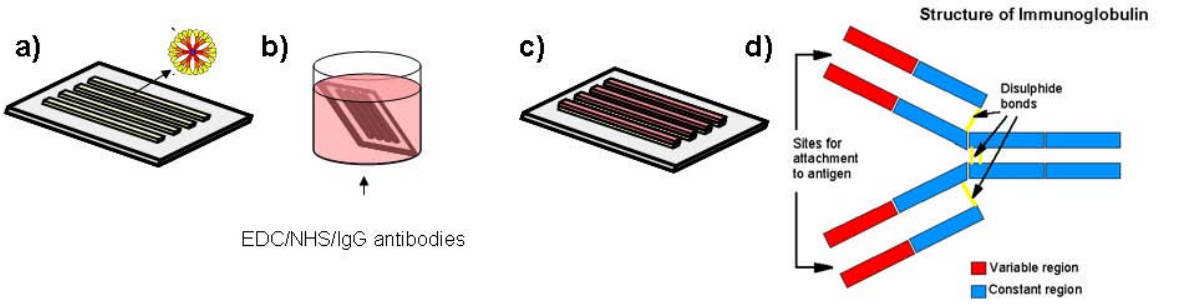

Figure 1-13 a),b),c) IgG patterning process on PAMAM membrane designed onto activated glass substrate. d) General structure of IgG molecule

Figure 1-14 shows the fluorescence image of the dendrimer template after incubation in the fluorescently labelled IgG solution: the antibodies present a regular and homogeneous architecture with 2 μm and 20 μm periodicity.These results clearly demonstrated the selective immobilization of IgG by the prefunctionalised dendrimeric surface via the formation of amidic bonds while non-patterned areas remained non reactive.

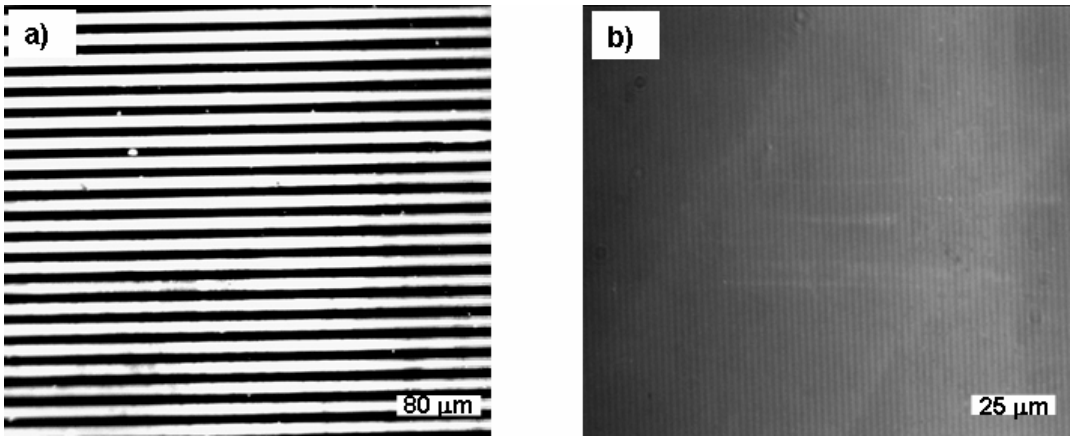

Figure 1-14 Fluorescence microcope images of IgG microstructures. PAMAM dendrimer deposited by fluidics through 20 μm (a) and 2 μm (b) periodic PDMS channels followed by covalent fixation of IgG

Since efficient biomolecule complexation was successfully achieved with micropatterned PAMAM surfaces, our research was then extended to the organization of ligand shell protected CdSe semiconducting nanoparticles. The organization of quantum dots into well defined structures is currently attracting much attention; it

represents indeed one of the crucial steps in evaluating the potential of nanoparticles in fields of application such as information storage, nano-electronics and nano-optics.

As described above, the dendrimeric micropattern was first created using soft-lithography techniques before being incubated in the CdSe nanoparticle solution. These 10 nm ligand protected particles, stabilized with a trioctylphosphine oxide (TOPO) outer shell were provided by EPFL.

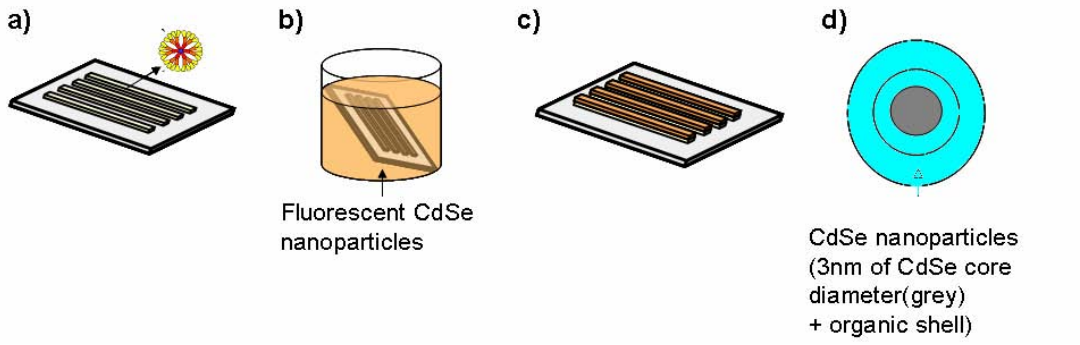

Figure 1-15 a),b),c) CdSe nanoparticles organization process on micropatterned PAMAM dendrimeric platform d) Core(grey)-shell(blue) structure of CdSe with diameter around 10 nm

The resulting fluorescence images showed regular and homogeneous CdSe architectures with 20 μm periodicities (Figure 1-16).

As for IgG, these results demonstrated that prefunctionalised dendrimeric surface selectively immobilize nanoparticles while non-patterned areas passivated by Optodex layer remain unreactive.

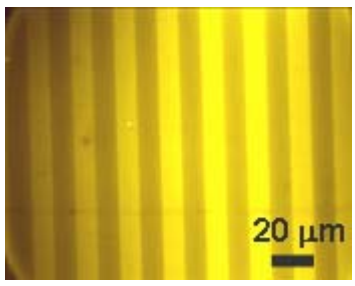

Figure 1-16 Fluorescence microscope image of CdSe nanoparticles microstructures. PAMAM dendrimer deposited by fluidics through 20 μm periodic PDMS stamp.

As preliminary conclusions, highly branched dendritic macromolecules were proved to be promising candidates as building units of organized structures and interfacing materials[75-77]. Thanks to their structural tunability dendrimers present versatile properties of complexation (eg. binding site nature and density) which can be used in a wide domain of applications such as biotechnology, electronics or optics.

1.3 References

[1] P. J. Flory, *J. Am. Chem. Soc.*, **1952**, 74, 2718

[2] E. Buhleier, W. Wehner, and F. Vogtle, *Synthesis-Stuttgart*, **1978**, 155

[3] D. A. Tomalia, H. Baker, J. Dewald, M. Hall, G. Kallos, S. Martin, J. Roeck, J. Ryder, and P. Smith, *Polymer Journal*, **1985**, 17, 117

[4] G. R. Newkome, Z. Q. Yao, G. R. Baker, and V. K. Gupta, *J. Org. Chem.*, **1985**, 189, 166

[5] E. M. M. deBrabandervandenBerg and E. W. Meijer, *Angew. Chem. Int. Ed.*, **1993**, 32, 1308

[6] C. Worner and R. Mulhaupt, *Angew. Chem. Int. Ed.*, **1993**, 32, 1306

[7] J. F. G. A. Jansen, E. M. M. deBrabandervandenBerg, and E. W. Meijer, *Science*, **1994**, 266, 1226

[8] J. M. J. Frechet, C. J. Hawker, and K. L. Wooley, *J. Macromol. Sci.-Pure and Appl. Chem.*, **1994**, A31, 1627

[9] C. J. Hawker, K. L. Wooley, and J. M. J. Frechet, *J. Chem. Soc.-Perkin Trans.*, **1993**, 1287

[10] R. Esfand and D. A. Tomalia, *Drug Discovery Today*, **2001**, 6, 427

[11] Y. Tomoyose, D. L. Jiang, R. H. Jin, T. Aida, T. Yamashita, K. Horie, E. Yashima, and Y. Okamoto, *Macromolecules*, **1996**, 29, 5236

[12] D. L. Jiang and T. Aida, *Chem. Commun.*, **1996**, 1523

[13] P. Bhyrappa, J. K. Young, J. S. Moore, and K. S. Suslick, *J. Am. Chem. Soc.*, **1996**, 118, 5708

[14] P. R. Ashton, V. Balzani, M. Clemente-Leon, B. Colonna, A. Credi, N. Jayaraman, F. M. Raymo, J. F. Stoddart, and M. Venturi, *Chem. Eur. J.*, **2002**, 8, 673

[15] M. Uyemura and T. Aida, *J. Am. Chem. Soc*, **2002**, 124, 11392

[16] P. J. Dandliker, F. Diederich, M. Gross, C. B. Knobler, A. Louati, and E. M. Sanford, *Angew. Chem. Int. Ed.*, **1994**, 33, 1739

[17] P. J. Dandliker, F. Diederich, J. P. Gisselbrecht, A. Louati, and M. Gross, *Angew. Chem. Int. Ed.*, **1996**, 34, 2725

[18] J. M. J. Frechet, *Science*, **1994**, 263, 1710

[19] M. Pittelkow, J. B. Christensen, and E. W. Meijer, *J. Polym. Sci. Part A: Polym. Chem.*, **2004**, 42, 3792

[20] M. J. Liu and J. M. J. Frechet, *Pharmaceutical Science & Technology Today*, **1999**, 2, 393

[21] E. R. Gillies and J. M. J. Frechet, *Drug Discovery Today*, **2005**, 10, 35

[22] M. Q. Zhao, L. Sun, and R. M. Crooks, *J. Am. Chem. Soc.*, **1998**, 120, 4877

[23] L. Balogh and D. A. Tomalia, *J. Am. Chem. Soc.*, **1998**, 120, 7355

[24] G. R. Newkome, C. N. Moorefield, J. M. Keith, G. R. Baker, and G. H. Escamilla, *Angew. Chem. Int. Ed.*, **1994**, 33, 666

[25] D. Astruc and F. Chardac, *Chem. Rev.*, **2001**, 101, 2991

[26] G. E. Oosterom, J. N. H. Reek, P. C. J. Kamer, and P. W. N. M. van Leeuwen, *Angew. Chem.Int. Ed.*, **2001**, 40, 1828

[27] J. W. J. Knapen, A. W. Vandermade, J. C. Dewilde, P. W. N. M. Vanleeuwen, P. Wijkens, D. M. Grove, and G. Vankoten, *Nature*, **1994**, 372, 659

[28] M. Slany, M. Bardaji, M. J. Casanove, A. M. Caminade, J. P. Majoral, and B. Chaudret, *J. Am. Chem. Soc.*, **1995**, 117, 9764

[29] C. Galliot, C. Larre, A. M. Caminade, and J. P. Majoral, *Science*, **1997**, 277, 1981

[30] A. M. Caminade, R. Laurent, B. Chaudret, and J. P. Majoral, *Coord. Chem. Rev.*, **1998**, 180, 793

[31] M. Slany, M. Bardaji, A. M. Caminade, B. Chaudret, and J. P. Majoral, *Inorg. Chem.*, **1997**, 36, 1939

[32] J. P. Majoral, A. M. Caminade, and R. Laurent, *Bulletin of the Polish Academy of Sciences-Chemistry*, **1998**, 46, 319

[33] M. Bardaji, A. M. Caminade, J. P. Majoral, and B. Chaudret, *Organometallics*, **1997**, 16(15), 3489

[34] M. Slany, M. Bardaji, M. J. Casanove, A. M. Caminade, J. P. Majoral, and B. Chaudret, *J. Am. Chem. Soc.*, **1995**, 117, 9764

[35] M. Slany, M. Bardaji, A. M. Caminade, B. Chaudret, and J. P. Majoral, *Inorg. Chem.*, **1997**, 36, 1939

[36] S. Jockusch, N. J. Turro, and D. A. Tomalia, *J. Inf. Recording*, **1996**, 22, 427

[37] H. F. Chen, Y. Q. Chen, B. G. Orr, M. M. B. Holl, I. Majoros, and B. H. Clarkson, *Langmuir*, **2004**, 20, 4168

[38] K. Naka, Y. Tanaka, Y. Chujo, and Y. Ito, *Chem. Comm.*, **1999**, 1931

[39] K. Naka in "*Dendrimers V: Functional and Hyperbranched Building Blocks, Photophysical Properties, Applications in Materials and Life Sciences"* by C.A. Schalley, F.Vögtle and V. Balzani, Springer, **2003**, 228,141

[40] K. Naka, Y. Tanaka, and Y. Chujo, *Langmuir*, **2002**, 18, 3655

[41] J. Haensler and F. C. Szoka, *Bioconjugate Chem.*, **1993**, 4, 372

[42] X. Q. Zhang, X. L. Wang, S. W. Huang, R. X. Zhuo, Z. L. Liu, H. Q. Mao, and K. W. Leong, *Biomacromolecules*, **2005**, 6, 341

[43] M. Hussain, M. S. Shchepinov, M. Sohail, I. F. Benter, A. J. Hollins, E. M. Southern, and S. Akhtar, *J. Control. Release*, **2004**, 99, 139

[44] C. Y. Guo, H. Wang, Y. H. Lin, and Q. L. Cai, *Prog. Biochem. Biophys.*, **2004**, 31, 804

[45] D. K. Smith, A. R. Hirst, C. S. Love, J. G. Hardy, S. V. Brignell, and B. Q. Huang, *Prog. Polym. Sci.*, **2005**, 30, 220

[46] V. Percec, W. D. Cho, P. E. Mosier, G. Ungar, and D. J. P. Yeardley, *J. Am. Chem. Soc.*, **1998**, 120, 11061

[47] V. Percec, A. E. Dulcey, V. S. K. Balagurusamy, Y. Miura, J. Smidrkal, M. Peterca, S. Nummelin, U. Edlund, S. D. Hudson, P. A. Heiney, D. A. Hu, S. N. Magonov, and S. A. Vinogradov, *Nature*, **2004**, 430, 764

[48] X. B. Zeng, G. Ungar, Y. S. Liu, V. Percec, S. E. Dulcey, and J. K. Hobbs, *Nature*, **2004**, 428, 157

[49] V. Percec, C. H. Ahn, G. Ungar, D. J. P. Yeardley, M. Moller, and S. S. Sheiko, *Nature*, **1998**, 391, 161

[50] S. Campidelli, E. Vazquez, D. Milic, M. Prato, J. Barbera, D. M. Guldi, M. Marcaccio, D. Paolucci, F. Paolucci, and R. Deschenaux, *J. Mater. Chem.*, **2004**, 14, 1266

[51] D. C. Tully and J. M. J. Frechet, *Chem. Commun.*, **2001**, 1229

[52] R. M. Crooks and A. J. Ricco, *Acc. Chem. Res.*, **1998**, 31, 219

[53] J. C. Love, L. A. Estroff, J. K. Kriebel, R. G. Nuzzo, and G. M. Whitesides, *Chem. Rev.*, **2005**, 105, 1103

[54] H. Tokuhisa, M. Q. Zhao, L. A. Baker, V. T. Phan, D. L. Dermody, M. E. Garcia, R. F. Peez, R. M. Crooks, and T. M. Mayer, *J. Am. Chem. Soc*, **1998**, 120, 4492

[55] A. Hierlemann, J. K. Campbell, L. A. Baker, R. M. Crooks, and A. J. Ricco, *J. Am. Chem. Soc.*, **1998**, 120, 5323

[56] H. Tokuhisa, M. Q. Zhao, L. A. Baker, V. T. Phan, D. L. Dermody, M. E. Garcia, R. F. Peez, R. M. Crooks, and T. M. Mayer, *J. Am. Chem. Soc.*, **1998**, 120, 4492

[57] A. Mecke, I. Lee, J. R. Baker, M. M. B. Holl, and B. G. Orr, *Eur. Phys. E*, **2004**, 14, 7

[58] R. Pericet-Camara, G. Papastavrou, and M. Borkovec, *Langmuir*, **2004**, 20, 3264

[59] T. A. Betley, M. M. B. Holl, B. G. Orr, D. R. Swanson, D. A. Tomalia, and J. R. Baker, *Langmuir*, **2001**, 17, 2768

[60] J. Li, L. T. Piehler, D. Qin, J. R. Baker, D. A. Tomalia, and D. J. Meier, *Langmuir*, **2000**, 16, 5613

[61] M. L. Mansfield, *Polymer*, **1996**, 37, 3835

[62] R. McKendry, W. T. S. Huck, B. Weeks, M. Florini, C. Abell, and T. Rayment, *Nano Lett.*, **2002**, 2, 713

[63] H. W. Li, D. J. Kang, M. G. Blamire, and W. T. S. Huck, *Nano Lett.*, **2002**, 2, 347

[64] X. C. Wu, A. M. Bittner, and K. Kern, *Langmuir*, **2002**, 18, 4984

[65] M. Rolandi, I. Suez, H. J. Dai, and J. M. J. Frechet, *Nano Lett.*, **2004**, 4, 889

[66] G. H. Degenhart, B. Dordi, H. Schonherr, and G. J. Vancso, *Langmuir*, **2004**, 20, 6216

[67] C. Minelli, N. Blondiaux, M. Losson, M. Liley, S. Jeney, C. Hinderling, R. Pugin, D. Joester, F. Diederich, J. Vancso, M. Hempenius, and H. Heinzelmann, *Chimia*, **2003**, 57, 646

[68] A. Friggeri, H. Schonherr, H. J. van Manen, B. H. Huisman, G. J. Vancso, J. Huskens, F. C. J. M. van Veggel, and D. N. Reinhoudt, *Langmuir*, **2000**, 16, 7757

[69] D. C. Tully, K. Wilder, J. M. J. Frechet, A. R. Trimble, and C. F. Quate, *Adv. Mater.*, **1999**, 11, 314

[70] H. C. Yoon, M. Y. Hong, and H. S. Kim, *Anal. Biochem.*, **2000**, 282, 121

[71] E. Emmrich, S. Franzka, and G. Schmid, *Nano Lett.*, **2002**, 2, 1239

[72] D. C. Tully, K. Wilder, J. M. J. Frechet, A. R. Trimble, and C. F. Quate, *Adv. Mater.*, **1999**, 11, 314

Chapter 2

Aim of the thesis

In contrast to conventional lithography techniques (ultimate miniaturization: top down approach) which will soon hit their limits of feature size and fabrication cost, recent years have seen considerable progress in the development of self-assembling structures and devices (bottom-up approach). Generally, self-assembly can be defined as a supramolecular concept which relies on non-covalent intermolecular interactions such as eg. hydrogen bonding, dipolar interactions and van der Waals forces. Such relatively weak interactions could then be used for the assembling of nanoscale building blocks in a controllable way. This results in the construction of self-assembled superstructures with new chemical and physical properties specific to the nanometer scale. Thus, the rational design of such complex nanoarchitectures is not merely of therotical interest but also has potential applications in many existing and emerging fields such as material science, optics, electronics and biotechnology.

Dendrimer chemistry is an additional field of research in nanoscience. Drawing on the geometric tunability (structure, size, shape) and ease of multiple functionalisation of dendrimer, we decided to work with commercially available as well as with newly designed amphiphilic dendrimers with the aim to investigate how their self-assembling properties could be used and tuned for the formation of complex nanoarchitectures.

In this context our first investigations have been focused on the self-organization of cyanine dye molecules for the formation of well-defined J-aggregates onto self-assembled PAMAM monolayers. Although J-aggregation of cyanine was first observed in the 1930's, the aggregation mechanism is not yet understood sufficiently to enable the rapid and reproducible formation of monolayered J-aggregates for industrial applications. In the chapter 3 we investigate how different substrates could be efficiently coated with PAMAM monolayers. Then, and based on previous studies which described dendrimer-assisted-dye-aggregation process in solution, the ability of such highly functionalised surfaces to behave as matrix for the molecular organisation of cyanine monomers into J-aggregates by self-assembling process has been tested. For a better understanding of surface J-aggregation mechanism, the influence of some experimental conditions (concentrations, pH) as well as the effect of the dendrimer nature and generation on the quality of the J-aggregation has been intensively studied.

In chapter 4 we investigated the potential of dendrimers in cell transfection technologies by studying the ability of dendrimers to behave as transport vectors for non viral gene therapy. Newly amphiphilic dendrimers were specially tailored to combine high charge density and buffering capacity with spontaneous self-assembling properties, both necessary for the complexation and delivery of foreign genetic material into targeted cells. Our contribution aimed first to investigate the intrinsic self-assembly properties of dendrimers with different sizes at the air/water interface using Langmuir Blodgett technique. Then, using atomic force microscopy and cryo-transmission electron microscopy the propensity of this dendrimer to strongly condense DNA into well defined polyplexes was evaluated. Thus, these studies allowed us to gain insight into the dendrimer structure-transfection activity relationship.

Chapter 3

J-Aggregation of cyanine dyes

3.1 Introduction

Loss-free propagation of optical excitation energy over a large number of non-covalently bonded molecules has been proved for a particular species of supramolecular assemblies called "J-aggregates"[1,2]. These aggregates arise from the self-assembling of cyanine dyes forming highly ordered crystal structures. As no vibrational relaxation or thermal destruction of the absorbed photons occurs, the lifetime of the excited state is close to that of molecular vibrations and is therefore in the pico-or subpicosecond range. This is supported by the fact that the resonance fluorescence of a J-aggregate can be quenched by a few molecules, which can be explained by migration of the excitation energy over a large number of cyanine monomers in this aggregate during the lifetime of the excited state[3].

Numerous devices have been proposed using the unique properties of cyanine J-aggregates. Examples are light harvesting systems for solar[4] and sensor devices[5], components for non-linear optics[6], electron- or energy acceptors for excited donors (e.g. spectral shifts in PLED's or OLED's[7]), fast optical recording systems, superquenching by long-range energy transfer in the resonating cavities of organic semiconductors between mirrors[8], enhanced light absorption by J-aggregate formation on metal (e.g. Au or Ag) quantum dots[9].

Although exciton delocalisation in J-aggregates of cyanine dyes was first observed[10,11] in the 1930's, it is not yet sufficiently understood to make use of this property for industrial applications (except for photography[12]).

In order to achieve the molecular organization of molecules into J-aggregates, the following methods/matrices have been described: Langmuir-Blodgett[1,13] (LB) and matrix-oriented layers[13,14] (MO-layers) using a fatty acid LB-matrix for dye organisation into J-aggregates, aqueous NaCl solutions[15], polymers[16] (gelatin[17], alginates[18], poly-lysine[5], polysoaps[19], polyacrylic acid layers[9]), nanocapsules[20], micelles[13], liposomes[21] . Inorganic surfaces like silver halide and semiconductor surfaces[22,23], brominated silver nanoparticles[24], mica[25], were also used as matrices for J-aggregate formation.

Most of the methods used to organize dye molecules into J-aggregates do not fulfill the desired requirements for using these supramolecular entities in devices for practical use. The main drawbacks are lack of reproducibility and stability, poor control of J-aggregate size and defect states, time for J-aggregate formation and preparation avoiding complex manufacturing techniques (e.g. LB- and MO techniques). Random-coiled matrices such as polymers, liposomes, bio-polymers, as well as crystallization processes from solutions do not allow size control, reproducibility and defect-free aggregation. Inorganic solid surfaces used for J-aggregate formation interact with the charge carriers formed after photonic excitation. Organic matrices have the highest chance to avoid such undesired interactions.

The only known nanoparticulate matrices used to self-assemble J-aggregates into organized monolayers without unwanted multilayer formation studied hitherto are stepped brominated silver nanoparticles[26] (diameter 20-30 nm, height 5-10 nm). They show interactions between surface plasmons in Ag and Frenkel excitons in the J-aggregates but no fluorescence (which is a disadvantage for energy transfer systems and light-harvesting). Polystyrene nanocapsules[27] of 500 nm diameters filled with 30 nm diameter J-aggregates behave like 3-dimensional crystals in “nanocontainers” and multilayer. Monoatomic steps on AgX microcrystal surfaces, as used in photography for certain products[28,29], or such steps on brominated silver nanoparticles come closest to nanocrystalline surfaces. However, the formation of atomic steps with controlled size and geometry is not possible, which often leads to J-aggregates larger than desired for exciton propagation. Both types of crystalline matrices interact with the charge carriers produced in the J-aggregate by exposure to electromagnetic radiation, thus quenching fluorescence, photocurrent and phosphorescence.

Other surfaces used as matrices for J-aggregates are either too disordered (polymers, gelatin, glasses, bio-polymers) or, if well defined (LB and MO-layers), they are too difficult and slow to allow commercial applications. For all devices of interest using the Frenkel exciton delocalisation property, the size and the perfection of J-aggregates in monolayers must be carefully controlled. In all systems described hitherto, J-aggregation is slow (1 hour or more), difficult to control (polymers, solutions), or only possible under very special conditions on special surfaces and using particular

cyanines. The lack of appropriate methods for obtaining perfect J-aggregates reproducibly by self-assembly and the considerable time required may be some of the reasons why J-aggregates have not yet lead to industrial applications except in photographic science.

The aim of the present research activity is to identify new templates for the self-assembly of cyanine J-aggregates without the disadvantages mentioned above. Such systems should enable optimum use of the unique exciton propagation properties of J-aggregates. It will be shown that polyamidoamine dendrimers (called PAMAM) provide an organizing matrix having the desired properties for the formation and control of J-aggregation process.

3.2 General properties of dyes

Archaeology teaches us that even prehistoric men used dyeing procedures: for furs, plant fibres and later for textiles. Usually the dyes or pigments came from plants and minerals. Over thousands of years the synthetic methods have improved resulting in the development of very effective dyes and pigments. According to the original theory of Witt in 1876, a coloured substance should contain one or more unsaturated groups, such as vinyl or carbonyl groups, which are called chromophores. Brooker and coworkers provided extensive documentation of major trends with two series of publications "Colors and Constitution and Steric Hindrance[30,31]". Later, resonance theories were developed to accommodate all the major trends in a highly successful manner.

Generally, dyes are molecules which have delocalized electrons along unsaturated bonds. The most important electronic transitions responsible for the absorption of light are the $\pi \rightarrow \pi^*$, $n \rightarrow \pi^*$ transitions; their frequency are proportional to the energy difference ΔE between the highest occupied molecular orbital (HOMO) and the lowest unoccupied molecular orbital (LUMO) (Figure 3-1).

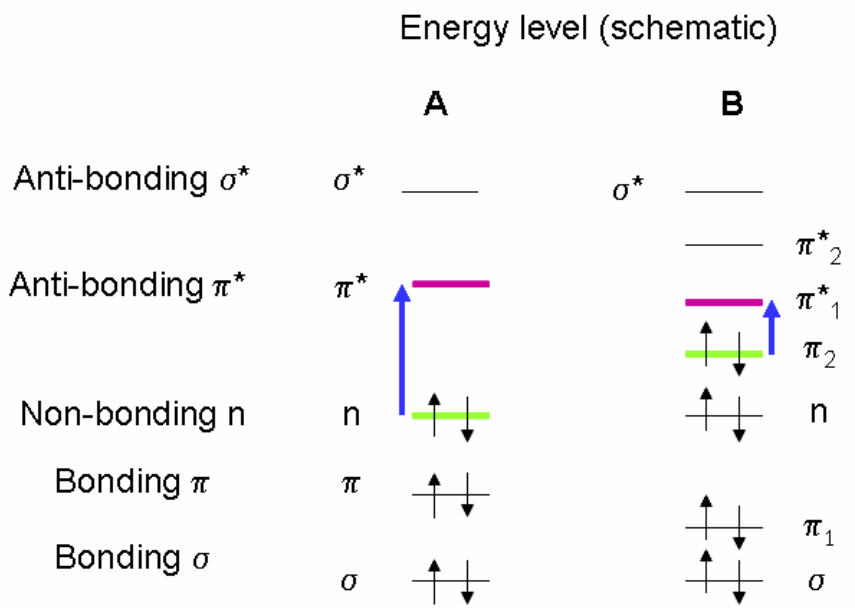

Figure 3-1 : Energy levels for electronic transitions

The energy difference ΔE is expressed by Planck's law (Equation 3-1):

$$\Delta E = h\nu = {}^{hc}\!/_{\lambda}$$

Equation 3-1: Planck's law

Planck's law forms the basis for the works of Lewis and Hückel, who established relationship between chemical structure and physics. An increase in the number of double bonds in a cyanine dye induces a strong electron delocalisation over the molecule, leading to a red shift (bathochromic effect) in the absorption spectrum.

If the absorbance spectrum is influenced by the chemical structure of the individual dyes, it is also strongly depending on the organisation of the dye-assembly at a molecular level. As we will describe below, a red shift (bathochromic effect) in absorption is characteristic for certain dye aggregates while a blue shift (hypsochromic shift) is recorded for dimers.

In contrast, the hyperchromic and hypochromic effects arise due to changes in concentration and solvent quality, but are not due to the aggregation of dye molecules.

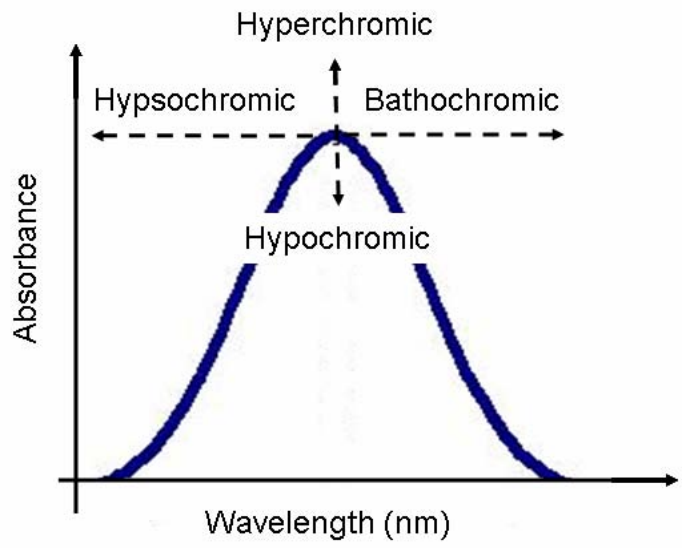

Figure 3-2 Absorbance spectrum shifts due to chemical structure modification and environmental factors

Further considerations will focus on polymethine dyes (cyanines and merocyanines). These dyes are versatile compounds and are nowadays used for novel technical applications such as photography, non-linear optics and OLEDs.

3.3 Structure of polymethine dyes: cyanines

Mono- or polymethine dyes (synthetic and natural origins) usually contain an electron donor and an electron acceptor group at the opposite ends of the polymethine chain. All these dyes derive from the following general structure:

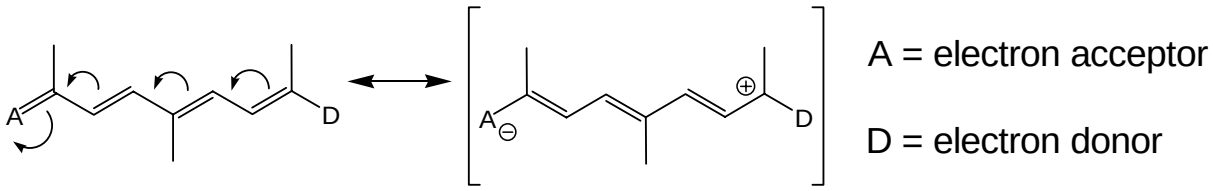

Figure 3-3 Resonance limiting structure of cyanine

The nature of substitutents in meso-position of the polymethine chain, influences cis-trans stereoisomerisation[32,33]. These dyes can be classified by the number of methine groups (n= 1, 2, 3 …) as mono, di, trimethines.

The formula can also be written as $R_2N\ [CH{=}CH]_nCHN^+R_2$ where n is an odd number for cyanines and an even number for merocyanines, respectively. The nitrogen atoms

are part of the delocalized π–electron system which can involve heterocycles such as,e.g, imidazole, pyridine, pyrrole, quinoline, thiazole, oxazole.

Figure 3-4 shows an overview of heterocycles which participate in electron delocalization. Generally, the polymethine chain is linked in α-position to the nitrogen of the heterocyclic group.

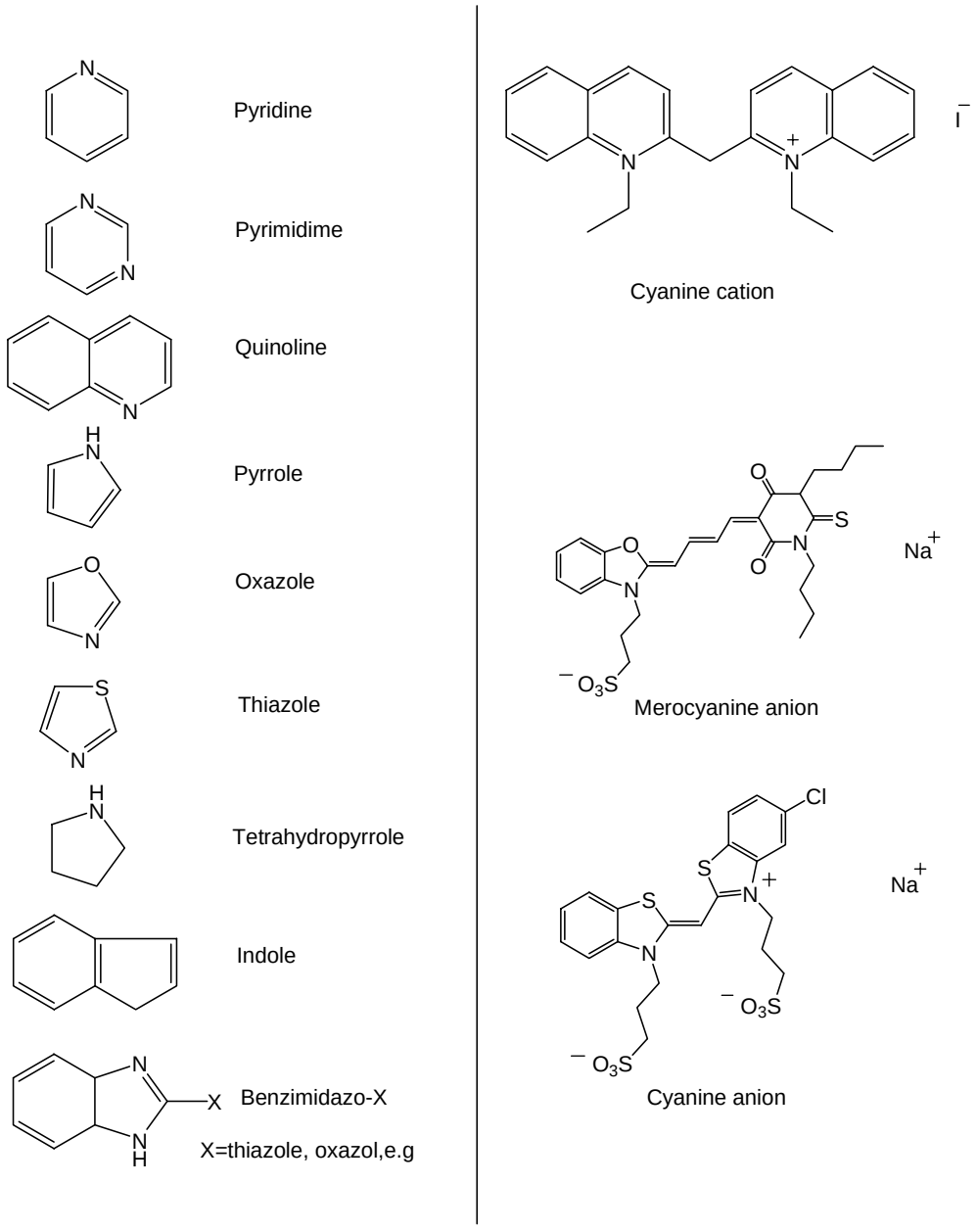

Figure 3-4 Different types of heterocycles and examples of polymethine dyes

Among the dyes, cyanines are substances exhibiting a variety of colours, but they are not widely used for dying purposes due to their low stability towards light. However,

they have been employed in photography as sensitizers, in optical disks as recording media, as photoreactive materials in light-harvesting systems, and as probes for biological applications.

Self-aggregation of dyes in solution or at the solid-liquid interface is a frequently encountered phenomenon in dye chemistry owing to strong Van der Waals attractive forces between molecules. The aggregates in solution exhibit distinct changes in the absorption band compared to the monomeric species. From the spectral shifts, various aggregation patterns of the dyes in different media have been proposed.

3.4 States of aggregation for cyanines

Some structural conformations of cyanine aggregates characterized by spectroscopic measurements [34,35] and microscopy [36,37] are represented in Figure 3-5.

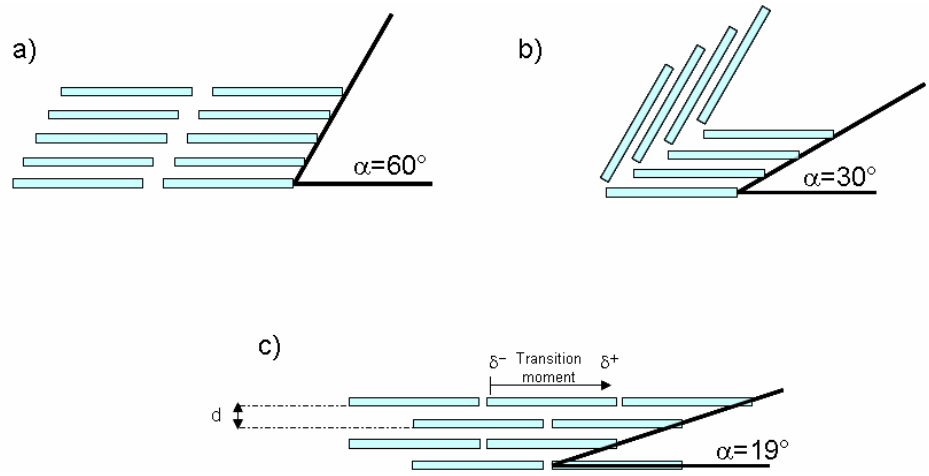

Figure 3-5 Organisation of cyanines monomers: a) H-aggregate (hypsochromic λ shift on absorption spectrum), b) J-aggregate "Herringbone structure" and c) J-aggregate "Brickstone structure". Structures b) and c) present a bathochromic λ shift of the absorption spectra.

Calculations based on an extended dipole model[38] are in agreement with experiments. The distance (d) between dye chromophore is almost identical for all types of aggregates (3-4 Å)[39,40]. Structural differences are due to different overlap angles (α) of molecules in parallel arrangement (Figure 3-5b, c)

In the case of cyanines, Van der Waals forces, electrostatic attractive forces, hydrophobic and π-π coupling are responsible for aggregation. For J-aggregates, it is

the strong π-π coupling between chromophores which is responsible for the particular structural arrangements[41] shown in Figure 3-5b) and c) XRD studies showed also that the crystal structure of J-aggregated cyanines presents the same features as 2-dimensional J-aggregates layers[42].

Changes in solvent properties (dielectric constant, ionic strength, hydrogen bonding) affect absorption maxima of J-aggregates. Moreover, parameters like electrolytes and temperature also are important factors that can influence the process of self-assembling. Depending on aggregation, different optical properties could be demonstrated.

In term of emission, while dimers and H-aggregates are generally non fluorescent, J-aggregates present very narrow emission spectra with low Stokes shifts (a few nm).

3.5 Exciton delocalisation and physical properties of cyanines

In semiconductors, electrons and holes interact pairwise to form an electron-hole pair called “exciton”. In J-aggregates, the exciton energy propagates like an energy particle (“soliton”) along the J-aggregate at sonic speed. The exciton theory was first explained by Frenkel[43], followed by Peierls[44] and further developed by Wannier[45].

Two conceptual approaches describe the electronic properties of all types of excitons. The Frenkel model, the most appropriate in our case, corresponds to a molecular system where the exciton is induced from delocalized molecular states. In the Wannier model, an exciton is formed by electron/hole interactions forming a particle-like electron-hole pair.

The most interesting property of J-aggregates is the formation and propagation of coherent Frenkel excitons. For this reason, many research projects actively focused on the understanding of this property for new technological applications.

Kuhn, Möbius and co workers [1,46] were the first to try to explain with an “exciton model” the appearance in J-aggregates of a narrow absorption band at longer wavelength than for the monomer absorption band. These investigations have first allowed them to demonstrate that the narrow J-band is due to the loss-free propagation of optical excitation energy over a large number of non-covalently bonded

molecules[46]. As shown below, the bathochromic shift is due to the specific brickstone architecture in J-aggregates where an attraction of the dipoles (cyanines polarized by external excitation) in the out-of-phase oscillation occurred decreasing the frequency (longer wavelength). The fluorescence of resonance is due to the fact that no vibrational relaxation or thermal destruction of absorbed photons occurs.

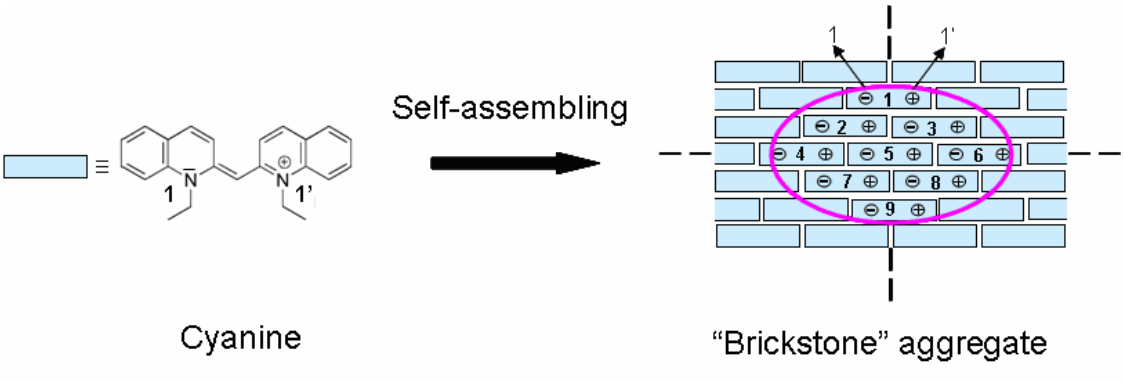

Figure 3-6 Brickstone aggregate (J-aggregate). Excited domain (pink noticed domain) of N=9 molecules represented by extended dipoles oscillating in phase (Model: H.Khun and C. Kuhn)

These conclusions were confirmed by observations where the fluorescence of the J-aggregate was quenched by insertion of highly efficient fluorescent probe molecules acting as energy acceptors into the J-aggregate lattice (Figure 3-8). These observations brought evidence that the J-aggregate acted as a cooperative molecular array which, after absorbing a photon, channelled the energy (excited domain) with a sufficient speed *v* to reach an acceptor molecule within J-aggregate life time τ_{agg} (Figure 3-7).

$$v = Za/(L_{exciton} * \tau_{agg})$$

Figure 3-7 Speed of exciton

$L_{exciton}$: width of the exciton

τ_{agg}: life time of exciton

Za: area of the aggregate where the acceptor molecule is present.

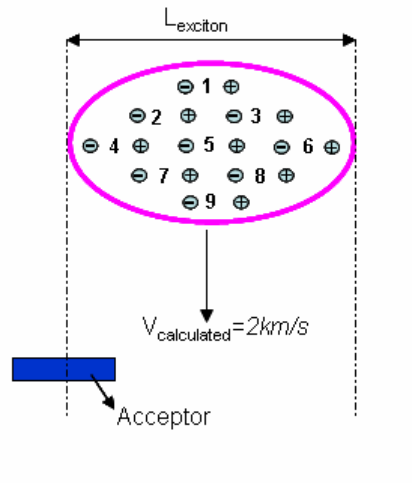

Figure 3-8 Exciton reaching an acceptor molecule, where it is trapped

When the light quantum has been absorbed, the excited domain is compressed due to the cohesive forces between the coherent oscillators (cyanines). The charge change sign simultaneously, thus nearest-neighbour charges are always opposite; the attraction of charges leads to a compression of the excited domain.

Additional experiments have also demonstrated the disappearance of the energy transfer when the J-aggregate rigidity and high supra-molecular order could not be guaranteed.

3.6 Current techniques for the preparation of well defined and highly ordered monolayered cyanine J-aggregates

The Langmuir-Blodgett (LB) technique is a reliable top-down method to obtain highly ordered mono- and multilayers of amphiphilic organic compounds. For amphiphilic cyanines, this method has first allowed one to form and determine structural data of well defined J-aggregates at the air/water interface[32,47-49]. One advantage of the LB-technique is that structural distorsions of J-aggregates, which may lead to the loss of their photophysical properties, is efficiently prevented. The study of pressure-area isotherms gives informations such as the influence of pressure on J-aggregate formation as well as the minimal molecular area in the compressed LB film[50,51].

Moreover, additional physical measurements directly performed at the air-water interface such as fluorescence measurements[52,53], X-ray diffraction measurements and IR reflection spectroscopy[54] have completed the optical and structural characterization of J-aggregate LB-films. Langmuir-Blodgett is also a particularly useful technique for studying the limiting distance for electron-hole recombination in the field of photographic sensitivity (so called "desensitization")[13]. Monolayers of mixed solutions of amphiphilic cyanines with electron accepting molecules were first prepared by LB. By changing the ratio between electron acceptor and cyanine donor concentrations, the mean distance between them could be varied. Such mixed LB-layers were then transferred to silver halide layers, and analyzed by absorption and fluorescence spectroscopy.

As an extension of the LB technique, Steiger *et al*[13] have organized cyanine molecules into J-aggregates by controlling the self-assembly process on a well defined fatty-acid matrix. The so called "matrix oriented layers" or MO-layers method) consists of adsorbing cyanine dyes dissolved in the aqueous subphase on a previously formed fatty-acid LB monolayer (Figure 3-9).

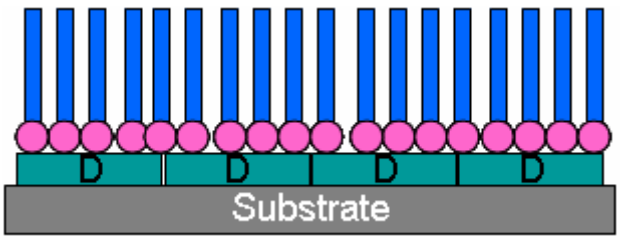

Figure 3-9 Schematic structure of a Matrix Oriented layer with a cyanine dye (D) transferred to solid substrates (AgBr, glass)

Here, adsorptive organization is mainly controlled by diffusion processes. Positively charged cyanine dye molecules strongly interact via attractive electrostatic forces with the negatively charged fatty acid LB layer. The subsequent progressive growth of the J-aggregate occurs by diffusion of remaining cyanine monomers from the aqueous subphase to the fatty acid layer. Such Matrix Oriented J-aggregate assemblies could then be transferred to AgBr surfaces and their photonic interactions spectroscopically studied.

J-aggregation could also be initiated directly on high-energy sites of microcrystalline silver halide surfaces. Contrary to previous experiments, the pre-formation of a monolayer at the air/water interface is not needed anymore. These experiments were carried out by forming new silver halide surface sites in the presence of the cyanine dye. The newly formed high-energy sites then acted as nucleation centres for J-aggregates which progressively grew along monoatomic steps formed at the AgX-surface by continuously adding silver and halide ions in the presence of the cyanine dye (Figure 3-10).

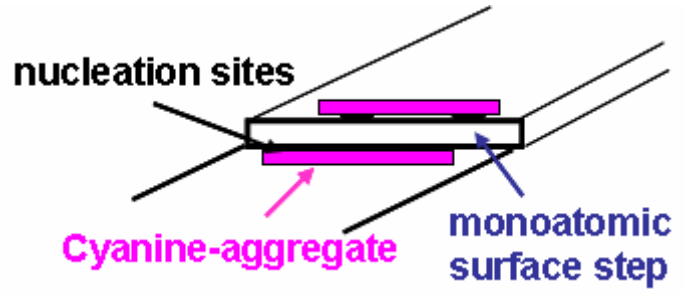

Figure 3-10 Growth of a J-aggregate along the edge of amonoatomic silver bromide surface step

Based on this concept, complementary investigations were reported by Sato *et al.*[55] who described the formation of J-aggregates on a nanoparticulate matrix formed of silver nanoparticles coated with a monomolecular silver bromide layer.

3.7 Proposed alternative self-assembly approach for highly controlled cyanine J-aggregation process

In all investigations mentioned above (using techniques such as LB, MO-layers, microcrystalline AgX surfaces and coated Ag nanoparticles) the main goal was to understand the mechanism of formation of dye J-aggregates as well as their resulting structure and photophysical properties. However such techniques are not appropriate to singly and reproducibly manufacture J-aggregates on solid substrates as well as for being scaled up to larger surfaces. Recently, many efforts have been made for the development of new matrices (polymers, gelatin, biopolymers or polysoaps) for a controlled J-aggregation process. Unfortunately, such matrices do not behave as an

ideal template since they lead to multilayered, poorly defined and unstable cyanine aggregates.

Our contribution to J-aggregate chemistry consisted in evaluating the potential of dendrimer functionalised surfaces to coordinate and organize cyanine molecules into highly ordered and monolayered J-aggregates. In contrast to linear or hyper-branched polymers, starburst dendrimers (PAMAM) present a very narrow size distribution as well as a highly defined structure, geometry and functional group density on their periphery. Even more interesting is the possibility to tune all these key parameters when varying the dendrimer generation. PAMAM dendrimers with tunable self-assembly properties are thus predicted as promising and flexible candidates for their use as "J-aggregate promoters".

3.8 Experimental work

3.8.1 Materials

PAMAM dendrimer, generation 1.0 (20%wt); generation 4.0 (10%wt); generation 6.0 (10%wt) were purchased from Sigma-Aldrich (Schnelldorf, Germany). For the preparation of solutions and for washing substrates, Uvasol acetone and ethanol were purchased from Merck (Darmstadt, Germany). H_2SO_4 (VLSI 96%) and H_2O_2 (VLSI 30%), used for preparing Piranha solution, were purchased from Rockwood (St Fromond, France). Glass substrates used are borosilicate glass wafer purchased from Bullen Ultrasonics Inc. (Eaton, United States of America) and diced into pieces with dimensions of 0.8 cm x 3cm. For the gold substrates, after cleaning glass wafers, gold was evaporated (rate of evaporation = 0.7 nm/s) on a preliminary evaporated chromium layer (rate of evaporation = 0.5 nm/s) acting as gold adhesion promoter. These slides with a Cr thickness of 4 nm and gold thickness of 32 nm are still transparent to visible light. Chromium and gold were purchased from Umicore.

UV-Visible Spectroscopy measurements were performed with a Perkin Elmer UV/Vis spectrometer Lambda 14. Fluorescence measurements were performed with a Perkin Elmer Luminescence spectrometer LS 50B.

Concerning PM-IRRAS spectroscopy and data acquisition, the gold sample was mounted within the compartment of a Bruker PMA 50, connected to an external beam port of a Bruker Tensor 27 Fourier Transform Infrared (FT-IR) spectrometer. After reflection at an angle of incidence of 80° the light was focused on a liquid nitrogen-cooled photovoltaic MCT detector in the PMA 50 cabinet. Polarization was modulated with a photoelastic modulator (Hinds, PEM 90) at a frequency of 50 kHz. Demodulation was performed with a lock-in amplifier SR830 DSP. All spectra were recorded during a sample scan time of 5 min at 4 cm^{-1} resolution.

Resulting PM- IRRAS reflectance spectra were calculated with the bare gold substrate as the reference.

3.8.2 Methods

Preparation of substrates

In order to clean substrates before the coating process, gold substrates were first treated under oxygen plasma for 3 minutes, (Oxford Plasmalab80 plus, 30 Watt, 50 mT, radio frequency). The plasma (high energy particles such as accelerated atomic ions and free electrons) is created between two capacitor plates by inducing a radio frequency (RF) electric current across the plates (Figure 3-11). The cleaning process consists in exposing the surface to the resulting oxygen plasma. The organic contaminants present at the surface of the substrate are thus degraded by the interaction with these highly energetic particles into smaller and volatile organic molecules. (AFM image of PAMAM on glass substrate is shown on Annexe1)

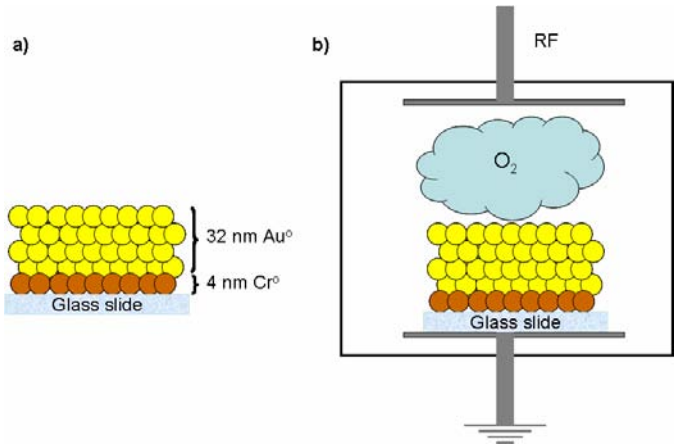

Figure 3-11 a) Gold evaporated on a glass substrate previously coated with a 4 nm thick chromium layer as adhesion promoter. b) Oxygen plasma etching, RF causes the ionization of oxygen

Glass substrates were washed by dipping them for 10 minutes in 120 °C Piranha solution (H_2SO_4/H_2O_2, 2:1). The slides were then rinsed with Millipore water before being dried under nitrogen flow. As already described for gold substrates the glass substrates were then activated with an oxygen plasma treatment.

3.8.3 PAMAM coating process

Gold and glass slides were dipped in a freshly prepared and slightly stirred ethanolic solution of PAMAM G4 ($1 \cdot 10^{-4}$M)[56]. After an 18 hours immersion period, dendrimer functionalised gold or glass slides were rinsed with pure ethanol in order to remove uncoordinated PAMAM molecules (Figure 3-12) and dried under nitrogen flow.

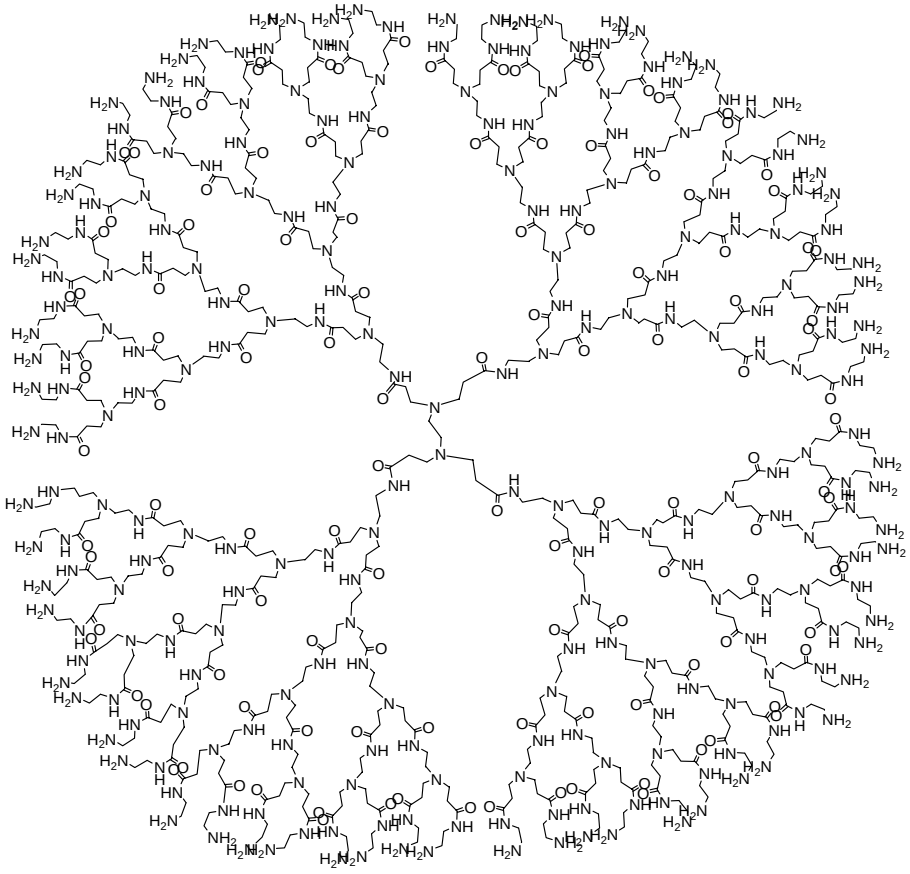

Figure 3-12 Structure of G4-Polyamidoamine (PAMAM)

3.8.4 Poly-lysine coating process

Poly-D-lysine or poly-L-lysine is known to strongly interact with negatively charged surfaces. Due to the large number of amine functions on poly-lysine polymers, poly-lysine layers have already been used as highly functionalised interfaces for promoting cell, proteins adhesion and DNA complexation. The poly-lysine coating glass substrate was a control experiment for J-aggregation process in comparison with PAMAM coated surfaces. Freshly cleaned glass slides were dipped into aqueous poly-lysine solution (0.1mg/mL). After a 18 hours immersion time, poly-lysine functionalised glass slides were rinsed with water Millipore in order to remove uncoordinated poly-lysine molecules (Figure 3-13), and dried in an oven at 45 °C for 40 minutes (AFM image of polylysine on glass substrate is shown on Annexe2).

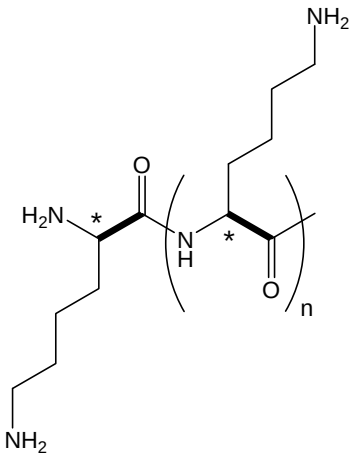

Figure 3-13 Structure of poly-lysine

3.8.5 Cyanine deposition process

Since cyanines are generally highly light sensitive, exposure to light has to be avoided during the entire process (solution preparation and coating process). Cyanines were dissolved in acetone ($7 \cdot 10^{-4}$ M; 15 seconds ultrasonic bath) and placed for 2 hours under magnetic stirring.

In order to promote the adsorption of negatively charged cyanine onto the PAMAM surfaces, the predeposited dendrimer monolayer has first to be protonated by dipping the PAMAM coated substrate into HCl solution (pH = 3.5; all amine functions are thus protonated). Protonated PAMAM coated substrates were then immersed into the cyanine solution, rinsed with pure acetone, dried with nitrogen flow before to be analysed with UV-Vis spectrophotometer. An example of cyanine we used is shown in Figure 3-14.

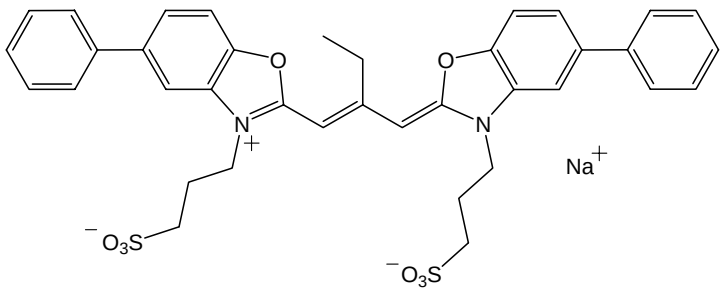

Figure 3-14 Chemical structure of [5, 5'-diphenyl-dibenzoxazolo-N, N'-propylsulfonate] 9-ethyl trimethine cyanine (myline1)

3.9 Results and discussion

Monolayers prepared by the direct adsorption of dendrimers on different substrates were extensively studied in the last few years because they present several important advantages[56,57]. Actually, they are highly stable in most cases since dendrimers are very strongly adsorbed to the surface in contrast to the monopodal surface attachment of linear alkyl-based self-assembled monolayers. The alternative strategy which consists in immobilizing linear polymers can also be used, but the inherent flexibility of these materials makes manipulation at the molecular level and self-organization difficult.

As shown in the introduction, we already used dendrimers such as Polyamidoamine (PAMAM) as anchoring functionalities for the immobilization of biomolecules or nanoparticles onto surfaces. The first method we presented has consisted first to pattern surfaces with PAMAM dendrimer microstructures by micro-contact printing (2 μm and 20 μm periodic features). PAMAM was subsequently covalently linked to the substrate by photoimmobilization (photolinker: Optodex) before the PAMAM coated surface can be used as highly functionalised and structured platform for the coordination of proteins.

In order to extend our investigations on PAMAM self-assembly properties, the main goal of this chapter 3 is to evaluate how predeposited PAMAM dendrimer monolayers can be used as templates for the coordination of cyanines on the functionalised surface. More interesting was to evaluate how such dendrimeric platforms could also self-organize cyanines into well-defined J-aggregates in a controlled way.

3.9.1 Interactions PAMAM / substrates

3.9.1.1 Interaction of PAMAM with gold substrates

As described in the experimental section, the coating of gold surfaces with different generations of PAMAM was achieved after 18 hours of immersion of freshly cleaned gold substrate in ethanolic PAMAM solution. Under such experimental conditions, the

Au oxide layer potentially formed during the plasma cleaning process (about 1nm thick)[58] is unstable and is removed before the PAMAM adsorption on the surface.

Concerning the nature of the Au/PAMAM interactions, Rahman *et al.*[59] already described that dendrimer adsorption is mostly driven by the weak favourable interaction between the peripheric primary amino groups of PAMAM and gold atoms of the surface. Actually, if dissolved in low molecular weight alcohols, primary amine end groups remain uncharged and the role of electrostatic forces in the formation of adsorbed PAMAM monolayer can be neglected. However, due to the large number of end groups on the dendrimer periphery, dendrimer layers present excellent adhesion properties and are very stable-

Using aqueous PAMAM solutions, the nature of Au/dendrimer interactions is completely different since the amino end groups tend to protonate resulting in positively charge peripheric groups. Thus, strong electrostatic forces when adsorbing on the surface become possible. However, under such conditions the formation of non-controlled multilayered systems has been reported[60].

3.9.1.2 Interaction of PAMAM with glass substrates

In the case of glass substrates, PAMAM molecules are adhering on the surface via strong acid-base interactions between the peripheric amine functions and the silanol groups of the glass surface (Figure 3-15). Possible proton exchange between silanol surface groups and the dendrimer periphery can even be considered. AFM image of PAMAM G4 adsorbed on glass is shown in Annexe1.

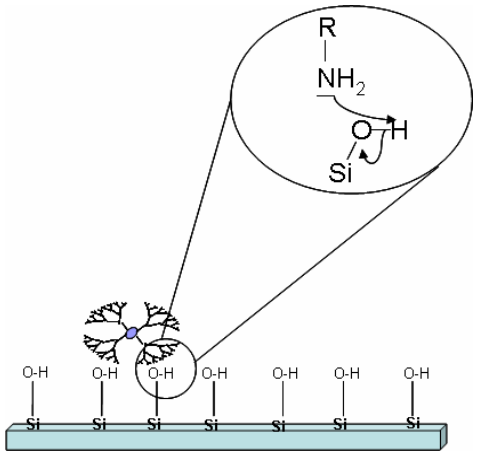

Figure 3-15 Surface chemistry of glass substrate and interaction with a PAMAM solution

3.9.2 J-aggregation of cyanines on PAMAM coated substrates

3.9.2.1 Characterization of myline1

Since most of our investigations are based on the cyanine myline1, some of its characteristics will be given. The cyanine myline1 is highly soluble in ethanol; however, the use of ethanolic (or methanolic) cyanine solutions never allowed us to prepare and characterize cyanine J-aggregates on PAMAM functionalised gold or glass substrates.

In contrast and as described below, when myline1 is dissolved in acetone, the formation of myline1 J-aggregates on PAMAM coated substrates could be demonstrated. This phenomenon could be explained by the presence of a few J-aggregate nuclei in acetone. Once adsorbed, these nuclei will progressively grow, and therefore promote and extend the J-aggregation process over the whole PAMAM monolayer (nucleation and growth mechanism). In order to evaluate the ability of PAMAM monolayers to self-organize myline1 into J-aggregates, optical characterization of pure and non-aggregated myline1 dissolved in acetone were first necessary.

In Figure 3-16 are showed absorption spectra of myline1 solutions with different concentrations. Concerning the supernatant, it was collected from the $7 \cdot 10^{-4}$M solution after 15 minutes centrifugation (25000 rpm, 25 °C).

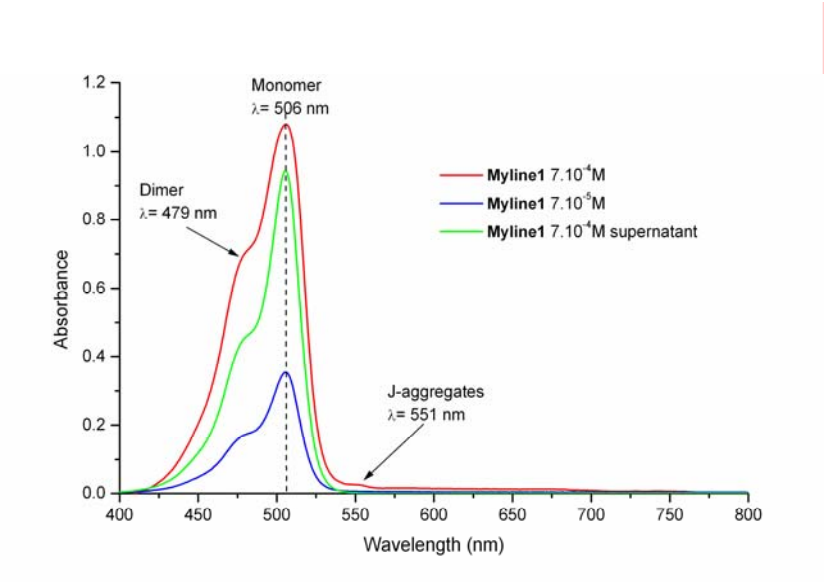

Figure 3-16 Absorption spectrum of myline1 in solution (solvent: acetone) as a function of concentration

In the absorption spectrum, shown in Figure 3-16 (red curve; [myline1] = $7 \cdot 10^{-4}$ M), three characteristic peaks could be detected at λ= 479, 506 and 551 nm. As already described in the literature[13], these 3 peaks correspond to the absorption by the dimer, the monomer and the J-aggregate, respectively. At $7 \cdot 10^{-4}$ M, the presence of some J-aggregate nuclei is observed while no aggregates were detected at lower concentrations. J-aggregation of the cyanine on top of the dendrimer layer is therefore expected to be favoured at $7 \cdot 10^{-4}$ M concentration. This minimum concentration has been maintained as a reference for the following experiments. Additionally, the emission properties of non aggregated myline1 were also investigated and are shown in Figure 3-17.

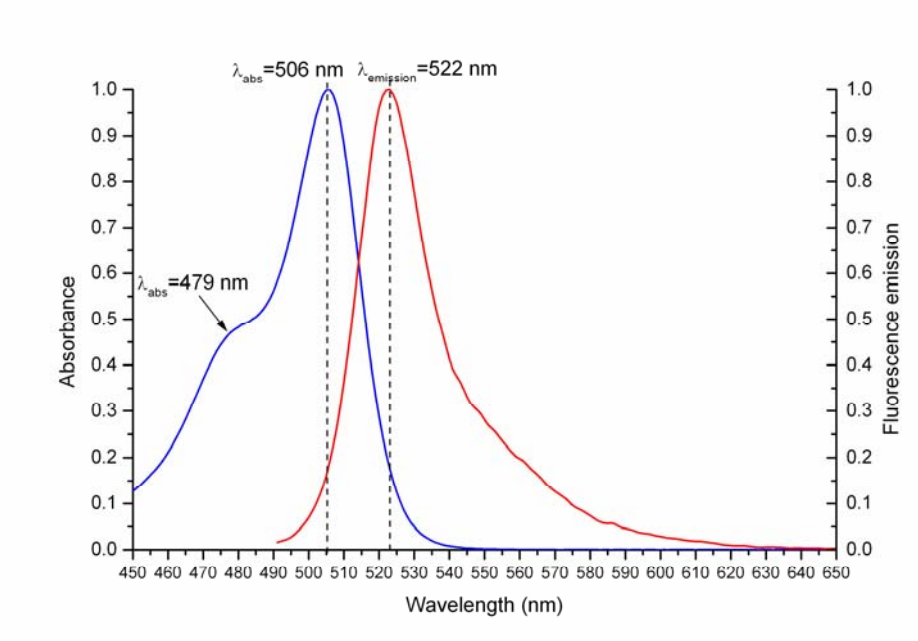

Figure 3-17 Absorption and emission spectra ($\lambda_{excitation}$=479 nm) of myline1 in solution (acetone) at concentration $7 \cdot 10^{-5}$M

To avoid potentially disturbing signals caused by the presence of J-aggregates in the emission spectra, such low concentrations of cyanine solutions have been used ([myline1] = $7 \cdot 10^{-5}$M). The emission is characterized by a relatively broad peak at 522 nm. Compared to the absorbance spectrum (λ_{abs} = 506 nm), a Stokes shift of 16 nm could thus be determined ($\lambda_{excitation}$ = 479 nm).

3.9.2.2 J-aggregation process on PAMAM coated gold substrate; influence of immersion time in myline1 solution on the J-aggregation process

After the functionalisation of initial gold substrates with a PAMAM G4 monolayer (see experimental section), the surface was acidified and then dipped into a myline1 acetone solution ($7 \cdot 10^{-4}$M) from 15 seconds to 12 minutes before being analyzed with a UV-Vis spectrophotometer. Spectra are shown in Figure 3-18.

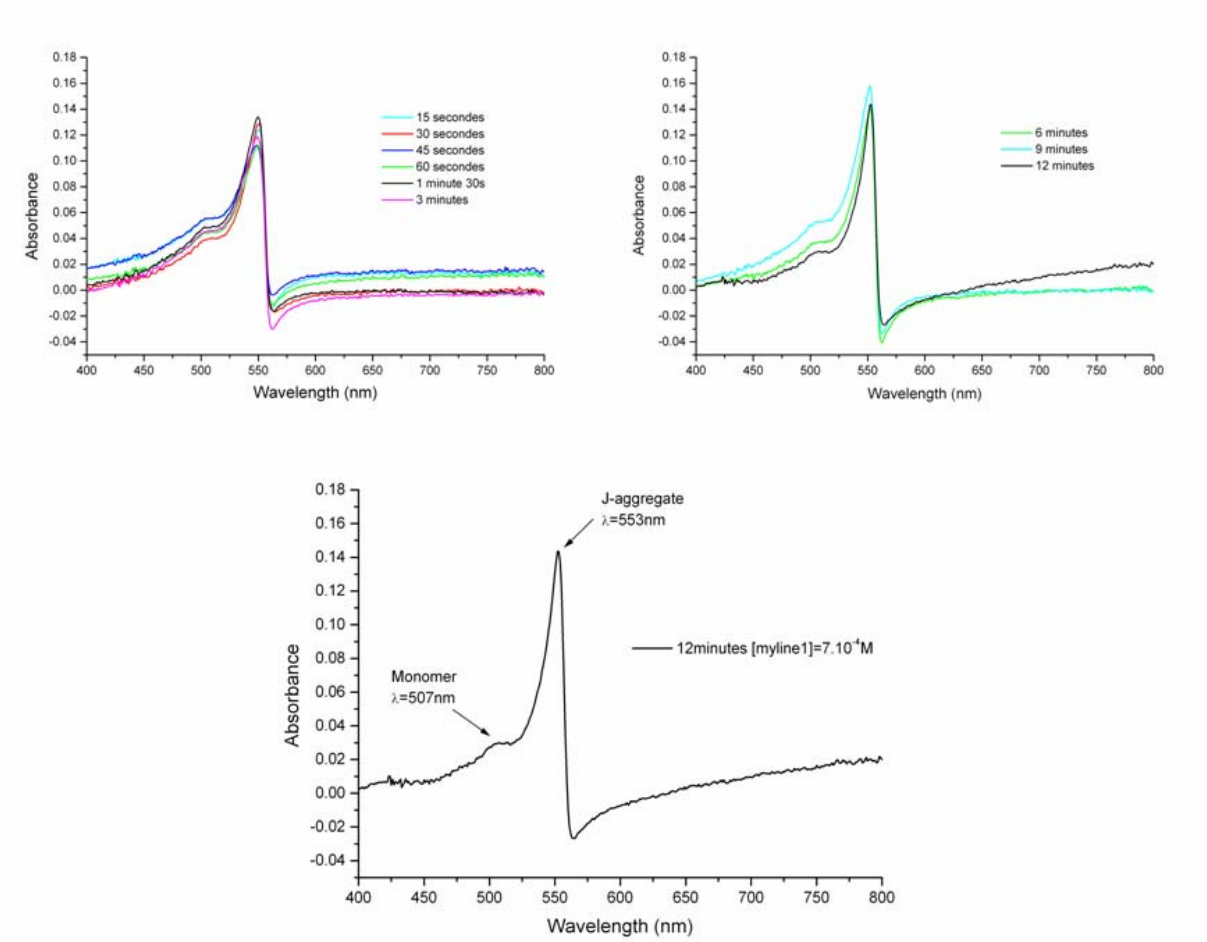

Figure 3-18 Absorption spectra of myline1 J-aggregate on G4-PAMAM coated gold surface as a function of the immersion time into cyanine solution (from 15 seconds to 12 minutes).

Compared to the spectra of non-aggregated myline1, the main observations are:

- Drastic decrease of the monomer absorption peak at λ_{abs} = 506 nm. The formation of a J-aggregate absorption peak at 549-552 nm (bathochromic shift) could already be detected after only 15 seconds immersion time.

- The absorbance of J-aggregates reaches a maximum (Abs max = 0.14±0.02) after 3 minutes of immersion; this value confirms the monolayer character of our myline1 J-aggregates already described by Steiger and Zbinden[13].

- The narrowest full width at half maximum (fwhm: 16 nm) is reached after 12 minutes immersion in myline1 solution.

- A negative absorbance is detected around 560 nm. We know from the Kramers-Kronig relation that a strong absorption peak has a corresponding strong modulation in

the real part of the refractive index, which reaches a maximum just on the long wavelength side of the absorption peak. This increase in the real part of the refractive index enhances the transmission through the Au-film and leads to the observed dip in absorbance. This was verified using a home-made program which allowed us to simulate the optical properties of our thin films.

We should insist here on the fact that all values (peak position, absorption maximum, fwhm) are in good agreement with previous results reported by Steiger and Zbinden[13] who described and characterized the formation of high quality myline1 J-aggregates by using Langmuir-Blodgett techniques and matrix oriented layers. However, the absorbance maximum is bathochromically shifted due to the different dielectric environment in the experiments presented by Steiger and Zbinden[13].

Moreover, the high quality of such self-assembled J-aggregates was confirmed after comparison of the absorption and emission spectra of the resulting Cyanine/PAMAM coating which demonstrated a low Stokes shift (4-5 nm shown in Figure 3-19).

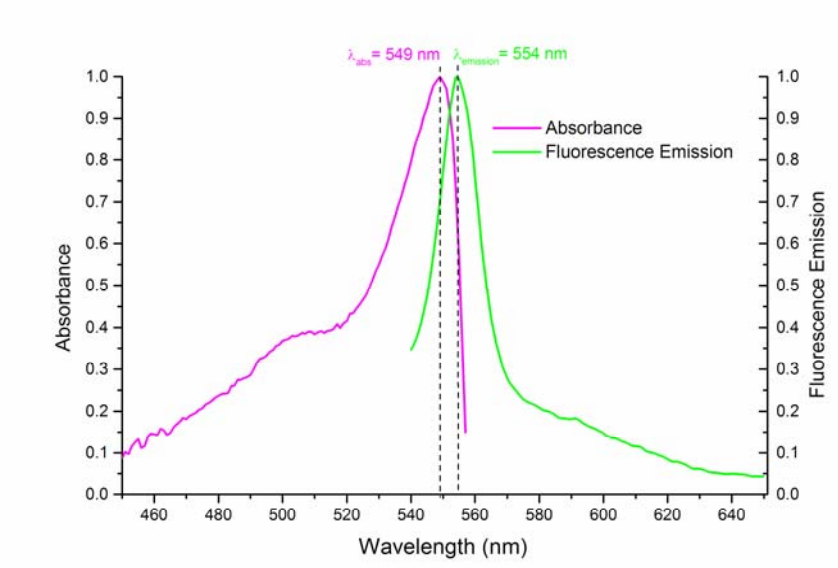

Figure 3-19 Absorption and emission ($\lambda_{excitation}$= 540 nm) spectra of myline1 J-aggregates onto G4-PAMAM coated gold substrate (normalized to 1.0 for comparison)

To further characterize PAMAM adsorbed monolayers on gold surface as well as cyanine J-aggregates on the dendrimeric layer, polarization modulation infrared

reflection absorption spectroscopy (PM-IRRAS) was used. This technique is well established for studying adsorbents on metal surfaces. The infrared light is reflected off a reflective surface rather than transmitted through the sample. With polarization modulation a higher sensitivity is achieved in order to analyse the chemical composition, configuration and conformation of very thin films and monolayers in the presence of an absorbing gas phase (Figure 3-20).

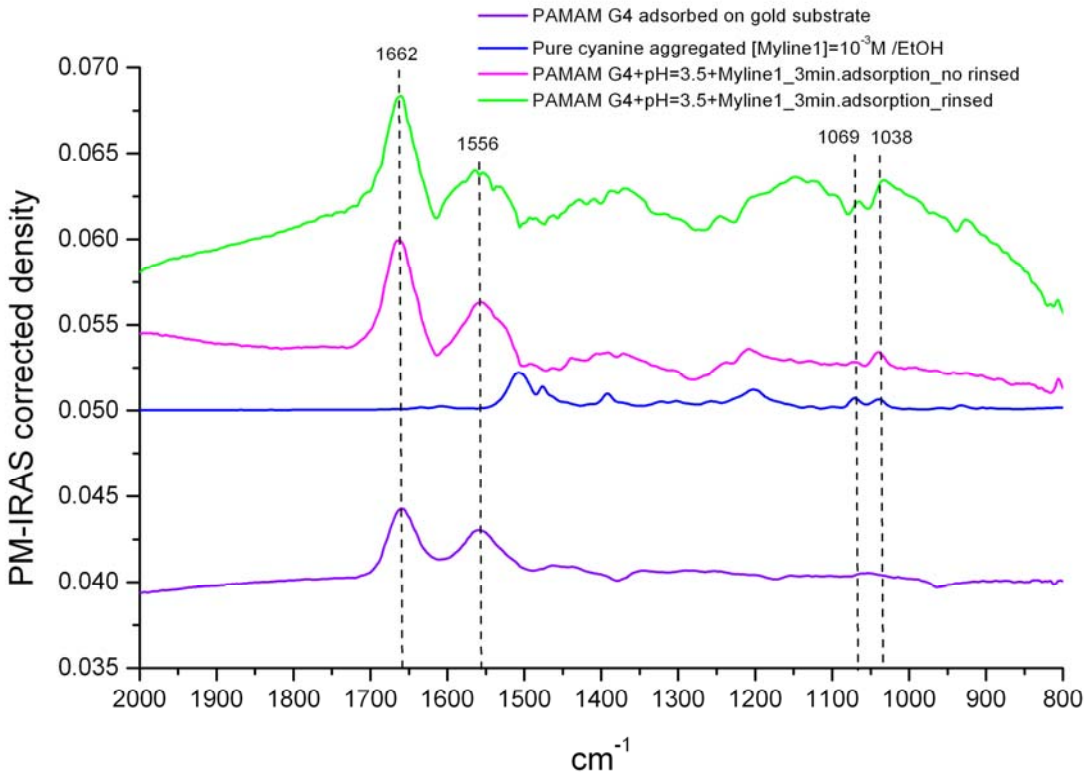

Figure 3-20 Polarization modulation infrared reflection absorption spectra (PM-IRRAS) on gold substrate coated with PAMAM G4 and cyanine (myline1). The spectrum with pure cyanine aggregated was measured by attenuated total reflection–FTIR (ATR-FTIR) on a germanium internal reflection element (control sample).

Adsorbed PAMAM monolayer onto gold substrate (violet curve) was first characterized by the presence of the strong amide I (carbonyl stretching) and amide II bands (C-N and N-H vibrations) at 1662 and 1556 cm^{-1} respectively.

The ATR spectrum of pure cyanine on Ge is indicated by the blue curve. The sample was prepared by evaporation of an ethanolic cyanine solution on the Ge internal reflection element and corresponds to a relatively thick film. Note that the spectrum was vertically scaled for comparison with the PM-IRRAS samples. The experimental conditions were determined for the formation of a J-aggregate, but the homogeneity in that case is not under control and the sample is expected to be randomly oriented. In the fingerprint region, characteristic peaks are observed at 1038 cm^{-1} and 1069 cm^{-1}, which are also observed in the pink and green (PM-IRRAS) spectra, but not in the PM-IRRAS spectrum of PAMAM on gold. The bands may be assigned to C-C or C-O vibrations.

When studying the PAMAM/cyanine J-aggregate system (pink and green curves) the following observations can be made:

- On the green (and pink) curve (Figure 3-20), both the signals due to PAMAM and cyanine are present. The main 4 peaks at 1662, 1556, 1069 and 1038 cm^{-1} were all detected. For the peak at 1556 cm^{-1}, a shoulder appears in the green and pink spectra. This band can be a combination of the signal at 1556cm^{-1} due to PAMAM and the signal at 1500 cm^{-1} due to the cyanine aggregated (blue curve).

- On the green and pink curves (Figure 3-20), the relative intensity of the amide I (1662 cm^{-1}) and amide II (1556 cm^{-1}) signals of PAMAM has changed with respect to the violet curve. Also the relative intensity of the cyanine signals has changed with respect to the blue curve.

The change in the relative intensity of the amide bands indicates a structural change of the PAMAM upon interaction with the cyanine. Furthermore, the change in relative intensity of the signals for cyanine at 1038-1069 cm^{-1} upon interaction with the gold/PAMAM surface points towards an orientation of the cyanine. Note that in the ATR experiment the cyanine is randomly oriented with respect to the surface (thick film). The relative intensity of the two bands therefore reflects the magnitude of the transition dipole moment of the corresponding vibrations. In the PM-IRRAS only the z-component of the transition dipole moment gives rise to a signal. The change in the relative intensity of two bands can therefore arise due to the different (average)

orientation of the corresponding transition dipole moments with respect to the surface normal.

These qualitative results show two important events. Firstly, the self-assembled structure (PAMAM /cyanine J-aggregate) is stable on the gold substrate. Secondly, cyanine and PAMAM interact strongly, leading to a deformation of the PAMAM and an orientation of the cyanine.

To complete our investigations, further measurements would be necessary to determine quantitatively the number of PAMAM functional groups adsorbed on the surface, and the way how cyanines are aggregated onto the dendritic matrix.

3.9.2.3 J-aggregation process on PAMAM coated glass substrates

In order to avoid fluorescence quenching phenomena on gold substrates, additional experiments were also performed on glass substrates. As for gold substrates, glass surfaces were first functionalised with PAMAM dendrimer, then dipped into a myline1 solution ($7 \cdot 10^{-4}$M, 3 minutes) before analyzing with a UV-Vis spectrophotometer (Figure 3-21).

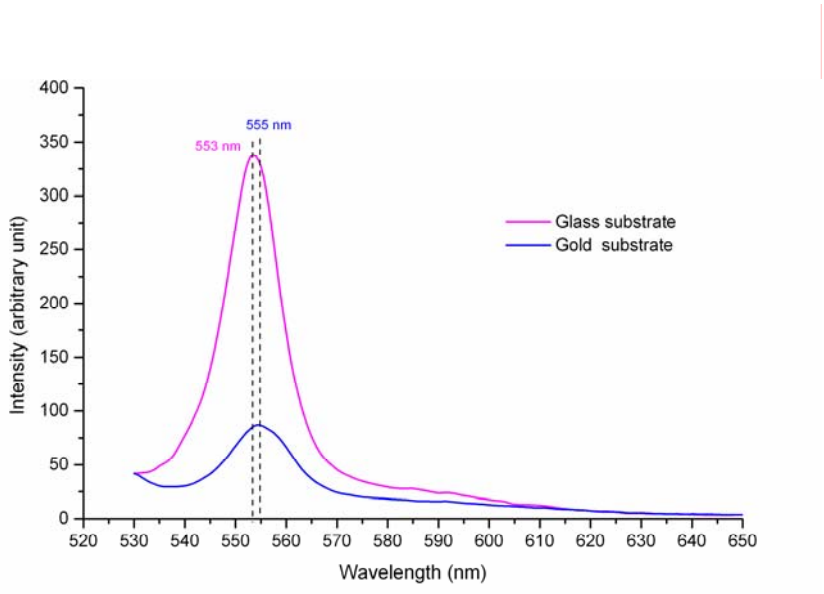

Figure 3-21 Comparison of fluorescence emission spectra of myline1 J-aggregated onto PAMAM G4 coating glass and gold substrate

As shown in Figure 3-21, the fluorescence intensity on gold is about 75% less than on glass substrate. Contrary to glass, gold has been shown to be an efficient electron acceptor for excited J-aggregates cyanines. In a previous work described by Khun *et al.*[61], an insulating fatty acid monolayer between the cyanine and the gold surface about 2nm ± 0.4 nm thick quenched the fluorescence to half its value as compared to the same assembly on glass. As it has been determined by XRD [60] the thickness of a G4-PAMAM monolayer is 1.8 nm ± 0.4 nm and we expected a fluorescence quenching of about 50%. The higher fluorescence quenching obtained in our experiments (Figure 3-21) is within error limits for the inverse exponential intensity-distance dependence expected for electron transfer.

J-aggregation experiments achieved onto glass substrates demonstrated once more the ability of predeposited PAMAM to assemble cyanines into well-defined J-aggregates characterized by a narrow full width at half maximum (17nm). A blank experiment when dipping a bare glass substrate (not coated with PAMAM) into myline1 solution has allowed us to confirm the crucial role of the PAMAM monolayer (Figure 3-22).

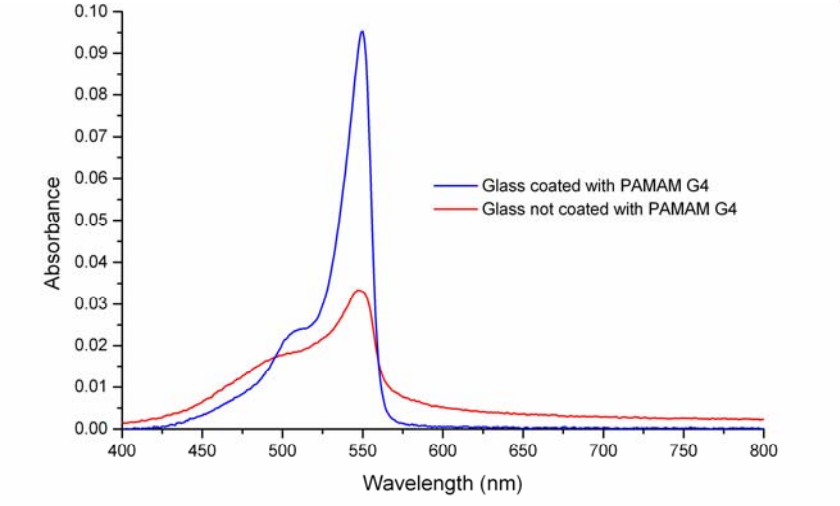

Figure 3-22 Absorption spectra showing the influence of PAMAM coating on J-aggregation phenomenom

As preliminary conclusion, all these results demonstrate clearly the propensity of PAMAM dendrimeric layers to behave as a highly functionalised platform which

enables the molecular organization of cyanine dye monomers into well defined J-aggregates. In absence of a predeposited PAMAM layer, the low absorbance value as well as the increase of the full width at half maximum demonstrates the poor definition of the resulting cyanine J-aggregates. Moreover, this flexible method, which is based on hierarchical self-assembly process, provides a new route for the formation of J-aggregated monolayer without multilayer formation within very short times and on different substrates.

3.9.2.4 Proposals for a mechanism of J-aggregation

As previously mentioned, the presence of J-aggregate nuclei in the initial cyanine solution seems to be crucial for the formation of well-defined J-aggregates onto the G4-PAMAM monolayer. A two steps nucleation and growth mechanism is therefore postulated for the J-aggregation process:

- Nucleation is promoted in solution by dissolving the cyanine in an appropriate solvent where the solubility is at its limits (acetone, concentration $\geq 7 \cdot 10^{-5}$M). Adsorption of a J-aggregate nucleus occurs at high-energy sites on the functionalised dendrimeric monolayer.

- Subsequent growth of the adsorbed nucleus occurs by diffusion of cyanine monomers from solution to the dendrimer surface. Defect-free growth of this J-aggregate nucleus is favoured by the highly perfect surface of a dendrimer nanoparticle, which itself is already highly ordered into a monolayer by adsorption on glass and on gold surface having only defects in the nanometer and sub-nanometer range[62].

Thus, the charges at the periphery of the PAMAM matrix are of primary importance. First, the positively charged end-groups of PAMAM (after acidification) strongly interact (attractive electrostatic forces) with the negatively charged cyanine which favours the adsorption of J-aggregate nuclei. This was confirmed when working with the positively charged cyanine show in Figure 3-23 which has a similar molecular structure as myline1 and which did not lead to J-aggregates when deposited onto protonated PAMAM monolayers.

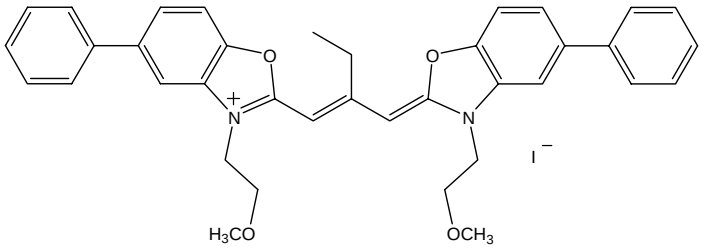

Figure 3-23 Chemical structure of [5, 5'-diphenyl-dibenzoxazolo-N, N'-propionate] 9-ethyl trimethine cyanine

On the other hand, J-aggregation was observed, in the same conditions as for myline1, with the following cyanine anion (Figure 3-24). When dissolved in acetone ([myline2] = $7 \cdot 10^{-4}$M) myline 2 monomer absorbs at 525 nm. The formation of a J-aggregate after 3 minutes of immersion time has been demonstrated by the presence of an absorption peak at 586 nm (bathochromic shift) with a full width at maximum equal to 20 nm. Compared to myline1, the fact that this cyanine presenting a different structure can still be aggregated in a controllable way by a PAMAM coated monolayer proves the versatility of such dendrimeric matrices for cyanine J-aggregation (Figure 3-24).

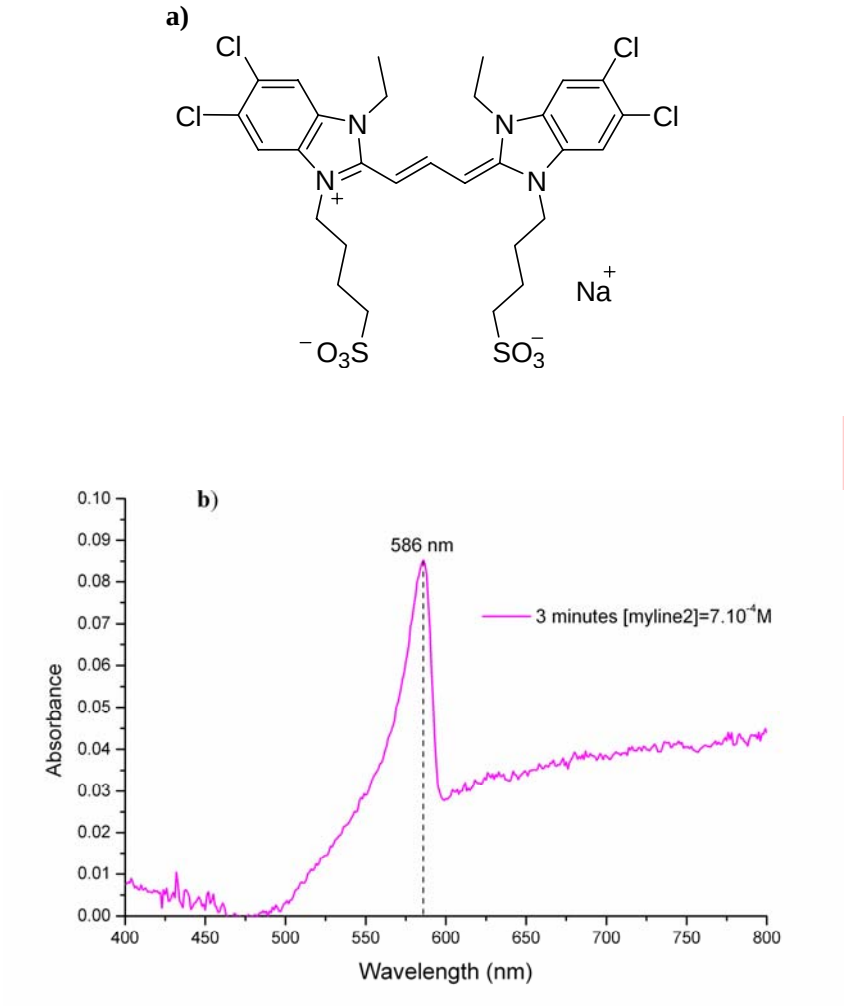

Figure 3-24 a) Chemical structure of [5, 5'-tetrachloro 1, 1'diethyl-dibenzoxazolo-N, N'-propionate-butylsulfonate] trimethine cyanine (myline2) b) Absorption spectrum of myline 2 J-aggregate on G4-PAMAM coated gold surface.

Moreover, the relatively high density of functional groups on the G4-PAMAM periphery may also promote nucleation as well as the mutual interaction between adsorbed cyanine molecules necessary for the growth of the aggregates (controlled mobility/diffusion for molecular self-organization).

Therefore, the possibility to tune the generation of the coated dendrimers is most interesting. Actually, this would allow us to modify the charge density on the PAMAM layer and to investigate thus how surface charge density may influence the J-aggregation process.

3.9.2.5 Influence of PAMAM generation on the J-aggregation process

The main goal here is to evaluate how the size, structure and surface charge density of the dendrimer can influence the formation of J-aggregates on the dendrimeric platform. The experiments have consisted in varying the dendrimer generation (G1, G4 and G6) and studying the J-aggregation of myline1 ([myline1] =$7 \cdot 10^{-5}$ M in acetone, dip-coating for 3 minutes) on surfaces functionalised with these dendrimers. Resulting absorbance spectra are shown in Figure 3-25.

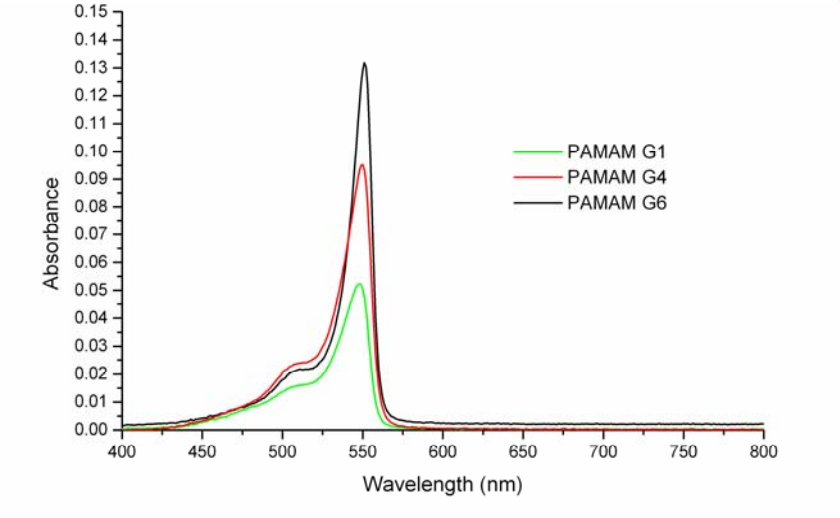

Figure 3-25 Absorbption spectra of myline1 J-aggregate on glass as a function of the PAMAM generation.

In contrast to adsorbed G4 and G6 PAMAM, surface functionalisation with G1 did not lead to the formation of high quality J-aggregates. This may be due to the much smaller number and surface density of amine functional groups on the G1 dendrimer periphery which may lead to a lower rate of surface functionalisation.

Additionally, as G1 adopts a flattened structure with most of the outer functional groups interacting with the surface, such G1 thin film show a lower reactivity for cyanine interactions.

Moreover, in order to better understand the influence of the dendrimer surface on J-aggregation some additional considerations on the geometry of deposited dendrimers have to be taken into account.

Atomic Force Microscopy (AFM, tapping mode) investigations on adsorbed PAMAM monolayers[63-66] give information on the dendrimer geometry when deposited on different substrates (gold or mica). Measurements in solution by dynamic light scattering demonstrated than the measured diameters are systematically larger than the molecular height in the adsorbed state as determined by AFM. This indicates that adsorbed molecules are no longer spherical but rather oblate when deposited on the surface (Figure 3-26).

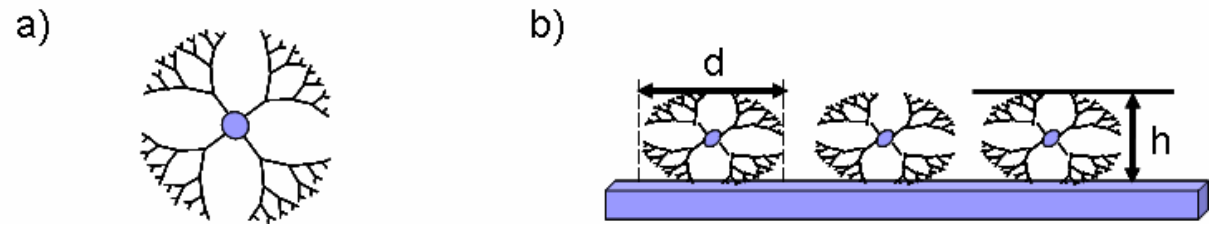

Figure 3-26 a) PAMAM dendrimer in solution: spherical shape b) adsorbed PAMAM: oblate structure

Tapping mode AFM investigations on G6-PAMAM monolayers adsorbed on mica has allowed one to determine a profile section of the deposited dendrimer corresponding to a molecule height (h) around 2.1 ± 0.2nm[63]. Based on AFM investigations[67] and mathematical considerations (elliptic representation of the dendrimer adsorbed on solid substrate) we can propose a calculation of the outer charge density on the dendrimer periphery (Table 1).

	Number of peripheric functions (½ Ellipse)	Diameter (d nm) AFM measurements	Height (h nm) AFM measurements	Outer Surface (nm^2) (Area of ½ Ellipse) $\pi\left[\frac{h^2(d/2)}{\sqrt{(d/2)^2-h^2}}\,arcsh\frac{\sqrt{(d/2)^2-h^2}}{h}+(d/2)^2\right]$	Surface density of functional groups (per nm^2)
G6	128	14	2.1	181.18	0.73
G7	256	21	2.1	378.77	0.68
G8	512	22	2.9	435.14	1.18
G9	1024	31	4.7	890.08	1.15

Table 1 Parameters such as outer surface and surface density of peripheric groups as a function of the adsorbed dendrimer generation under pH=1 (adsorbed onto mica) (AFM data described in the publication of Betley *et al.*[67])

Compared to the measured diameter in solution (6.7 nm), this value demonstrated the substantial distortion and flattening of the adsorbed molecule (-69%) which tends to maximize its interaction with the surface. For higher generations (G7-G9), similar investigations demonstrated that the height is increasing much faster when increasing the generation. This result suggests that the rigidity of deposited dendrimers increases significantly when increasing the generation. As expected from surface group dense packing considerations, dendrimers of high generations tend to become rigid as their periphery becomes highly populated and sterically crowded.

As a consequence, while a lower surface concentration of end-groups (compared to the theoretical maximum expected for close-packed lattice of spherical dendrimers) is expected for low generations (G1-G4) and highly distorted dendrimers, higher surface density of end-groups is expected with higher generations (>G4-G6) and globular

shaped PAMAM dendrimers. In our case, a higher density of amine groups is expected on G6 to G9-PAMAM functionalised substrates (than for G1 and G4).

Concerning the J-aggregation process on PAMAM functionalised surfaces, the influence of geometry and surface density is now quite well understood. While adsorbed high generation dendrimers (≥ G6) present a more spherical structure and a high density of end-groups both ideal for templating the formation of J-aggregates (charge density of myline1= 0.95), this is no longer the case with G1 which may adopt a much more ellipsoid flat conformation on the substrate as well as a much lower surface density of amine functions.

3.9.2.6 Influence of temperature on the J-aggregation process

These investigations have consisted in the formation of myline1 J-aggregates on G4-PAMAM and G6-PAMAM glass coated substrate at 40°C and 55 °C in comparison with J-aggregates formed at room temperature. The acetone solution of cyanine ([myline1] =$7 \cdot 10^{-5}$M) was warmed up (with a “water-bath”) and the temperature of the medium was controlled. Preliminary results obtained are shown in Figure 3-27.

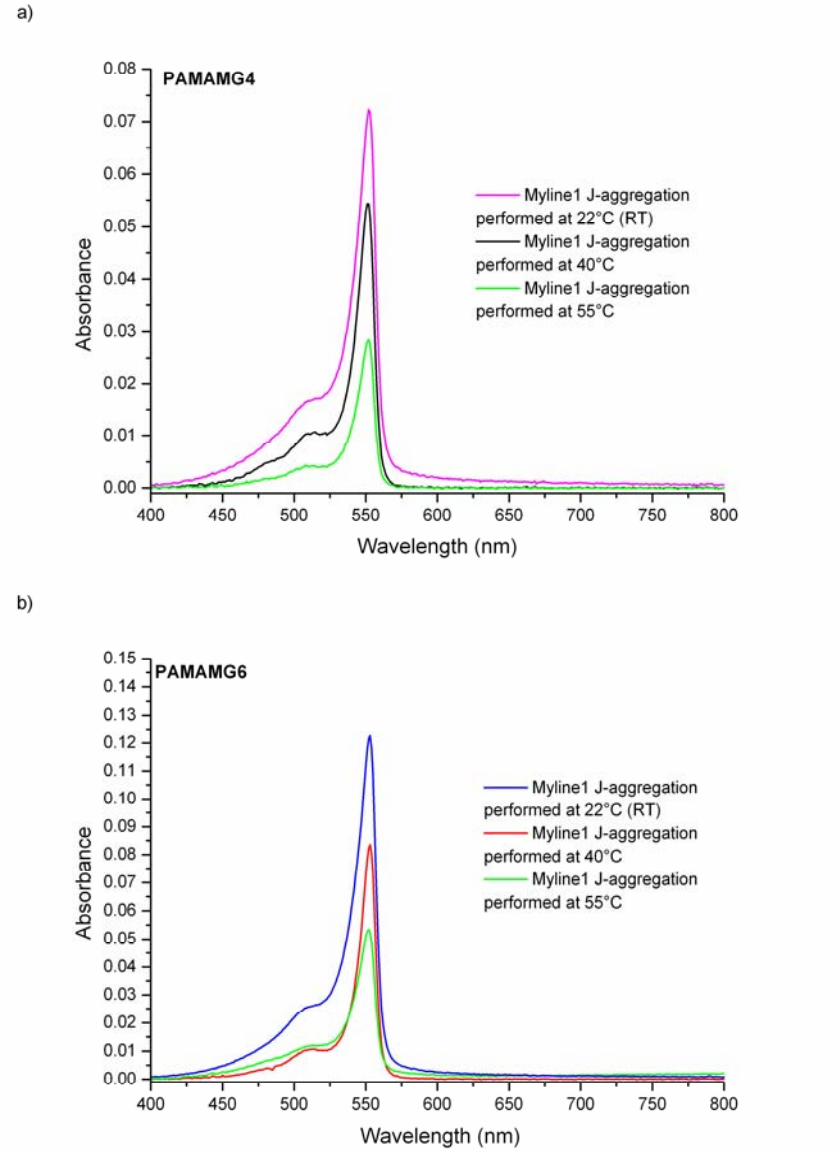

Figure 3-27 Absorption spectra of myline1 J-aggregates performed at different temperatures on a) G4-PAMAM glass coated substrate and b) G6-PAMAM glass coated substrate

Generally, the influence of temperature on the J-aggregation process does not depend on the dendrimer generation and could be detected in a similar way for both G4- and G6-PAMAM coated glass substrates. Compared to the spectra obtained at 22°C, the absorbance of J-aggregates prepared from 40°C cyanine solutions is slightly decreased (from 0.07 to 0.055 and from 0.12 to 0.085 for G4 and G6 respectively) but the full width at half maximum is considerably reduced (from 17 nm to 15 nm and from 18 nm to 13 nm for G4 and G6 respectively). These observations demonstrate that J-aggregation did not lead to a complete monolayer at this temperature; however better organised cyanine 2-dimensional structures could be obtained on the dendrimeric

matrix. On one hand, the increase of cyanine solubility at higher temperature may decrease the formation and adsorption of nuclei which allows the formation of a dense cyanine monolayer. On the other hand, the increase of temperature is expected to favour the diffusion and mobility of cyanine monomers, both needed to guarantee during the growth step the high ordering of J-aggregates. Concerning the low rate of J-aggregation observed at 55°C, it can be explained by fast acetone evaporation and a strong thermal agitation which did not allow the formation of well defined J-aggregates.

3.9.2.7 Comparison between PAMAM G4 and poly-lysine as templates for cyanine J-aggregation

In that context the aim here was to compare the self-assembly properties of dendrimers with poly-lysine and to evaluate for these two molecules their ability to self-organize cyanines into J-aggregates on surface (Figure 3-28). It as been reported that the morphology of such polyelectrolyte on solid substrate is linked to the molecular weight and the presence of salt , in solution, limiting the charges repulsion internal to the polymer random-coil structure[68,69]. In our experiments poly-lysine has been solubilized in Millipore water without salt addition. Poly-lysine coated glass substrates were characterized by AFM in tapping mode in ambient conditions (Annexes). AFM images show the presence of a 60 nm thick homogeneous layer on glass substrate. For the J-aggregation investigations on the poly-lysine control functionalized surface myline1 cyanine has been used according the J-aggregation process already described above ($7 \cdot 10^{-4}$M; 3 minutes).

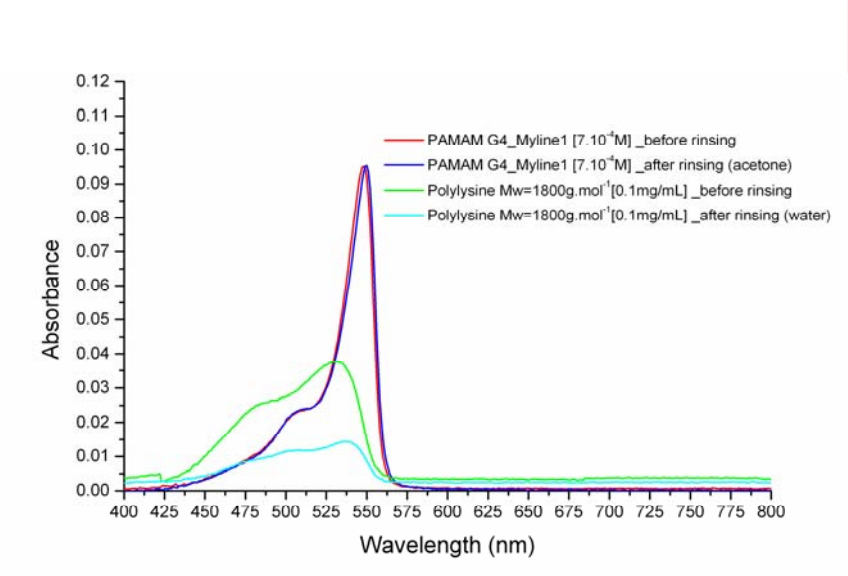

Figure 3-28 Comparison of absorption spectra of myline1 J-aggregation on G4-PAMAM and poly-lysine (Mw =1800g·mol^{-1}) coated glass slides

Compared to experiments on PAMAM layer, the main observations on poly-lysine layer are:

- Results are not reproducible, although weak J-aggregation on poly-lysine has been observed here and by other authors[70] .

- Drastic decrease and broadening of the absorbance peak corresponding to the cyanine J-aggregates

- The position of the absorbance peak characteristic of the formation of the J-aggregate is very poorly defined (λ: from 530 to 544 nm)

- Full width at half maximum could not be determined

- Absorbance is decreased and spectra are red shifted after rinsing which indicates the instability and some reorganisation of cyanine molecules at the surface

As an emphasis, while a PAMAM monolayer is a very efficient template for the formation of well-defined cyanine J-aggregates, poly-lysine layers never allowed us to obtain similar results. Additional experiments with higher molecular weights poly-lysine (Mw=9000 g.mol^{-1} and Mw=150000 g.mol^{-1}) and other cyanines were not successful either (Figure 3-29).

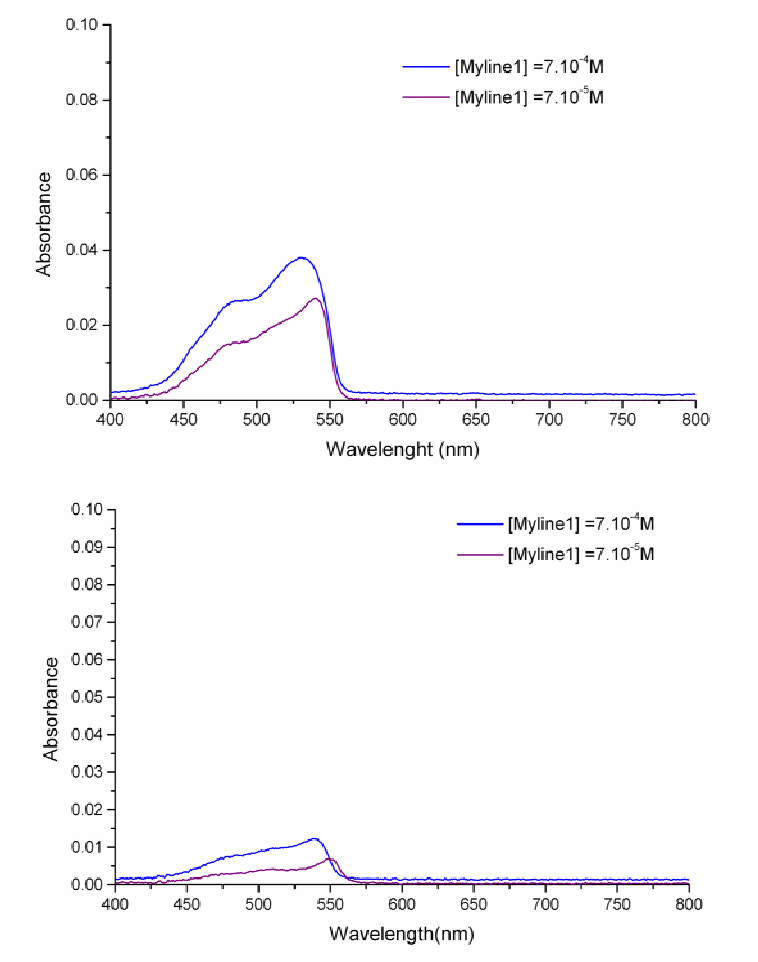

Figure 3-29 Absorption spectra of myline1 aggregation on Poly-L-lysine (Mw = 9000g.mol^{-1}) coated glass slides, before and after slide rinsing with cyanine solvent (acetone)

In contrast to classical polymers, dendrimers are particularly monodisperse, highly branched macromolecules with defined structure, shape, size and functionalities. All these advantages over randomly coiled polymers seem to be a key factor for a controlled and efficient cyanine J-aggregation process.

3.9.2.8 Stability in time of J-aggregates

In order to evaluate the potential of dendrimer/J-aggregate films in terms of applications, the stability of such systems in obscurity has been determined. In this paragraph, we will present the variation of absorbance of J-aggregates formed on glass substrates coated with different generations of dendrimers. Following the cyanine aggregation process, slides were kept at room temperature in darkness during several weeks before being re-analysed with a UV-Vis spectrophotometer (Figure 3-30).

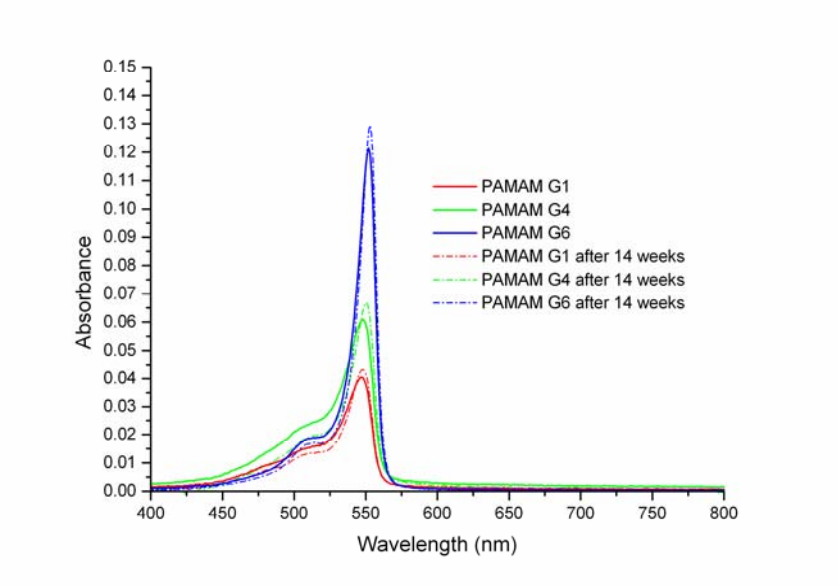

Figure 3-30 Variation of absorption spectra of J-aggregates formed on glass substrate coated with G1, G4 and G6 after 14 weeks

Generally, a slight increase of the absorbance values (around 5% for the different generations PAMAM coated glass substrate) as well as a reduction of the full width at half maximum could be observed for G1, G4 and G6 PAMAM on glass substrate. These observations confirm the high stability as well as the high quality (ordering) of the initial J-aggregates. The slight improvement with time of the J-aggregate quality can be explained by the presence of remaining solvent molecules between cyanine monomers into the initially formed J-aggregate which may disturb the growth of a highly well defined 2-dimensional J-aggregate. As a function of time the progressive evaporation of solvent may induce a structural improvement of the self organized molecules which results in the narrowing of the fwhm.

3.9.2.9 Stability of J-aggregates towards light exposure

In order to evaluate the stability of our system toward actinic light, J-aggregates formed on PAMAM coated glass substrates were exposed to the ambient daylight during 10 minutes, 30 minutes, and 1 hour (Figure 3-31).

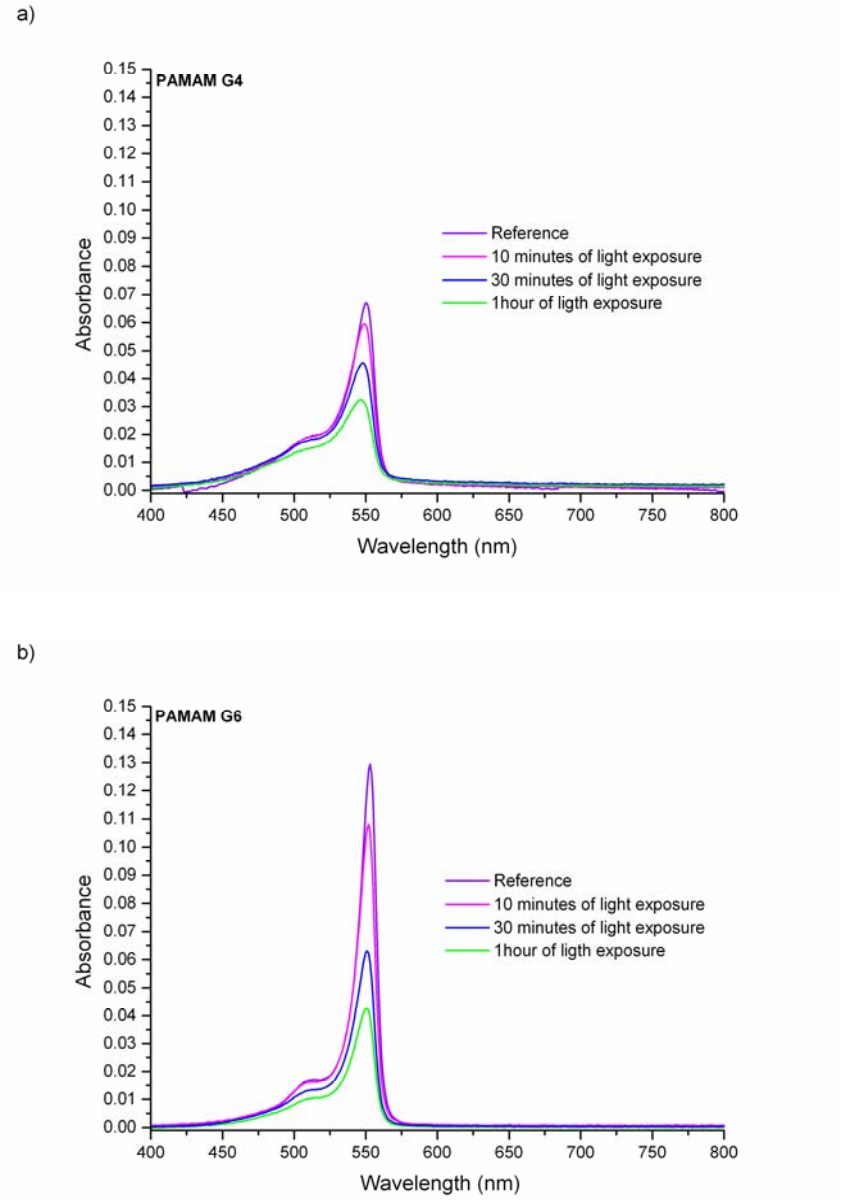

Figure 3-31 Absoprtion spectra showing the light stability of J-aggregates of myline1 formed on b) G4-PAMAM coated glass substrate and c) G6-PAMAM coated glass substrate in function of time exposure to daylight (around 100 Lux)

These experiments have shown that the half life of J-aggregates formed on G4-PAMAM coated glass substrate is equal to one hour. In comparison, the half life time of J-aggregate formed on G6-PAMAM is equal to 30 minutes. As already reported in literature, these observations confirmed that the higher the quality of the J-aggregate, the better the photochemical properties (higher absorbance and fluorescence intensity, lower Stokes shift) but the shorter the life time of the system due to strong photo-oxidative degradation.

3.9.2.10 First tests on fluorescence quenching by the electron acceptor paraquat

The following experiments have been carried out in order to evaluate and visualize potential electron transfer between an electron acceptor (paraquat) and excited cyanine J-aggregates. Whereas excited cyanines J-aggregates offer resonance fluorescence with high emission intensity, the presence of an electron acceptor (electron trap) on the cyanine monolayer is quenching the fluorescence of the J-aggregates. There is an electron transfer from the first excited singlet state (E1) of the J-aggregate to the unoccupied state (E1) of the electron acceptor, forming a free radical. In other words, measuring the fluorescence quenching may allow detecting the presence and the concentration of an electron acceptor.

Our first investigations were based on paraquat (1, 1'-dimethyl-4, 4'-bipyridinium or methyl viologen; Figure 3-32) as a very strong electron acceptor

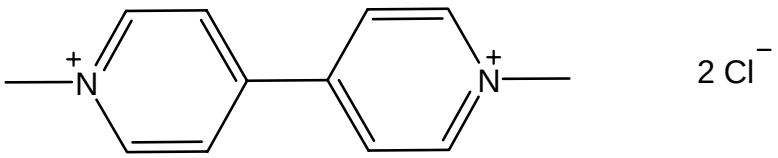

Figure 3-32 Chemical structure of paraquat (1, 1'-dimethyl-4, 4'-bipyridinium or methyl viologen)

Paraquat was widely used as an herbicide since it destroys plant tissue by disrupting the photosynthesis. Nevertheless, paraquat is acutely toxic and damages the lungs, heart, kidneys, adrenal glands, central nervous system, liver, muscles and spleen. As a tiny amount present in the body, paraquat can be lethal; even more problematic, there is no available antidote.

Detection of this molecule with a very high sensitivity is still an important challenge. Monitoring fluorescence quenching of myline1 J-aggregates in presence of paraquat was thus identified as a potential detection scheme.

Myline1 J-aggregates were first prepared on G4-PAMAM functionalised glass slides as described above. The resulting surfaces were then dipped for 1 hour into aqueous paraquat solutions with different concentrations. Slides were then excited at $\lambda_{excitation}$ = 510 nm and their fluorescence emission properties were recorded (Figure 3-33). One additional slide was dipped for 1 hour into water and was used as a blank.

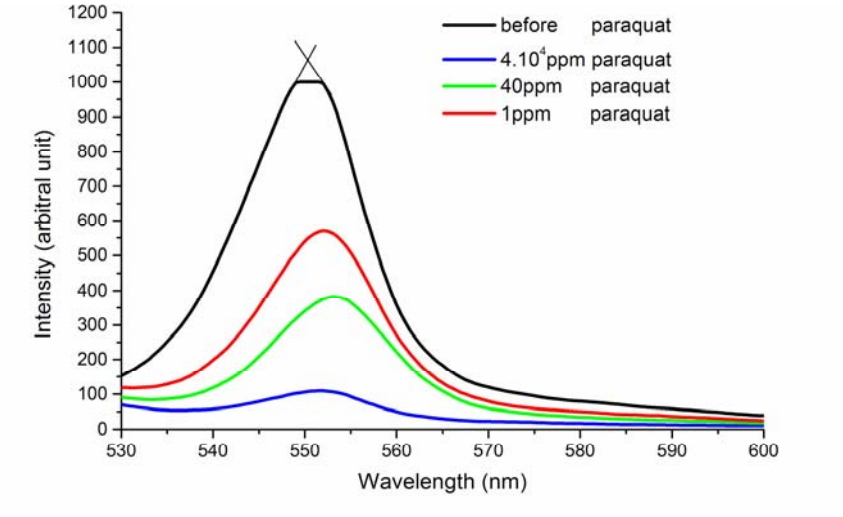

Figure 3-33 Extinction of myline1 J-aggregate fluorescence in presence of paraquat aqueous solutions ($\lambda_{excitation}$ =510 nm)

Figure 3-33 shows how the fluorescence intensity of preformed cyanine J-aggregates is dramatically decreased in presence of paraquat. As demonstrated here the detection of paraquat by monitoring the fluorescence quenching is achieved for concentrations as low as 1ppm.

3.10 Conclusions

In this chapter, a new method for the formation of well defined cyanine J-aggregates on dendrimer functionalised substrates has been reported.

This method is very versatile since it allows tuning the surface chemistry of the platform by changing the nature of the dendrimer (nature and number of the periphery groups, size and shape of the dendrimer). Moreover, the process can easily be adapted to different substrates (gold, glass, metal oxides). In order to improve the stability of the deposited dendrimer layer, alternative methods which result in the formation of covalent bonds between the dendrimer and the substrates are currently under investigations (e.g. via EDC coupling)

J-aggregation of cyanines on the dendrimer surfaces was described by a two step nucleation and growth mechanism. Moreover, our investigations have allowed us to demonstrate that the spherical shape and the high density of functional groups make dendrimers very good candidates for the self-organization of cyanines on surfaces. In contrast, this could not be achieved when functionalizing the substrates with polymers (e.g. poly-lysine, poly-ethylenimine) which generally do not present a highly defined monodispersity and geometry.

In terms of applications, we demonstrated the high stability at room temperature of our dendrimer/J-aggregate films as well as the possible use of such systems as sensors (detection of paraquat). Additional investigations will allow us to describe the huge potential of this system for light harvesting devices, photovoltaic cells or organic light emitting diodes.

3.11 References

[1] J. A. Tuszynski, M. F. Jorgensen, and D. Mobius, *Phys. Rev. E*, **1999**, 59, 4374

[2] H. Kuhn and C. Kuhn in T.Kobayashi "J-aggregates", World Scientific, **1996**

[3] S. Dähne, Bunsen Magazin, 2002, 81, 4

[4] F. Nuesch, J. E. Moser, V. Shklover, and M. Gratzel, *J. Am. Chem. Soc.*, **1996**, 118, 5420

[5] R. M. Jones, L. D. Lu, R. Helgeson, T. S. Bergstedt, D. W. McBranch, and D. G. Whitten, *Proc. Natl. Acad. Sci. U. S. A.*, **2001**, 98, 14769

[6] R. Gadonas in T.Kobayashi "J-aggregates", World Scientific, **1996**

[7] E. I. Mal'tsev, D. A. Lypenko, B. I. Shapiro, M. A. Brusentseva, G. H. W. Milburn, J. Wright, A. Hendriksen, V. I. Berendyaev, B. V. Kotov, and A. V. Vannikov, *Appl. Phys. Lett.*, **1999**, 75, 1896

[8] D. G. Lidzey, D. D. C. Bradley, A. Armitage, S. Walker, and M. S. Skolnick, *Science*, **2000**, 288, 1620

[9] A. Naber, U. C. Fischer, S. Kirchner, T. Dziomba, G. Kollar, L. F. Chi, and H. Fuchs, *J. Phys. Chem. B*, **1999**, 103, 2709

[10] G. Scheibe, *Angew. Chem.* **1926**, 49, 563

[11] E. Jelly, *Nature*, **1936**, 138, 1069

[12] R. Steiger, R. Kitzing, R. Hagen, and H. Stoeckli, *Chimia*, **1973**, 27, 660

[13] R. Steiger and F. Zbinden, *Journal of Imaging Science*, **1988**, 32, 64

[14] C. H. Tian, G. Zoriniants, R. Gronheid, M. Van der Auweraer, and F. C. De Schryver, *Langmuir*, **2003**, 19, 9831

[15] B. Herzog, K. Huber, and H. Stegemeyer, *Langmuir*, **2003**, 19, 5223

[16] J. Wullschleger and R. Steiger in J.R. Cox "Photographic sensitivity" Acad. Press, **1983**

[17] EU Patent 0437135A1

[18] US patent 6013430

[19] H. Fukumoto and Y. Yonezawa, *Thin Solid Films*, **1998**, 329, 748

[20] C. S. Peyratout, H. Mohwald, and L. Dahne, *Adv. Mat.*, **2003**, 15, 1722

[21] N. Kato, J. Prime, K. Katagiri, and F. Caruso, *Langmuir*, **2004**, 20, 5718

[22] R. Steiger, *Chimia*, **1994**, 48, 444

[23] R. Steiger, J. N. Aebischer, and E. Haselbach, *Journal of Imaging Science*, **1991**, 35, 1

[24] T. Sato, F. Tsugawa, T. Tomita, and M. Kawasaki, *Chem. Lett.*, **2001**, 402

[25] H. Kuhn, D. Möbius in "Physical methods of chemistry", 2nd ed. Vol.IXB, J.Wiley and sons, **1993**

[26] T. Sato, F. Tsugawa, T. Tomita, and M. Kawasaki, *Chem. Lett.*, **2001**, 402

[27] C. S. Peyratout, H. Mohwald, and L. Dahne, *Adv. Mat.*, **2003**, 15, 1722

[28] R. Steiger, *Helv. Chim. Acta*, **1971**, 54, 2645

[29] R. Steiger, *Chimia*, **1994**, 48, 444

[30] L. G. S. Brooker, G. H. Keyes, R. H. Sprague, R. H. Vandyke, E. Vanlare, G. Vanzandt, F. L. White, H. W. J. Cressman, and S. G. Dent, *J. Am. Chem. Soc.*, **1951**, 73, 5332

[31] L. G. S. Brooker, A. C. Craig, HESELTIN.DW, P. W. Jenkins, and L. L. Lincoln, *J. Am. Chem. Soc.*, **1965**, 87, 2443

[32] R. Steiger, R. Kitzing, and P. Junod, *Journal of Photographic Science*, **1973**, 21, 107

[33] R. Steiger, R. Kitzing, R. Hagen, and STOECKLI.H, *Journal of Photographic Science*, **1974**, 22, 151

[34] K. Minoshima, M. Taiji, K. Misawa, and T. Kobayashi, *Chem. Phys. Lett.*, **1994**, 218, 67

[35] H. Nakahara, K. Fukuda, D. Mobius, and H. Kuhn, *J. Phys. Chem.*, **1986**, 90, 6144

[36] T. Tani, M. Saeki, Y. Yamaguchi, T. Hayashi, and M. Oda, *Journal of Luminescence*, **2004**, 107, 339

[37] Y. Hamanaka, O. Kawasaki, H. Kurasawa, T. Yamauchi, Y. Mizutani, S. Kuroda, and A. Nakamura, *Colloids Surf. A*, **2005**, 257-58, 105

[38] H. Kuhn and C. Kuhn in T.Kobayashi "J-aggregates", World Scientific, **1996**

[39] H. Bücher and H. Kuhn, *Chem. Phys. Lett.*, **1970**, 6, 183

[40] V. Czikkely, H. D. Försterling, and H. Kuhn, *Chem. Phys. Lett.*, **2005**, 6, 11

[41] C. A. Hunter and J. K. M. Sanders, *J. Am. Chem. Soc.*, **1990**, 112, 5525

[42] R. Steiger, R. Kitzing, R. Hagen, and H.Stoekli, *Journal of Photographic Science*, **1974**, 22, 151

[43] J. I. Frenkel, *Phys. Rev.* **1931**, 37, 17

[44] R. Peirls, *Annal Phys.*, **1932**, 13, 905

[45] H. G. Wanier, *Phys. Rev.*, **1937**, 52, 195

[46] V. Czikkely, H. D. Försterling, and H. Kuhn, *Chem. Phys. Lett.s*, **2005**, 6, 207

[47] M. Matsumoto, *J. Photochem. Photobiol. A* , **2003**, 158, 199

[48] M. Matsumoto, T. Nakazawa, R. Azumi, H. Tachibana, Y. Yamanaka, H. Sakai, and M. Abe, *J. Phys. Chem. B*, **2002**, 106, 11487

[49] M. Lan and K. Ikegami, *Synthetic Metals*, **2003**, 137, 977

[50] D. Mobius, H. Bucher, H. Kuhn, and SONDERMA.J, *Berichte der Bunsen-Gesellschaft fur Physikalische Chemie*, **1969**, 73, 845

[51] L. Wolthaus, M. Gnade, and D. Mobius, *Adv. Mat.*, **1995**, 7, 453

[52] S. Kirstein and H. Mohwald, *Makromolekulare Chemie-Macromolecular Symposia*, **1991**, 46, 463

[53] S. Kirstein and H. Mohwald, *Adv. Mat.*, **1995**, 7, 460

[54] N. Kato, M. Yamamoto, K. Itoh, and Y. Uesu, *J. Phys. Chem B*, **2003**, 107, 11917

[55] T. Sato, F. Tsugawa, T. Tomita, and M. Kawasaki, *Chem. Lett.*, **2001**, 402

[56] H. Tokuhisa, M. Q. Zhao, L. A. Baker, V. T. Phan, D. L. Dermody, M. E. Garcia, R. F. Peez, R. M. Crooks, and T. M. Mayer, *J. Am. Chem. Soc.*, **1998**, 120, 4492

[57] D. C. Tully and J. M. J. Frechet, *Chem. Commun.s*, **2001**, 1229

[58] H. Ron and I. Rubinstein, *Langmuir*, **1994**, 10, 4566

[59] K. M. A. Rahman, C. J. Durning, N. J. Turro, and D. A. Tomalia, *Langmuir*, **2000**, 16, 10154

[60] V. V. Tsukruk, F. Rinderspacher, and V. N. Bliznyuk, *Langmuir*, **1997**, 13, 2171

[61] H. Kuhn, D. Möbius in "Physical methods of chemistry", 2nd ed. Vol.IXB, J.Wiley and sons, **1993**

[62] C. O'Dwyer, G. Gay, B. V. de Lesegno, and J. Weiner, *Langmuir*, **2004**, 20, 8172

[63] J. Li, L. T. Piehler, D. Qin, J. R. Baker, D. A. Tomalia, and D. J. Meier, *Langmuir*, **2000**, 16, 5613

[64] H. G. Abdelhady, S. Allen, M. C. Davies, C. J. Roberts, S. J. B. Tendler, and P. M. Williams, *Surf. Sci.*, **2004**, 558, 99

[65] K. H. Jung, H. K. Shin, Y. S. Kwon, and C. Kim, *Colloids Surf. A*, **2005**, 257-58, 191

[66] R. Pericet-Camara, G. Papastavrou, and M. Borkovec, *Langmuir*, **2004**, 20, 3264

[67] T. A. Betley, M. M. B. Holl, B. G. Orr, D. R. Swanson, D. A. Tomalia, and J. R. Baker, *Langmuir*, **2001**, 17, 2768

[68] R. Steitz, V. Leiner, R. Siebrecht, and R. von Klitzing, *Colloids Surf. A*, **2000**, 163, 63

[69] M. Dijkstra, R. van Roij, and R. Evans, *Phys. Rev. Lett.*, **1999**, 82, 117

[70] I. Place, T. L. Penner, D. W. McBranch, and D. G. Whitten, *J. Phys. Chem. A*, **2003**, 107, 3169

Chapter 4

Study of self-assembly properties of newly designed amphiphilic dendrimers as transport-vectors for cell transfection

4.1 Introduction: Gene delivery therapy

The technique of gene delivery was developed by biologists to efficiently deliver and express, foreign genetic material, commonly plasmid DNA, into the nucleus of host cells. Production of foreign proteins affords, for example, a therapeutic effect. The major issue of gene transfection remains however the transport process of DNA from the outside of the cell to the nucleus via the successive penetrations into the cell membrane, the cytoplasm and the nuclear membrane[1-3]. Biologists therefore need an efficient carrier, most often an engineered and attenuated virus unable to replicate. If viral vectors have already proven their efficiency and versatility for the transfection of the genetic material[4,5], safety problems and unpredictable immune response are still limiting their systematic therapeutic use[6]. To circumvent these drawbacks, new strategies have been developed towards the design of synthetic non-viral vectors, especially cationic lipids, cationic polymers[7,8], or amphiphilic block copolymers[9]. In this approach, DNA plasmids are first condensed by the cationic vectors, resulting in the formation of stable complexes. While naked DNA, with its high negative surface density charge is unable to cross biological membranes because of electrostatic repulsions to the negatively charged cell surface, complexation not only allows the reduction of the DNA surface charge but also minimizes its effective hydrodynamic radius[10]. Subsequent penetration of the polyplexe into the cell occurs via the formation of a vacuole, an endosome (internalization phase), followed by intracellular transport, endosomal escape, nucleus entrance and gene expression (Figure 4-1).

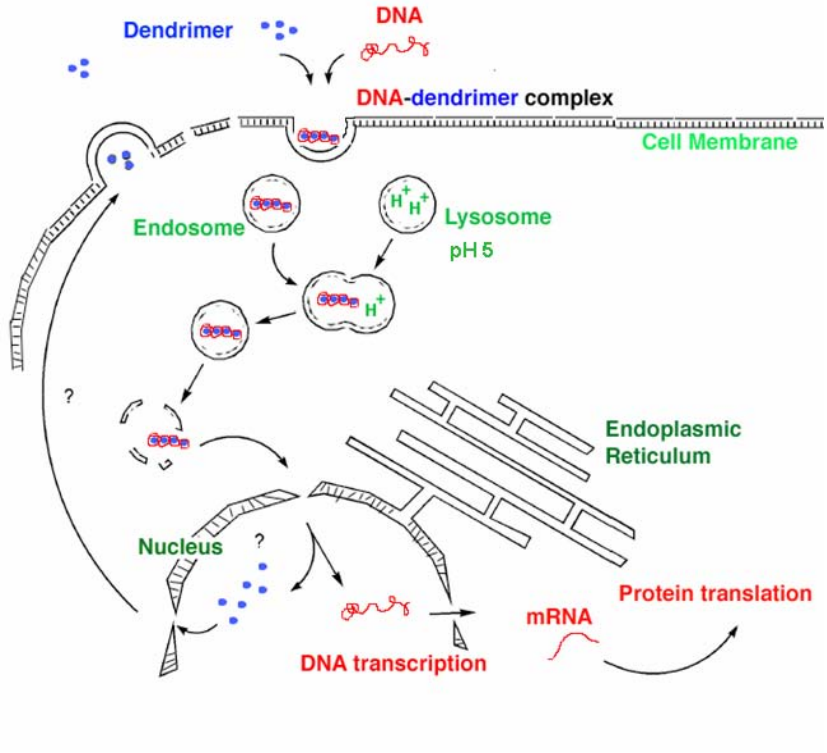

Figure 4-1 Gene delivery mechanism via non viral vector (The non viral vector described is a cationic dendrimer, but could be replaced by a cationic lipid (N-[1-(2,3-Dioleoyloxy)propyl]-N,N,N-trimethylammonium methyl-sulfate :DOTAP) or a polymer (Poly-ethylenimine :PEI))

Although the mechanisms by which such polyplexes are transported into the targeted cells are still not understood in detail, recent papers reported that endosomal escape could be facilitated by cationic vectors, typically protonated amines. Their buffering capacity protects DNA when vacuoles are progressively acidified. A pH drop occurs naturally in the compartments of living cells[11]. The resulting structural modifications of the polyplexe, such as swelling, favour a late endosomal escape[12] and the release of DNA close to the nucleus.

Contrary to classical polymers, dendrimers are monodisperse and hyperbranched macromolecules with precisely defined structure, shape, size and functionalities[13]. Their low toxicity, geometric tunability and controlled structure allows one to combine multiple cationic functionalisation and, together with self-assembling properties and making good candidates as transfection agents[14]. The first investigation with a particular dendrimer was made by Haensler and Szoka[15]. Using polyamidoamine

polymer (PAMAM) for the *in vitro* experiment, they showed that with a lower pKa than polylysine, this molecule could lower the cytoxicity by buffering the pH changes inside the endosomal compartment. Dennig[16] determined that PAMAM activated (irregular globular shape) dendrimer could enhance the gene delivery efficiency due to a higher flexibility allowing a better release of DNA from endosome. In this context, the design of a new class of amphiphilic dendrimers based on a rigid tolane (diphenylethyne) core and their activity as gene transfection vectors with structure-activity relationship[17] will be described (Figure 4-2).

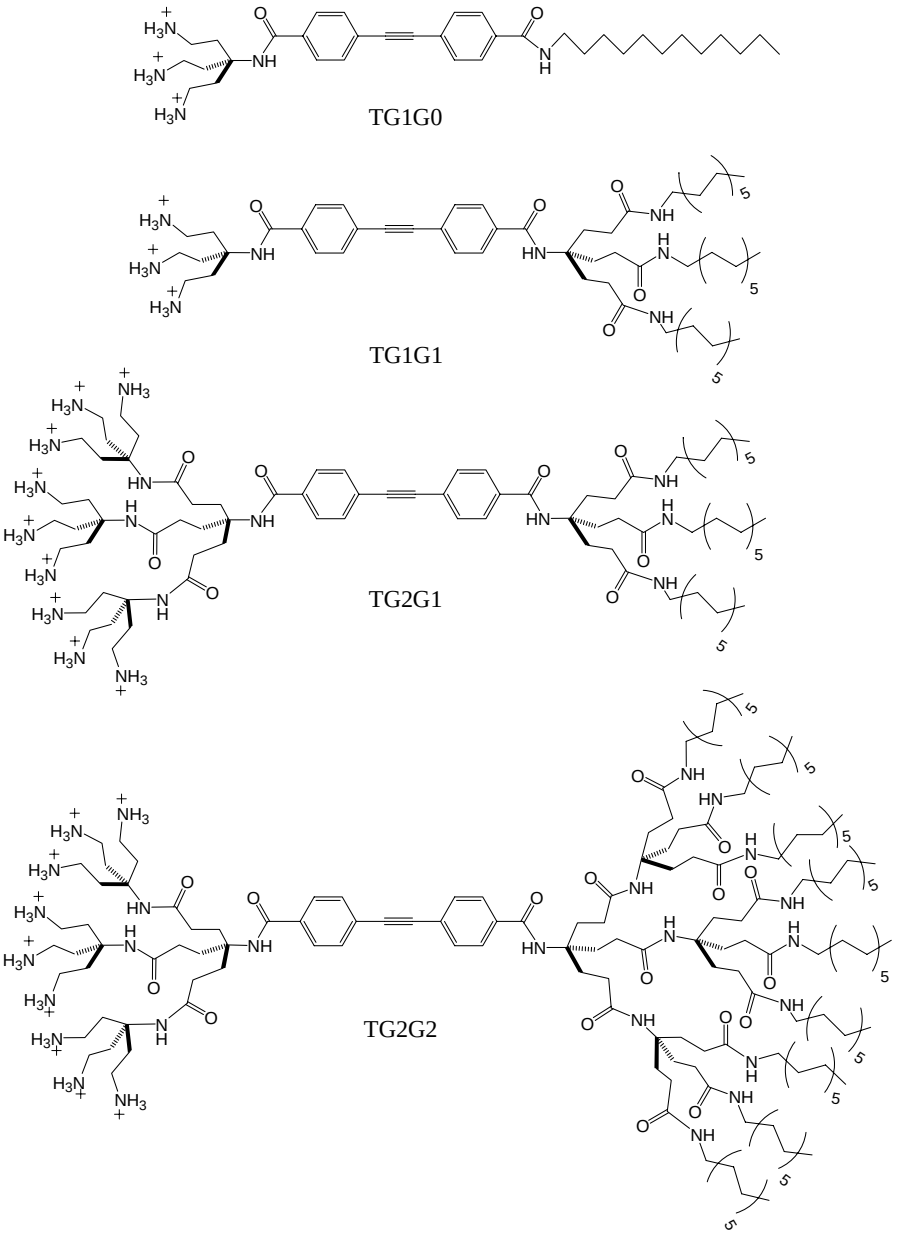

Figure 4-2 New amphiphilic dendrimers

In contrast to classical cationic dendrimers, a very strong influence of the lipophilic part of the dendron on the cell transfection efficiency has been demonstrated. In order to investigate the fundamental self-assembling properties of such amphiphilic dendrimers, the use of the Langmuir-Blodgett (LB) technique with the two compounds TG1G1 and TG2G1 (Figure 4-2), which have shown the highest efficiency as transport vectors for cell transfection.

By studying the surface pressure-area (π-A) isotherms on pure water subphase, the minimal area per molecule could be determined for TG1G1 and TG2G1. In order to simulate the pH changes which occur in living cells, the influence of the pH subphase has also been investigated. In both cases the (π-A) isotherm exhibits a strong pH dependence. Brewster angle microscopy (BAM) has been used for observation of the film homogeneity during its formation and for the determination of its optical thickness. The resulting Langmuir films have then been transferred onto solid substrates. X-Ray Diffraction (XRD) analysis has been used to determine the film thickness. The film stability and homogeneity have been studied by Atomic Force Microscopy (AFM). A qualitative study of the condensation properties of the amphiphilic dendrimers TG1G1 and TG2G1 with DNA has been also performed by LB and AFM. Additional cryogenic Transmission Electron Microscopy, investigations which allowed us to visualize the conformation of TG1G1/DNA plasmid polyplexes, are also reported.

4.2 Novel tolane based amphiphilic dendrimers: structure-activity relationship.

It has to be mentioned that concerning this part of the work, my personal contribution has mainly consisted of leading the Langmuir, SPM, and cryo-TEM investigations described below as well as taking an active part in very fruitful discussions with our partners for the interpretation of the biological results (collaboration within the NCCR Nanoscience network with ETH Zurich, Prof. Diederich – dendrimer synthesis, pharmaceutical assays; ETH Zurich, Prof. Merkle - pharmaceutical assays).

4.2.1 New amphiphilic dendrimers

As described in the introduction, and in order to avoid the drawbacks of viral vector, a new route for non viral gene therapy was recently opened. Recently, the synthesis of a novel class of cationic amphiphilic dendrimers has been described as promising non-viral gene delivery vectors for cell transfection[18](Figure 4-2). Such amphiphilic dendrimers were specially tailored to combine a high charge density and buffering capacity (hydrophilic part) with spontaneous self-assembly properties (lipophilic part), both necessary for the complexation and delivery of foreign genetic material in targeted cells.

Because of the presence of ammonium groups on their periphery, such amphiphilic dendrimers were expected to strongly interact and complex DNA. Protection of complexed DNA during pH change occurring within the cell is assured by the buffering capacity of the amine end-groups.

The presence of a triple-chained hydrophobic part may confer intrinsic self-assembly properties to such vectors, crucial for the penetration, transportation and release of the DNA into the nucleus. The rigid tolane linear spacer allows us to control the architecture geometry in space and therefore the self-assembly properties of the dendrimers.

The synthesis of these dendrimers was carried out at ETHZ using the convergent approach [17].

4.2.2 Amphiphilic dendrimers TG1G1 and TG2G1 as efficient transport vectors for cell transfection[17]

In collaboration with D. Joester, F. Diederich, E. Walter and H.P. Merkle, the ability of TG0G1, TG1G1, TG2G1, and TG2G2 to behave as efficient transport vectors for cell transfection via non-viral gene therapy has been investigated. Dye exclusion experiments were carried out in order to evaluate the potential binding affinity of the dendrimers to DNA. The experiments consisted of monitoring the fluorescence of Picogreen-DNA complex as a function of the concentration of added amphiphile. The

result was the progressive loss of fluorescence as the dye was displaced from its complex with DNA while the concentration of the amphiphile was progressively increased. By this method, a DNA binding affinity ranking could be established which demonstrated a very strong affinity of TG1G1 and TG2G1 while TG0G1 and TG2G2 did not interact as efficiently with DNA.

To complete these observations, the evaluation of the transfection efficiency (TE) of a defined transport vector was determined by the ratio of the number of cells that are transfected by a given amount of foreign genetic material (polyplexe DNA/vector) divided by the total number of cells submitted to the treatment. In practice, the cell transfection experiments have consisted of transfecting human embryonic kidney HEK293 cells with plasmid pGFP which encode the green fluorescent protein. After transfection, and once the GFP gene is expressed by the cell, the transfected cells may become fluorescent (Figure 4-3). After a 24h incubation time, treated cells were analysed with a fluorescence microscope and the number of transfected cells could be easily determined by simply counting those that were fluorescing.

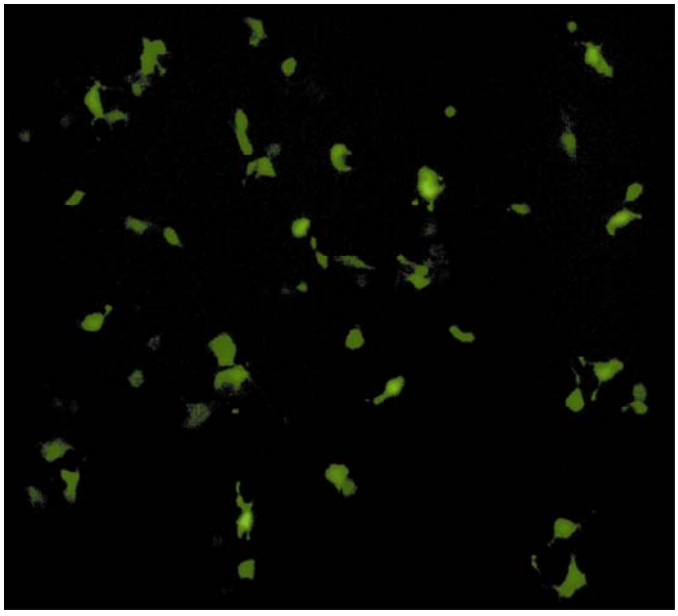

Figure 4-3 Fluorescence micrograph of HEK293 cells transfected with a polyplex prepared from pGFP and TG1G1 (Diameter of one cell is around 15-20μm)

By studying the transfection efficiency as a function of the dendrimer/DNA charge excess ratio (CE), strong maxima were obtained for dendrimers TG1G1 and TG2G1.

The charge excess is defined as the number of positively charged centers present in the protonate vectors divided by the number of negative charges carried by the DNA in the sample. Indeed, dendrimers TG1G1 and TG2G1 presented very high transfection efficiency respectively for CE=8-12 (c_{max}=20-30 μM) and CE=12-16 (c_{max}=10-15 μM) (see Figure 4-4). On the other hand, dendrimers TG0G1 and TG2G2 did not show any significant transfection activity.

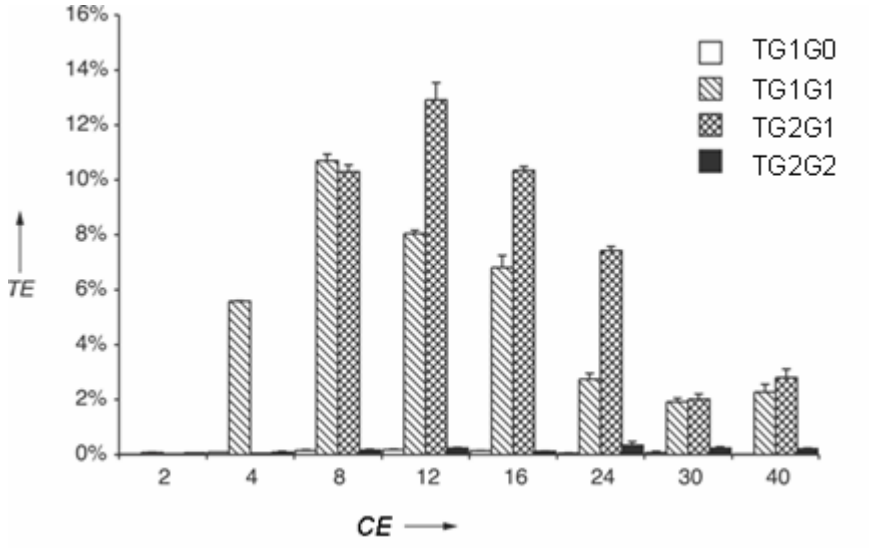

Figure 4-4 Transfection efficiency of TG1G0 to TG2G2 as a function of the charge excess ratio CE

As first conclusion and in agreement with dye exclusion experiments, it could be assumed that the influence of the hydrophobic dendron on the DNA binding and cell transfection efficiency was much stronger than anticipated. The self-assembly properties defined by the lipophilic dendritic side of the amphiphile dominate the transfection activity as can be seen through the comparison of the two dendrimers with identical hydrophilic dendron (TG0G1 vs. TG1G1 and TG1G1 vs. TG2G1). Alternatively, if the hydrophobic dendron is influencing the size, the shape as well as the solubility properties of the dendrimer (c_{max} of TG2G1 is one half the value of TG1G1), it does not significantly influence the transfection efficiency. A dendrimer structure with three lipophilic chains is thus strongly favoured for reaching high transfection efficiency (TE).

It should also be mentioned that these first results were all the more promising as the maximal TE values of TG1G1 and TG2G1 were found to be twice larger than those of commercially available vectors (DOTAP: cationic lipids, PEI: cationic polymer, Superfect: dendrimer) as shown in Figure 4-5. Moreover, the cytotoxicity of TG1G1 and TG2G1 in the optimum CE range (8-16) was found to be low.

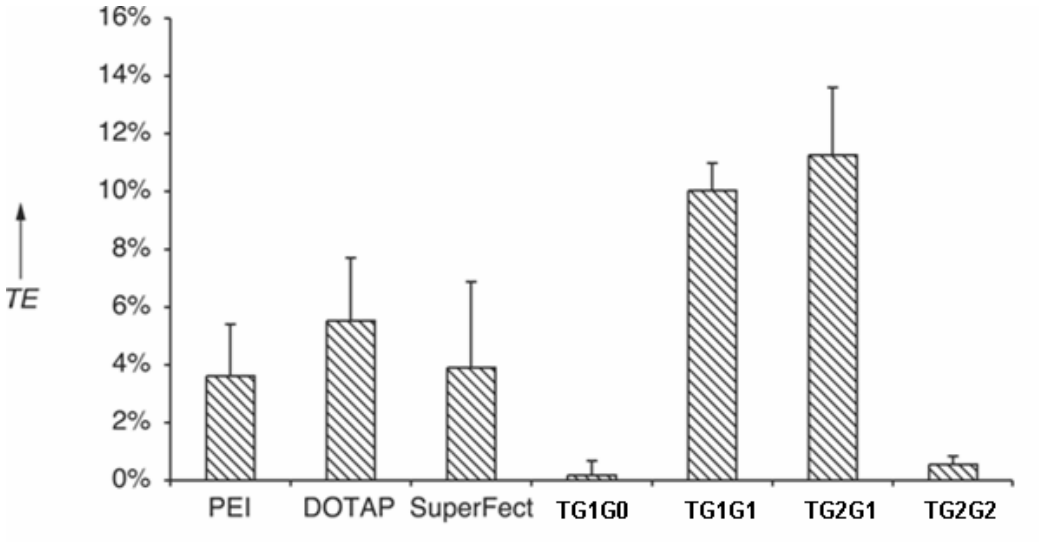

Figure 4-5 Maximum TE of TG1G0 to TG2G2 at optimum conditions are compared to reference commercial non viral vectors PEI, DOTAP and Superfect

Extension of this work has been undertaken at ETHZ to design new dendrimers (to evaluate e.g. how the tuning of the length of the rigid tolane spacer may affect the self-assembly properties and thus the TE; by the introduction of additional functionalisation into the lipophilic dendron in order to control endosomal escape).

At CSEM, our researches were extended to Langmuir techniques, Atomic Force Microscopy (AFM) and Transmission Electron Microscopy (TEM) in order to better understand and control the relationship between dendrimer structure, intrinsic self-assembly properties and activity for cell transfection.

4.2.3 Langmuir films: structural studies of TG1G1 and TG2G1 Results and Discussion.

Compound TG1G1 dissolved in $CHCl_3$ was first spread onto water subphase. After the rapid solvent evaporation and a 30 minutes equilibration period, Brewster Angle

Microscopy has been performed in order to study the homogeneity of the initial layer before compression. As shown in Figure 4-6a, this revealed the presence of a 2D foam at the water/air interface, indicating clearly that the deposited molecules have a tendency to form a condensed phase, contrary to more classical amphiphiles which form a gas phase at low surface pressure. As already described in the literature[19-21], this phenomenon is due to intermolecular attractive forces such as hydrophobic and/or Van de Waals interactions induced by the presence of alkyl chains. Once the compression was started, BAM monitoring allowed us to image the progressive formation of an homogeneous and dense monolayer (Figure 4-6). At the end of the compression, the film is homogeneous (the fringes that can be seen are artefacts due to the coherent lighting). The initial 2D foam is recovered after progressive decompression of the film (Figure 4-6d); the compression-decompression process is thus reversible. The AFM studies (see below) performed on monolayer transferred onto silicon bring another proof that the Langmuir films are nearly defectless.

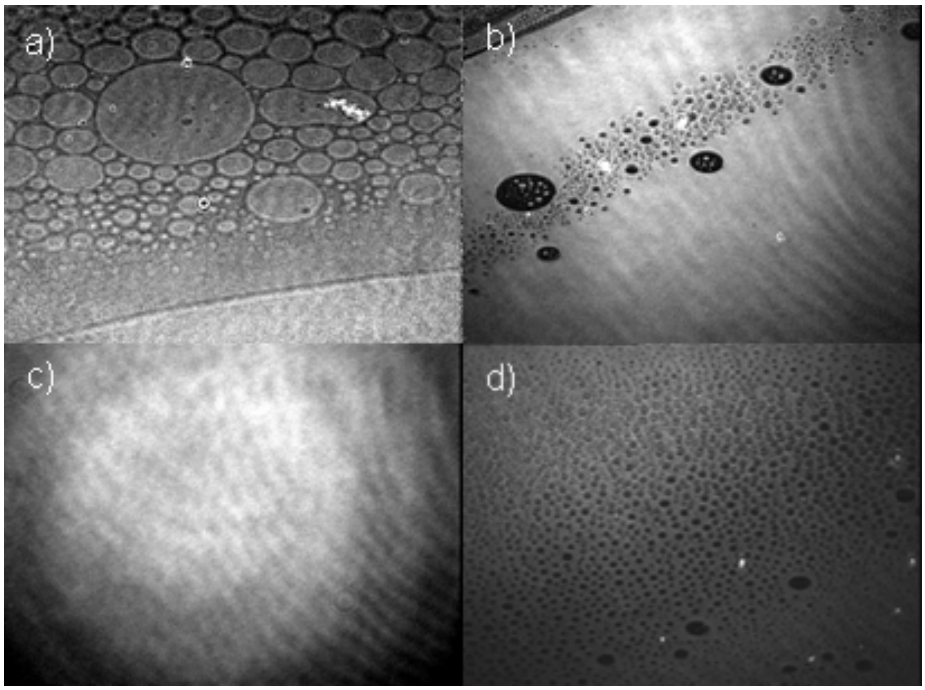

Figure 4-6 a), b), c), d). BAM images (500μm×600μm) of TG1G1 at minimal area per molecule a) 110 Å^2 b) 90 Å^2 c) 75 Å^2 d) 105 Å^2. These images show the formation of foam at very low pressure and the ultimate formation of a homogeneous Langmuir film upon compression

This reversible behaviour has been confirmed by recording surface pressure-area (π-A) isotherms during successive compression and decompression cycles (Figure 4-7). The surface pressure starts to increase around 110Å^2 per molecule, and then steadily increases until the collapse of the film at 47mN.m^{-1}. The film remains in a liquid-condensed state until the collapse, without any phase transition to a solid state. Upon decompression the behaviour of the film is reversible.

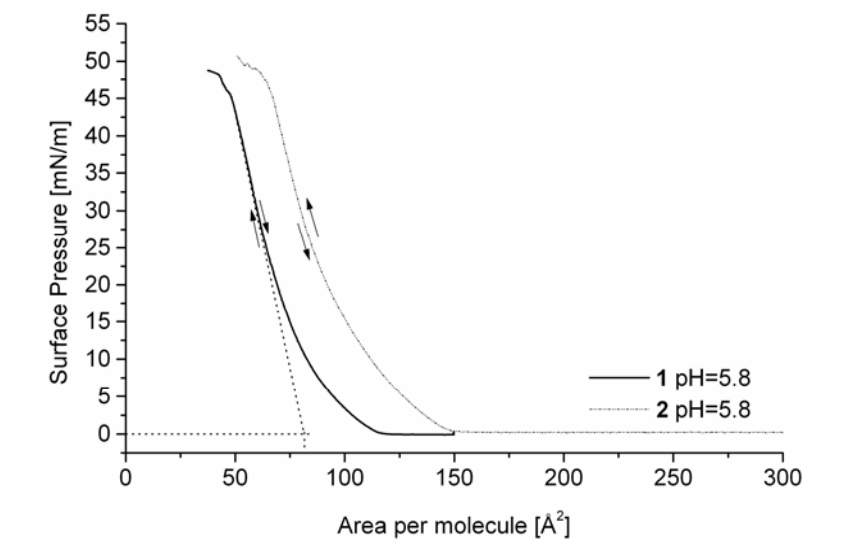

Figure 4-7 Comparison of the surface pressure-area (π-A) isotherms of TG1G1 and TG2G1 on water subphase

Extrapolation to zero surface pressure of a handling line tangent to the final part of the isotherms afforded a minimal area per molecule of 80 Å^2 ± 8 Å^2 for TG1G1. Such a value implies that once compressed and densely packed the molecules should be almost perpendicular to the air-water interface and that their packing is essentially limited by the steric hindrance and self-assembling properties of their three lipophilic alkyl chains. Brewster angle microscopy also enables an estimation of the Langmuir film thickness through the measurement of the intensity of the reflected light. Assuming a refraction index of 1.45 for the Langmuir film in its compressed state, its thickness has been determined to be around 35Å. Molecular modelling with ViewerLite4.2 (Accelrys) giving a maximum length of about 38Å for a fully extended

molecule, the perpendicular configuration of TG1G1 to the interface at the end of the compression is confirmed.

The thickness of the film has been also, indirectly confirmed by X-Ray Diffraction studies (Figure 4-8).

A monolayer transferred onto a hydrophilic Si <100> substrate with a transfer ratio of 1.0 has been analyzed and its thickness found to be 32.5 ± 2.6 Å. The fact that the transfer ratio is 1.0 implies that no or minor molecular reorganization took place during the transfer and so the thickness of the LB film should be close to that of the film on water.

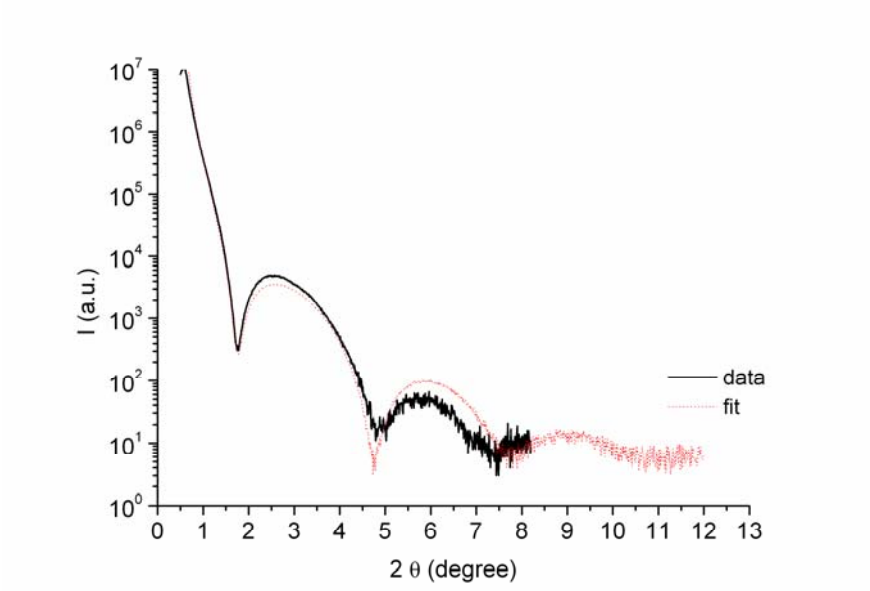

Figure 4-8 X-Ray diffraction analysis of TG1G1 LB-film transferred onto Si <100> at π= 25mN·m^{-1} with a unity transfer ratio

AFM investigations on a monolayer LB film of TG1G1 transferred from pure water (Figure 4-9) corroborate the film thickness determined by XRD and demonstrate that the resulting film is mostly free of any structural defect (aggregates, holes or cracks). A statistical analysis of the image gives a Root Mean Square (RMS) roughness of 0.180 and 0.09 nm on Si (100) and Mica respectively, confirming the good quality of the transferred film.

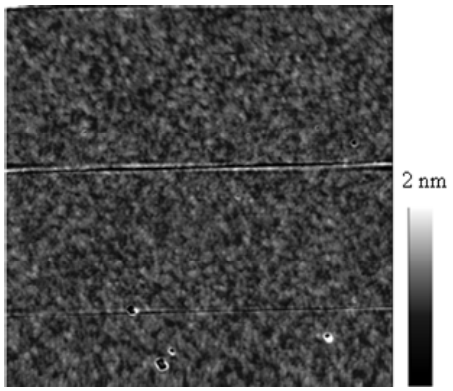

Figure 4-9 Tapping mode AFM image (1µm×1µm) of a monolayer of TG1G1 transferred onto silicium<100> with a unity transfer ratio

Compound TG2G1 which presents a hydrophilic dendron containing nine peripheric amine functions has been studied in a similar way, in order to evaluate the influence of the polar head groups on the self-assembling properties. The compression isotherm on pure water (Figure 4-7), is nearly identical to that of TG1G1 except for a shift towards larger molecular areas. Similarly to those of compound TG1G1, the isotherms of TG2G1 are reversible and the collapse pressure around $47 mN \cdot m^{-1}$. The surface pressure starts to increase around a minimal area per molecule of $150 Å^2$ and the final molecular area is $110 Å^2 \pm 11 Å^2$. Compared to those of TG1G1, this larger value indicates that the process limiting the molecular packing is different. This had to be expected as the second generation polar head is now much larger. The steric and electrostatic forces between polar heads of adjacent molecules must limit the compression. In order to compensate the larger molecular area, the tolane core and the alkyl chains are necessarily tilted.

BAM observations have also been performed during the formation of the films (Figure 4-10). The images collected are very similar to theses taken for TG1G1, the main difference being the presence of bright "spots" in the films. These highly reflective domains could either be defects or, more probably, some kind of supramolecular organization, e.g. micelles[22]. This phenomenon would potentially originate in the pronounced conical shape of TG2G1 which may favour the formation of this type of aggregates.

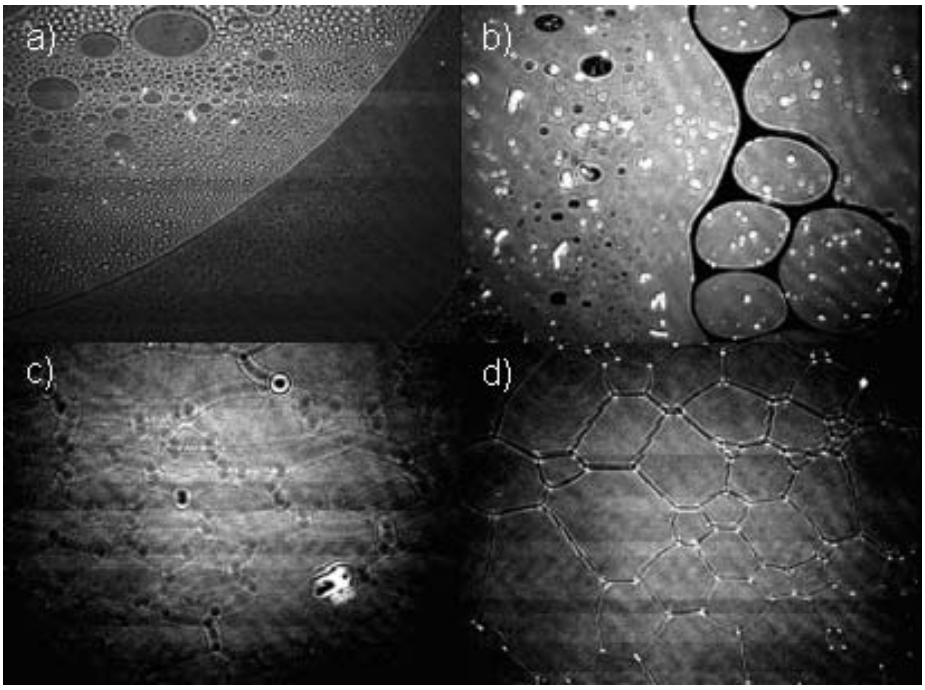

Figure 4-10a, b, c, d BAM images (500µm×600µm) of TG2G1 at minimal area per molecule a) 150Å^2 b) 130Å^2 c) 102 Å^2 d) 108Å^2

In order to determine the optical thickness of the LB-film in its compressed state, additional BAM measurements were performed. Unfortunately, these measurements confirmed the presence of dendrimer TG2G1 supramolecular structures and therefore the non homogeneity of the LB film. No stable reflectivity intensity could be recorded, so no significant value for the thickness of the film could be determined. We were no more successful with XRD measurements which confirmed the high propensity of TG2G1 to self-reorganize during the film transfer.

In contrast to TG1G1, the balance between hydrophilic head and hydrophobic tail of TG2G1 does not allow the control of the formation of a homogeneous monolayer at the air/water interface as well as the transfer of a homogeneous LB film onto different substrates.

Langmuir films: pH and complexation studies

In relation to our previous cell transfection experiments, the influence of pH on the self-assembling properties of TG1G1 and TG2G1 has also been investigated. Inside cells, significant drop of the pH value from pH=7.4 in the physiological medium to

pH~4-5 in lysosome has already been reported[23,24]. The influence of pH on the different internalization and transport mechanisms occurring during cell transfection is therefore considerable; the study of the pH influence on the self-assembly properties of the transfection agents thus becomes crucial. The pH of the subphase has been adjusted at 3.0 with trifluoro acetic acid (TFA) before the dendrimer was deposited on water. Under such acidic conditions, the protonation of all peripheric amines functions was expected.

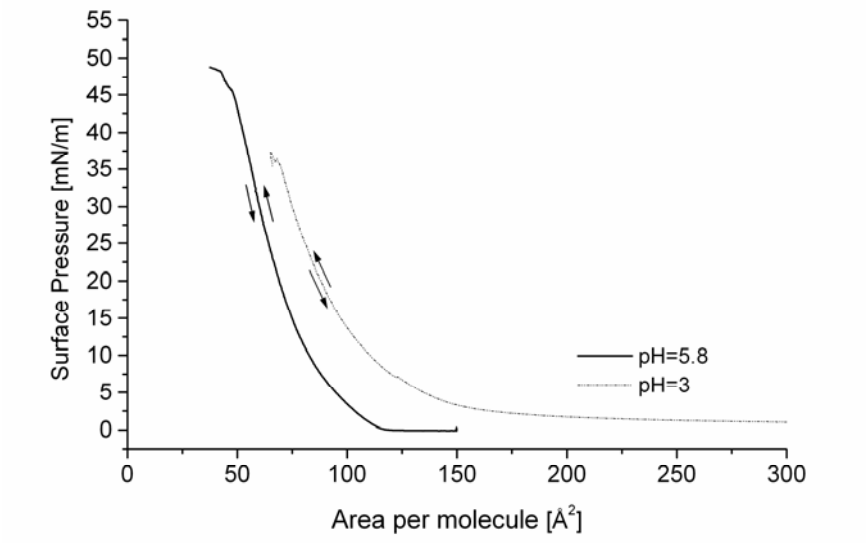

Figure 4-11 Surface pressure-area (π-A) isotherms of TG1G1 on pure water subphase and on acidic subphase

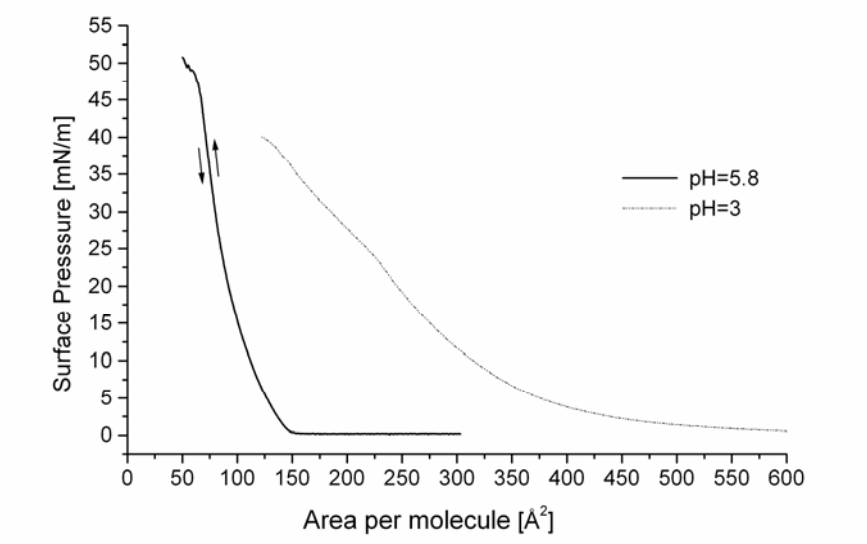

Figure 4-12 Surface pressure-area (π-A) isotherms of TG2G1 on pure water subphase and on acidic subphase

Isotherm of TG1G1 shows an increase of the surface pressure at larger molecular areas as well as an important shift of the minimal area per molecule from 80 $Å^2$ to 115 $Å^2$ (+40%) is observed (Figure 4-11). The increase of the initial surface pressure is attributed to stronger and longer range repulsive electrostatic intermolecular interactions between the positively charged molecules TG1G1 at lower pH. Additionally, the protonation of the amine groups also causes repulsive intramolecular interactions between these groups, resulting in a swelling of the hydrophilic dendron and in an increase of the minimal molecular area. A closer look at the shape of the isotherm at the pressure lift-off also reveals a somewhat more progressive transition. This is due to the larger "elasticity" of the molecules induced by this swelling. A similar behaviour has been reported for a fullerene-based amphiphile with dendrimeric polar head[25]. Therefore, while the self-assembling properties of TG1G1 mainly depend on the lipophilic dendrons at pH= 5.8, they are strongly influenced by the protonation of the polar head at lower pH.

Similar investigations have then been performed with TG2G1. Because of a higher number of amine functions on the dendrimer periphery, a stronger influence of the pH on the (π-A) isotherm was expected. As anticipated, the isotherm in Figure 4-12 shows dramatic modifications relative to the one recorded on pure water. On the isotherm taken with the acidic subphase the surface pressure steadily increases from molecular areas as large as 600$Å^2$ down to 150$Å^2$, with a much greater a compressibility than that observed on pure water. The collapse pressure is slightly smaller (about 35 $mN \cdot m^{-1}$) and the film formation process is no longer reversible. While the steric hindrance between the head polar groups is balanced by the weak interactions between the lipophilic chains when monolayer of TG2G1 is formed on pure water, the intermolecular interactions are completely governed by electrostatic repulsive forces and most of the initial self-assembling properties are lost when peripheric amine functions are protonated. Moreover a dramatic increase of the solubility of protonated TG2G1 in the water subphase might explain the irreversibility of the compression-decompression cycle.

In order to complement our investigations on the influence of pH on the self-assembling properties of TG1G1, the influence of the pH on the morphology and stability of a pre-existing Langmuir film has also been studied (Figure 4-13). A monolayer of dendrimer TG1G1 was first prepared on pure water (pH=5.8) and compressed into the condensed phase (π=25 mN·m^{-1}). The compression was then stopped. Using a specially designed system, 1mL of TFA (pH=3) was added into the subphase under the LB film and close to the surface while keeping constant the position of the barriers. Moreover, these experimental conditions ensure that all terminated amine groups could be protonated at the air-water interface.

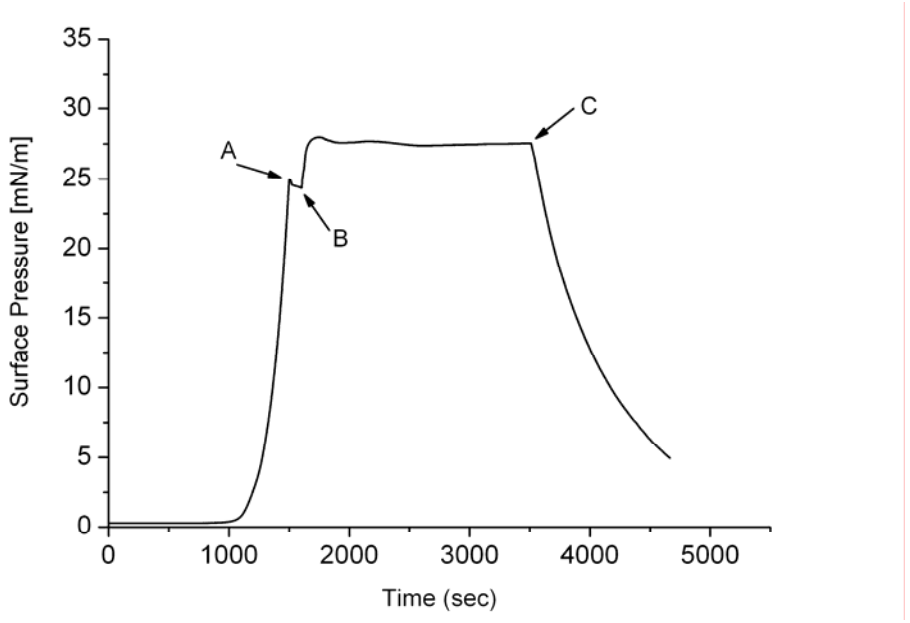

Figure 4-13 Surface pressure variation as a function of addition of TFA into the subphase: film relaxation while barrier position is kept constant (A), addition of 1mL TFA (B) and film swelling due to the protonation of amine functions and subsequent film decompression (C) by extending the barriers.

Figure 4-13 shows an increase of around 3 mN·m^{-1} for the surface pressure induced by the swelling of the TG1G1 LB-film when the amine functions are progressively protonated after the addition of TFA into the subphase. To confirm that these observations are due to the injection of acidic solution, we stress that the addition of an equivalent volume of pure water did not generate any significant change in the surface

pressure (< 0.4mN·m^{-1}). After calculation of the compressibility coefficient, this 3 mN·m^{-1} surface pressure increase was found to correspond to a variation of the area per molecule of 3.2 Å^2, i.e. much smaller than the increase of 35 Å^2 observed when dendrimer TG1G1 monolayer was formed onto an acidic subphase (pH=3). This low value is mainly explained by the higher resulting pH of the water subphase (from 5.8 to 5.6) after the injection of 1 mL TFA (pH=3) but also by the lower accessibility of amines groups in the condensed state. Compared to the protonation of TG1G1 in the gas phase, the protonation rate in a compressed LB film is dramatically decreased minimizing therefore the influence of the pH on the area per molecule. However, if such film swelling experiments did not allow us to quantify the influence of low pH on the configuration of individual molecules, the propensity of dendrimer TG1G1 LB film to swell under different pH conditions could still be demonstrated.

Based on our previous cell transfection studies[17], additional investigations have consisted in investigating whether the LB technique could also allow us to qualitatively observe the expected strong interactions between amphiphilic dendrimers and DNA plasmids at the air/water interface (Figure 4-14). Several groups have already reported the expansion of a monolayer of an insoluble surfactant when polyelectrolytes are added in the water subphase[26]. Similar observations might be therefore expected in the case of complex formation between amphiphilic dendrimers and plasmid DNA. Because of the low toxicity and better propensity of TG1G1 to behave as an efficient transport vector for cell transfection, this LB study has been limited to this compound. In contrast to previously described experiments where the surface pressure-area (π-A) isotherm of TG1G1 was recorded on pure Millipore water, DNA plasmids (pUC18-4915 base pairs) were first dispersed in the water subphase before TG1G1 was deposited and compressed.

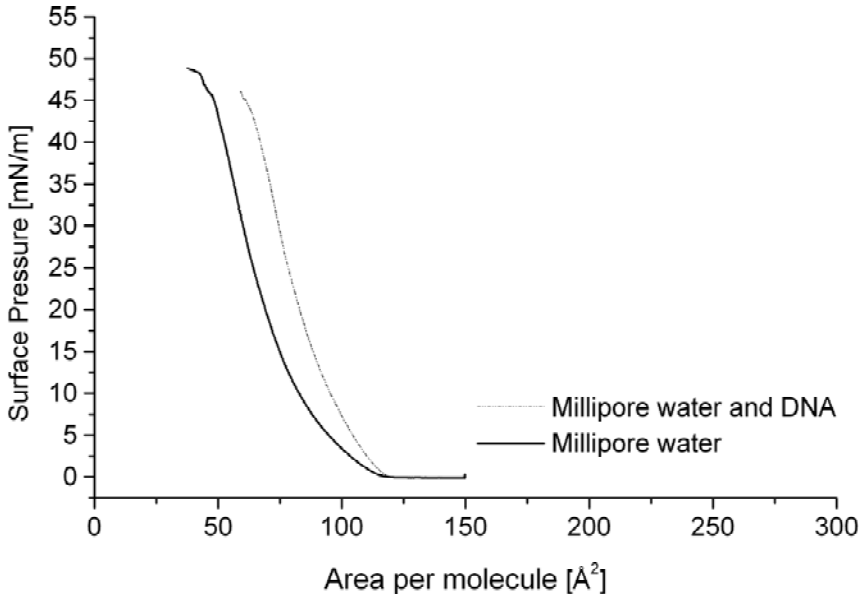

Figure 4-14 Surface pressure-area (π-A) isotherm of TG1G1 on a water Millipore subphase containing plasmid DNA pUC18-4915bp (0.6mg/L); the (π-A) isotherm for TG1G1 on pure water subphase is included as the reference.

As shown in Figure 4-14, the overall shape of the surface pressure-area (π-A) isotherm recorded on a DNA containing subphase is almost parallel to the one on pure water and no effect on the collapse pressure is detected; however, a shift of the (π-A) isotherm of +20 $Å^2$ (corresponding to an increase of 25%) to higher molecular values is observed while the surface pressure starts to increase. The strong electrostatic interactions between the DNA and the dendrimer induce a swelling of the cationic polar head, which results in an increase of the molecular area. Similar conclusions have already been reported by several groups describing the influence of the DNA subphase on the self-assembling properties of cationic surfactants[27,28]. McLoughlin *et al.*[29] reported recently the effects of divalent cations on the interaction between DNA and phospholipids at the air/water interface and thus demonstrated the ion specificity of the DNA-lipids binding with the LB technique.

Additional BAM measurements were performed on the same DNA-dendrimer system and compared to those in Figure 4-6 for dendrimer TG1G1 deposited on a pure water subphase. The homogeneity of the compressed film in the presence of DNA could be demonstrated. Nevertheless, despite the strong dendrimer/DNA electrostatic interactions at the air/water interface, neither structural modifications nor the presence of macroscopic domains could be observed. Such results could be related to the mentioned film stability and preservation of both liquid-expanded and liquid-condensed phases in the presence of DNA.

In order to visualize the strong electrostatic interactions between amphiphilic dendrimer and plasmid DNA, AFM investigations have been carried out. Scanning probe microscopies (SPM) are becoming versatile and powerful analytical tools for imaging biological specimens[30] such as single protein[31], DNA[32,33], membrane-liquid and cells in their native environment[34]. Recent developments in SPM techniques allow scientists to investigate the elastic properties of living cells and to identify the binding sites on proteins by performing AFM measurements with sub-molecular resolution[35]. Quantification of biomolecule interactions as well as the determination of some DNA mechanical properties can even be studied by single-molecule force spectroscopy[36,37].

In our case, AFM studies were restricted to the influence of dendrimer TG1G1 on DNA structure. First, when pure DNA plasmid was deposited by drop casting onto freshly cleaved mica, individual stretched plasmids could be imaged by tapping mode AFM (Figure 4-15).

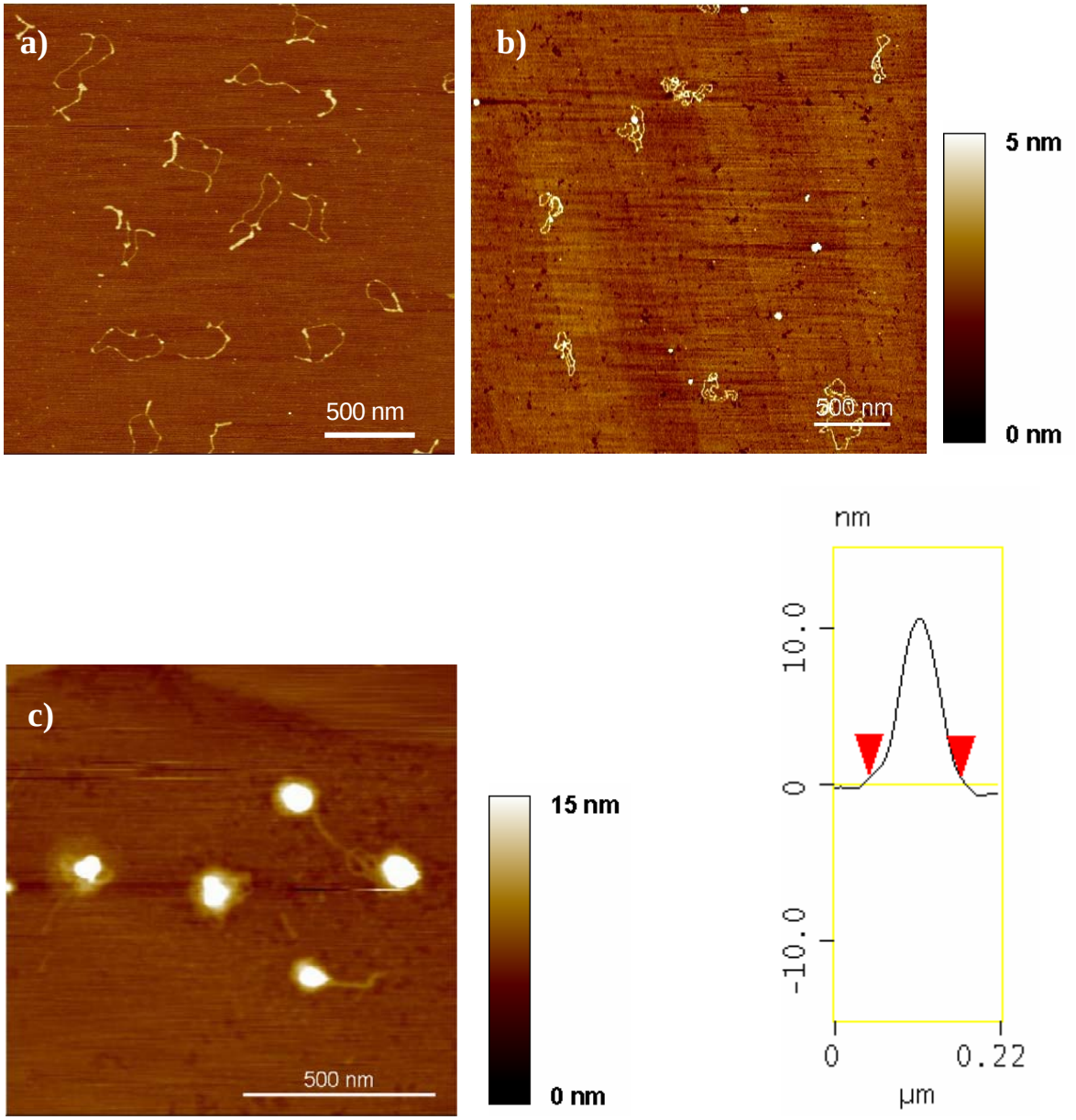

Figure 4-15 AFM images in tapping mode onto mica a) pure plasmid, b) first states of DNA coiling after addition of a few droplets of an aqueous solution of TG1G1 c) TG1G1/DNA with a positive to negative charges ratio of 6 (CE=6) preformed in solution before mica coating and on the right a polyplexe cross section

When a drop of an aqueous solution of TG1G1 was subsequently deposited onto this sample, the preliminary DNA coiling states could be imaged. This demonstrated the strong electrostatic interactions between TG1G1 and the previously deposited plasmids (Figure 4-15b). When TG1G1 and plasmids are first mixed, before being deposited onto the substrate, no individual plasmids could be detected (Figure 4-15c). This result, with experimental conditions (concentrations, charge excess ratio) close to

those used for cell transfection experiments, demonstrated that TG1G1 strongly interacts and condenses DNA into well-defined structures. While individual pure plasmids are stretched over several hundreds of nm (height: 2.0 ± 0.2 nm), dendrimer/plasmid polyplexes present a flattened spheroidal shape with diameters ranging from 100 to 120 nm and a height around 11 ± 0.5 nm (Figure 4-15c); uncondensed small portion of DNA could be still observed. Previous investigations describing DNA condensation by dendritic block-copolymers already reported the AFM imaging of similar polyplexes[38,39]. More recently, a molecular level structural model of DNA molecules wrapped around dendronized polymers has also been proposed by Rabe *et al.*[40]. In all these cases, the resulting alteration of the DNA charge density by cationic molecules and the drastic decrease of the DNA effective hydrodynamic radius are all promising for efficient plasmid internalization during cell transfection tests.

AFM and Langmuir techniques are valuable tools to study the DNA affinity of amphiphilic dendrimers and therefore should help to elucidate the biological mechanisms of DNA complexation. As dye exclusion and transfection experiments are rather time demanding, AFM studies might allow the detection of dendrimers with a high DNA affinity (by imaging dendrimer/DNA polyplexes), and thus to anticipate their ability to behave as efficient non-viral transport vectors. However, all the above advantages of the AFM are accompanied by limitations and present drawbacks. The price to pay for most high resolution techniques is that one can only look at a small part of the specimen at a given time: the higher the resolution the lower the sampling abilities of the instrument. When performing AFM investigations on biological samples, the interactions between dissolved biomolecules and substrates are not negligible and do not represent at all in vivo/vitro conditions. Even if AFM investigations are performed in a liquid environment (measurement inside an AFM liquid cell which may help to prevent the denaturation of some proteins once dried onto the substrate), the influence of the substrate on the configuration of the adsorbed biomolecules has still to be considered.

In order to circumvent this drawback, a structural characterization of DNA/dendrimer polyplexes by cryogenic-Transmission Electron Microscopy (cryo-TEM) has been performed. This analysis allowed the characterization of the self assembly properties of TG1G1 and TG2G1 in solution (formation of vesicles and micelles), as well as the imaging of the structure of vitrified dendrimer/DNA polyplexes.

4.2.4 Self-assembling properties of TG1G1 and TG2G1 and DNA binding DNA: Transmission electron microscopy study

In contrast to previous AFM measurements, the vitrification processes allow us to freeze the sample in an amorphous thin film of ice on top of a TEM grid. Interactions with the supporting film (physisorption or covalent attachment) are thus drastically reduced and distortion or flattening of the imaged molecules against the TEM grid is efficiently prevented. Moreover, samples are never dried before being analysed and the rapid cooling process ensures the preservation of the original sample structure. These analytical conditions were meant to reflect the ones under which the biological cell transfection experiments were carried out.

Cryoelectron microscopy has already been used to study the reorganization of vesicles upon the addition of DNA. Although the spontaneous formation of cationic lipids/DNA complexes when adding DNA to a suspension of lipid vesicles has already been reported, the precise nature and outcome of DNA interactions with lipids in such formulations are still not completely understood. A deeper understanding is therefore needed to obtain an insight into the DNA/vector interactions and mechanisms for the synthesis of more efficient artificial gene delivery systems (such as amphiphiles dendrimer as a new DNA carrier).

In that context, our first cryo-TEM investigations have consisted in studying the self-assembly properties of pure TG1G1 and TG2G1 by characterizing the type of aggregates they tend to form when dissolved in buffer solution. Then after addition of DNA to the amphiphile solution, our main goal was to define the geometry of the DNA/amphiphile polyplexes which might be responsible for cell transfection efficiency. Imaging such polyplexes at different DNA/Dendrimer charge excess ratio

has also allowed us to confirm a DNA/Dendrimer complexation mechanism recently described in the literature.

Concerning TG1G1, cryo-TEM images have been performed on TE (Tris-EDTA pH = 8) buffer solution at the concentration of 10 $mg \cdot mL^{-1}$. When directly analysed after dissolution, deposition on TEM grid and vitrification, lamella-forming amphiphiles as well as vesicles with a high polydispersity could be imaged (Figure 4-16).

In both cases (lamellar structures, vesicles), a membrane thickness of around 6-8 nm corresponding to twice the theoretical length of TG1G1 (3.5-3.8 nm), demonstrated the bilayer character of TG1G1 aggregates.

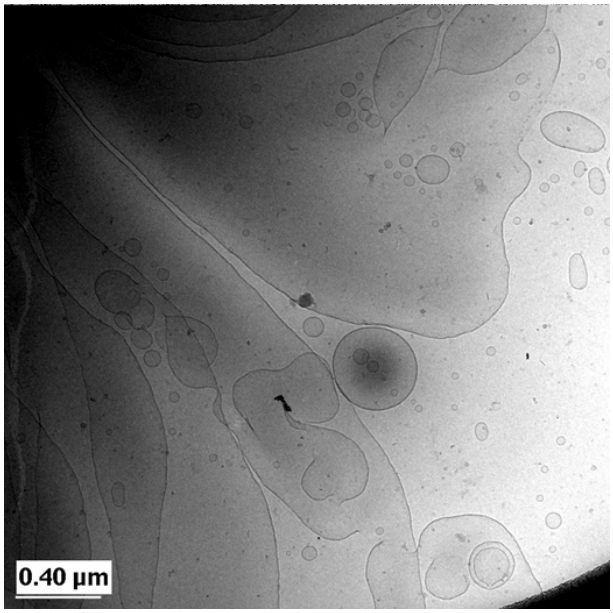

Figure 4-16 Cryoelectron microscopy images of giant membranes (several µm long) and polydisperse vesicles formed by after relaxation of TG1G1 at 10 $mg \cdot mL^{-1}$ in TE buffer (pH = 8)

However, when the sample was sonicated prior to the deposition, bilayered vesicles were still observed but lamellar structure could no longer be imaged. This result demonstrated that if TG1G1 vesicles do not easily form spontaneously (i.e. vesicles are not the most thermodynamically stable form for TG1G1), the formation of vesicles is strongly favoured by bringing additional energy to the system through sonication (Figure 4-17).

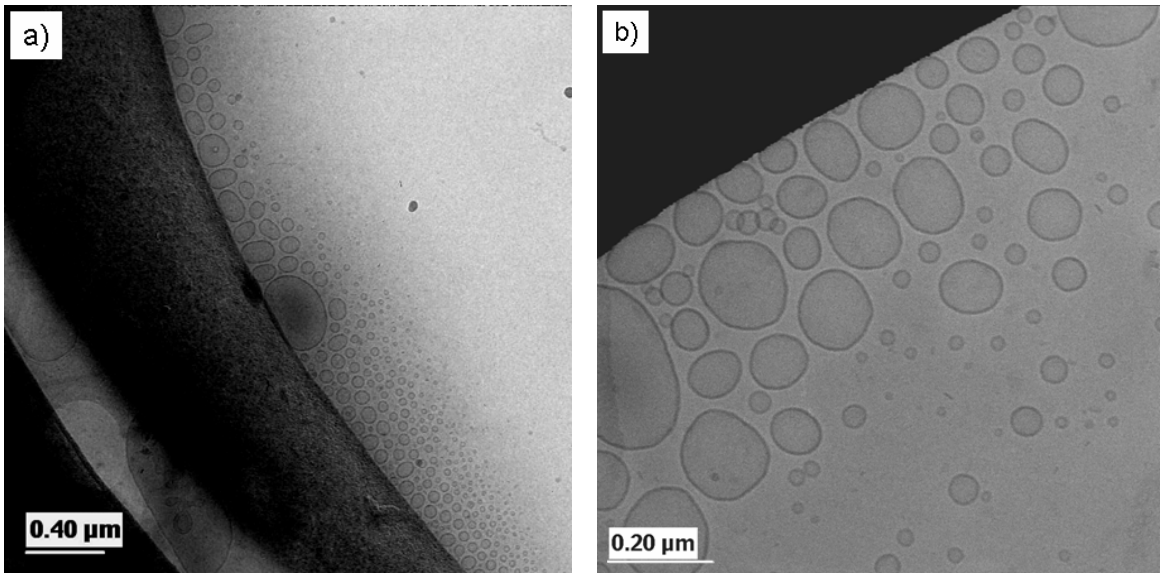

Figure 4-17 a) and b) Cryoelectron microscopy images of bilayered vesicles formed by sonication of TG1G1 at 10 mg ·mL^{-1} in TE buffer (pH = 8)

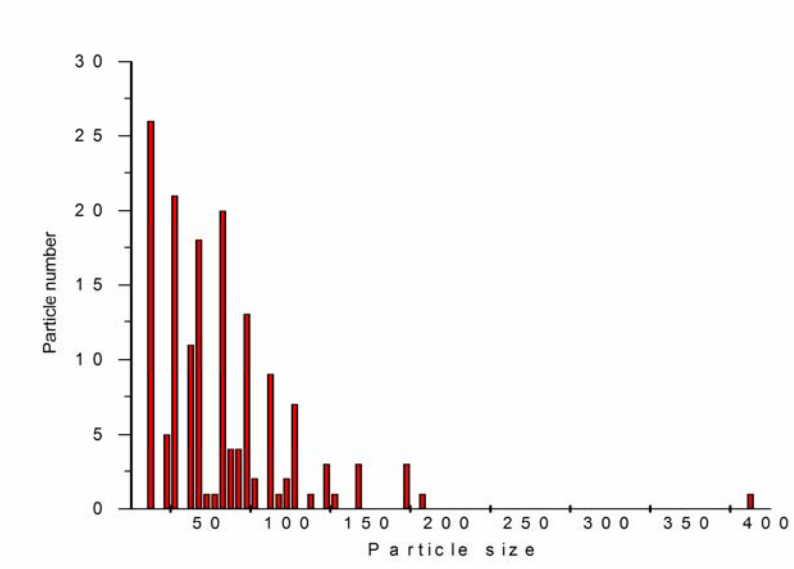

Figure 4-18 Representative size distribution of particles of TG1G1 vesicles at 10mg·mL^{-1} in TE buffer (pH=8).

In the absence of sonication, the self-assembly of TG1G1 into lamellar structure is due to the cylindrical shape of TG1G1 molecule (triple alkyl chains, triple hydrophilic chains). This observation is in agreement with the critical packing parameter of TG1G1 (cpp =1.66) determined with the Equation 4-1 proposed by Israelachvili[22] for lipids, assuming a polar head diameter equals to 7Å (molecular modelling with

ViewerLite 4.2 software) and a number of carbon atoms equals to 12 for the critical length of lipophilic chain.

$$v / a_0 l_c$$

Equation 4-1 Critical packing parameter or shape factor with v corresponding to the hydrocarbon chain(s) volume, a_0 corresponding to the optimal surface area of the polar head and l_c corresponding to the critical chain length of the amphiphilic molecule characterized

To this value is corresponding a critical packing shape of truncated cone allowing preferentially the formation of lamellarstructure (ccp from 1 to 2) and inverted micelles (ccp ≥ 2). The TG1G1 vesicles diameter size estimated in most of cases is between 50 nm and 150 nm (± 5 nm) but larger vesicles could also be visualized (Figure 4-18). Such a polydispersity could be explained by the fusion of vesicles as already reported by Israelachvilli[22] and was confirmed by Dynamic Light Scattering which showed a very broad size distribution in TE buffer and in HEPES buffer with a maximum at a radius of 180 nm (Annexe3). Distribution with radii around 100 nm-200 nm is typical for lamella-forming amphiphiles after sonication[41]. Such a giant vesicles (diameter higher than 500nm) could not be fully visualized in cryo-TEM due to the vitrification process drawbacks. Indeed the thickness of the vitrified water layer formed is around 150-200 nm which excludes the giant structures formed by self-assembled amphiphilic molecules in buffer solution. Cryo-TEM measurements were also performed with different concentrations of TG1G1 (from 1mg to 20mg). Generally, the dilution of the vesicles solution did not change the shape but small variation on the average size of the vesicles can be characterized, as well as differences in terms of vesicles density.

Concerning TG2G1, the most stable self-assembling structure we determined by cryo-TEM is micelle. Compared to TG1G1, TG2G1 presents a much larger hydrophilic polar head (17Å in diameter determined by ViewerLite4.2 molecular modelling software). The TG2G1 critical packing parameter calculated with Equation 4-1 equals 0.28. This value is lower than 0.33, it corresponds to a conic critical

packing shape. With such geometry, the formation of higher curvature radius aggregates such as micelles could be anticipated.

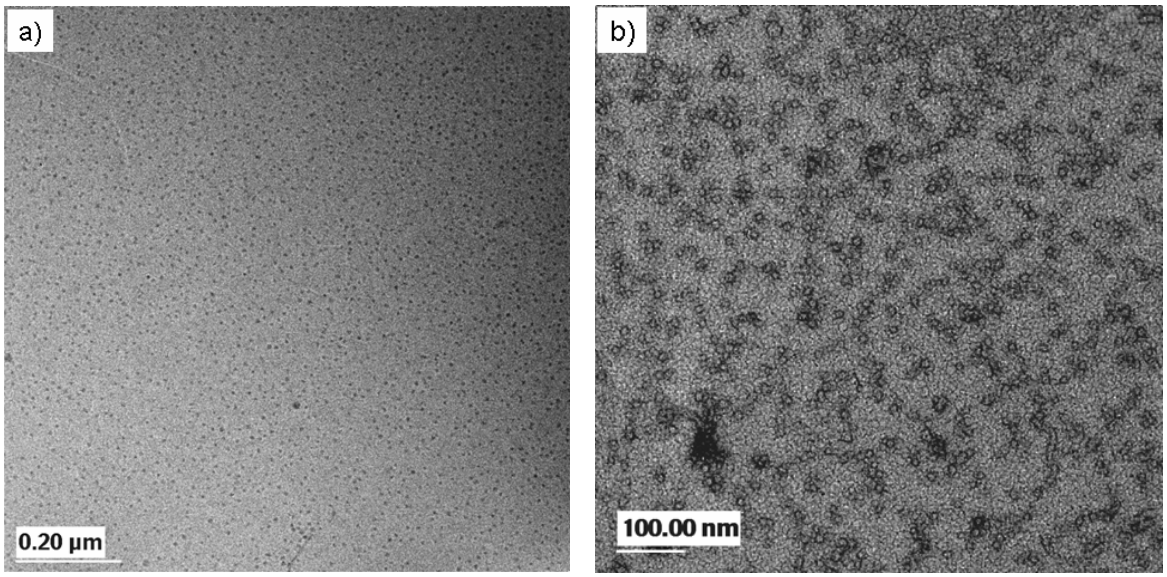

Figure 4-19 a) Cryo-electron microscopy images of TG2G1 micelles formed by sonication of TG2G1 at 20 mg / mL in TE buffer (pH=8); b) Electron microscopy image of TG2G1 micelles concentration 10mg/mL in TE buffer (pH=8) after negative staining with uranyl acetate pH=6 On both images small particles (6-9 nm of diameter) can be observed homogeneously dispersed onto samples.

By cryo-TEM the diameter of TG2G1 micelles was found to be around 6-9 nm representing twice the theoretical size of TG2G1 (~ 4 nm).

Those micelles were found to be monodisperse. This monodispersity has been confirmed both by the negative staining method (Figure 4-19b) and by DLS (Annexe3) which showed a narrow size distribution with a maximum at 5 nm ± 2nm (Annexe3). This analysis could not be used for the characterization of TG1G1 vesicles due to the dehydratation phenomenon and the resulting denaturation of the vesicles induced by the contrasting agent.

In order to complete the characterization of all compounds involved in the cell transfection process, additional cryo-TEM investigations were carried out with pure DNA plasmids. In this case, an additional staining step was required during the sample preparation in order to increase the image contrast (see experimental section).

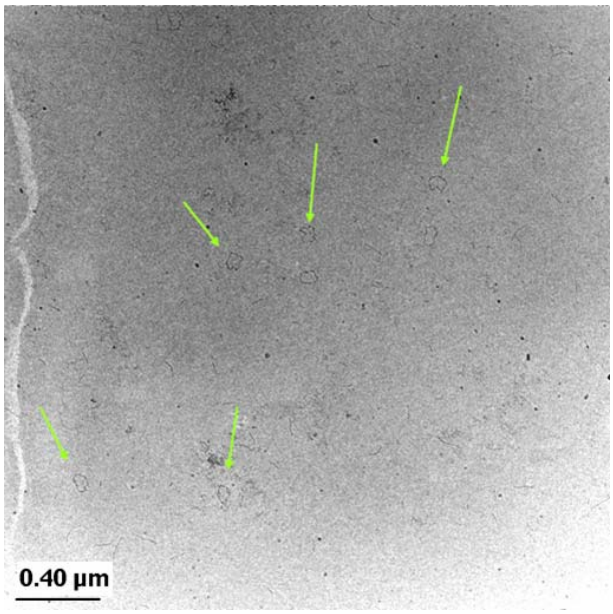

Figure 4-20 Cryo-electron microscopy image of plasmid DNA pBr (4361bp) at concentration 0.025mg·mL^{-1} in TE buffer at pH=7.6. The specimen has to be stained with a solution of ammonium molybdate (pH=7) in order to enhance the contrast.

In this way and as shown in Figure 4-20, individual, stretched and not denaturated DNA plasmids were imaged with a high resolution.

In order to evaluate the effect and interactions of DNA plasmid on the amphiphilic dendrimers, subsequent cryo-TEM investigations have been carried out to study the reorganization of TG1G1 vesicles upon the addition of DNA plasmids into the initial dendrimer solution.

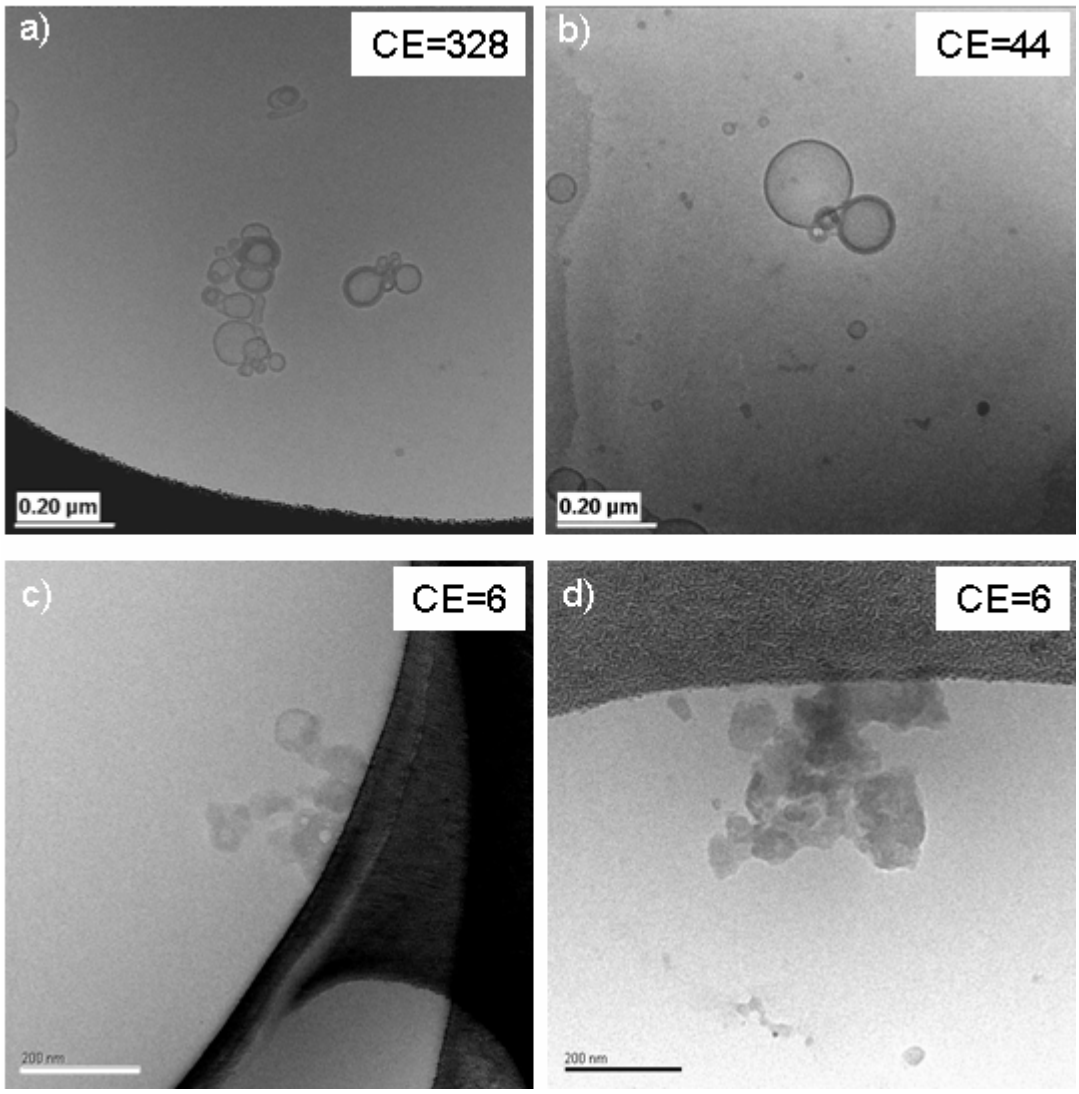

Figure 4-21 Cryo-electron microscopy images of TG1G1 /plasmid DNA polyplexes at a) CE=328; b) CE= 44; c) and d) CE=6.

The images show the formation of vesicles aggregates and the presence of multilamellar vesicle membranes (Figure 4-21). This is characterized by an increase of membrane thickness. Figure 4-21 shows cryo-TEM images corresponding to different Charge Excess (CE) ratio between TG1G1 and plasmid DNA. On Figure 4-21d), it is no more possible to visualise the vesicle membrane. In the presence of DNA, neither individual dendrimer vesicles nor single free DNA plasmid could be observed and the sample shows only spontaneously formed DNA/dendrimer aggregates. DNA does not induce a clear vesicle fusion phenomenon as observed by Huebner *et al.*[42]. The

particle size distribution shows a maximum at 51 nm (± 5nm), corresponding to the approximate value determined for pure TG1G1 specimens.

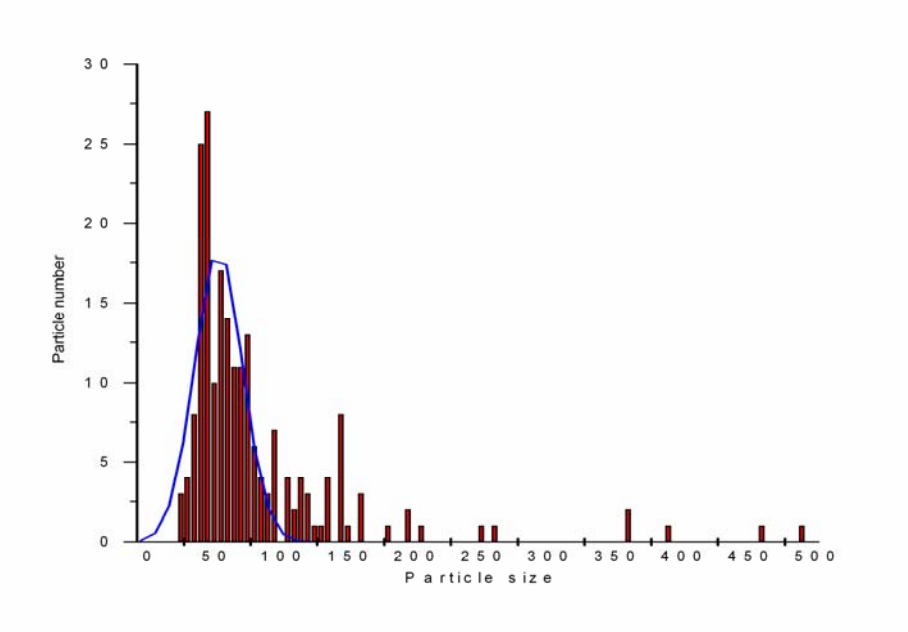

Figure 4-22 Representative distribution of size particles for polyplexe TG1G1/DNA specimens. The distribution curve is done by a Gaussian fit.

These experiments were carried out, changing the CE (charge excess ratio) by decreasing the amphiphiles concentrations while keeping constant DNA concentration. In this way, it was possible to reach CE similar to those used for cell transfection experiments, while maintaining the solution homogeneous for a performant cryo-TEM imaging.

With a CE of 6 (a condition similar to that previous AFM analysis), only very dense vesicles were imaged due to many successive aggregation processes (Figure 4-21).

Compared to the original TG1G1 solution which presents well separated vesicles (with 52 nm ± 5nm), the vesicles aggregation upon addition of DNA is here clearly demonstrated. After addition of DNA, electrostatic attractive interactions between the negatively charges phosphate groups of DNA and the positively charged polar head groups of the dendrimer vesicles are favoured, which results in the covering of the vesicles by DNA. Progressive apposition of neighbouring vesicles where one adsorbed DNA is sandwiched between two vesicles thus leads to their fusion (phenomenon not

clearly observed in these samples) or aggregation. Such strong association can be correlated to the already reported formation of highly turbid suspensions or precipitates when adding very low amounts of additional DNA to solutions of amphiphilic molecules [43,44].

Since cryo-TEM technique provides excellent resolution, it was also possible to detail the morphology of the Dendrimer/DNA polyplexes. Actually, when focusing on the vesicles or aggregates periphery, some of them presented a thicker outer layer than usual (Figure 4-23).

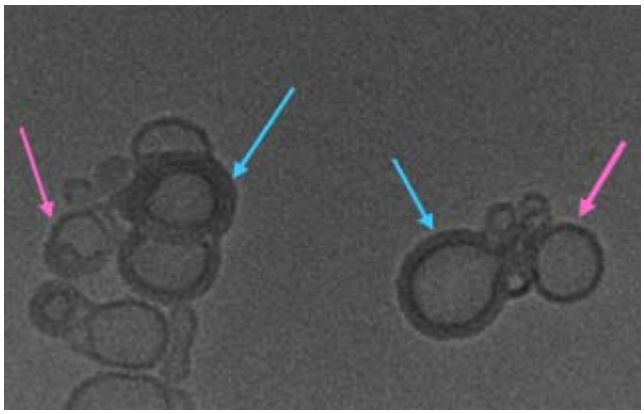

Figure 4-23 Zoom of a cryo-electron microscopy of Figure 4-21a). The vesicle bilayer is pointed with pink arrow and the presence of multilammelar is pointed by the blue arrow.

In most cases, thicknesses from 13 to 18 nm were observed which represent more than twice the initial thickness of pure TG1G1 vesicles (6-8 nm). Based on these results, we propose that such an increase is attributed to the formation of multilamellar structures of the vesicles membranes. In such systems negatively charged DNA molecules are intercalated between the two vesicles membrane after one adsorbed vesicle ruptures and rolls its bilayer over a host Dendrimer/DNA complex. Such a reorganisation may theoretically result in the thickness increasing from one bilayer thickness (6-8 nm in our case) to two bilayers with intercalated DNA (12-16 nm ± 2 nm for the adsorbed DNA[45,46]) which is in perfect agreement with our experimental observations.

Such mechanisms (fusion and/or formation of multilamellar vesicles) were already reported for cationic lipids/DNA polyplexes by Huebner *et al.*[47] (Figure 4-24) who

proposed both of them as participating to the reorganisation of vesicles bilayers upon the addition of DNA.

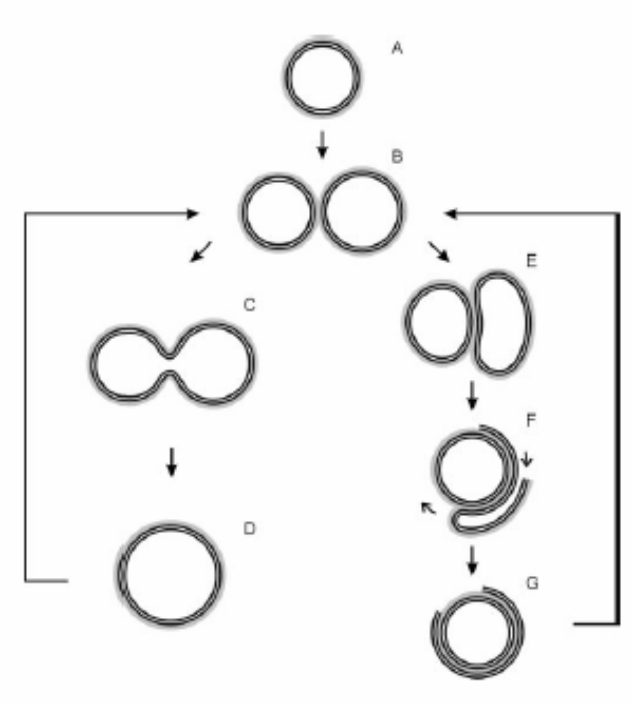

Figure 4-24 Reproduced from Huebner *et al.* DNA spins around a unilamellar vesicle (A) Two vesicles with one partially covered with DNA adsorb to each other (B) Fusion of 2 vesicles (C) The vesicle subsequently minimizes its membrane energy by adopting a near-spherical shape (D) Multilamellar structures form if one vesicle ruptures (E) Such a vesicle then rolls its bilayer over an host DNA/vesicle polyplex (F), forming one adsorbed bilayer with an open edge.(G) By such a mechanism further layers could get adsorbed.

To extend our research and in order to investigate the correlation between the structure of Dendrimer / DNA polyplexes and their transfection efficiency preliminary cryo-TEM analysis have been performed on TG2G1/DNA formulations.

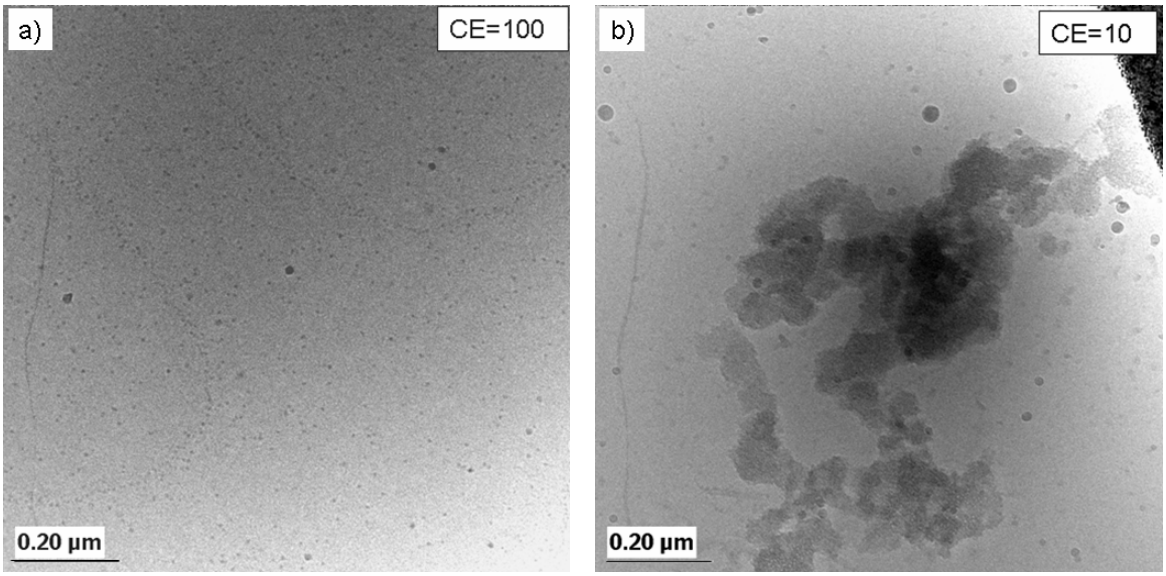

Figure 4-25 Cryo-electron microscopy image of TG2G1 /plasmid DNA polyplexes at a) CE=100; b) CE= 10. On the image a) no significative changes on TG2G1 micelles induced by plasmid DNA. With CE=10, the presence of large dendrimer/DNA aggregates are characterized.

Generally and as shown in Figure 4-25, similar observations could be made in the sense that the formation of large Dendrimer/DNA aggregates occurs upon the addition of DNA. However, compared to TG1G1, a larger amount of DNA is needed to induce the reorganization of TG2G1 initial micelle structure (no effect with CE = 100 while a CE of 328 was sufficient to modify the initial vesicle structure of TG1G1). Additional cryo-TEM investigations with such formulations are still needed here for a more complete understanding of the Dendrimer /DNA complexation mechanism.

4.3 Conclusions

After very promising cell transfection investigations, the self-assembly and film-forming properties of a new class of amphiphilic dendrimers have been investigated at the air-water interface using Langmuir-Blodgett techniques and Brewster Angle Microscopy.

The influence of pH on two amphiphilic dendrimers configuration as well as the electrostatic dendrimer/DNA interactions was qualitatively observed by LB and BAM techniques.

Atomic Force Microscopy measurements confirmed the propensity of dendrimer TG1G1 to strongly condense DNA into well defined polyplexe.

Additional cryogenic Transmission Electron Microscopy has also allowed better evaluation of the conformation of TG1G1/DNA and TG2G1/DNA plasmid polyplexes and of the DNA condensation mechanisms under physiological conditions. The main advantage with such techniques is that the samples can be prepared artefact-free due to conventional staining or drying procedures. Moreover the ultra fast cooling rate ensures a minimum perturbation of the original structure. For TG1G1 (which showed the highest transfection efficiency) the thickness of the initial TG1G1 vesicles membranes was determined first to be 6-7 nm (± 1 nm), twice the theoretical length of a single amphiphilic dendrimer which demonstrated the bilayer character of the vesicles. In the presence of DNA, individual dendrimer vesicles could no longer be observed and the sample consisted of spontaneously formed multi-lamellar DNA/dendrimer aggregates. As already reported for cationic lipids/DNA polyplexes, such aggregates are formed by fused and multilamellar vesicles in which the negatively-charged DNA molecules are intercalated between two positive lipid bilayers. Similar observations could be made with TG2G1/DNA formulations. Imaging of Dendrimer/DNA polyplexes using cryo-TEM is therefore very promising and gives valuable insights into the fundamental mechanisms that play a role in Dendrimer/DNA complex formation. However, because some complex structures such as multilamellar Dendrimer/DNA systems are difficult to elucidate (eg. transcription

of 2D pictures in 3D objects), additional investigations such as Small Angle X-ray Scattering (SAXS) would be very helpful to confirm structural parameters of Dendrimer/DNA aggregates.

All these complementary investigations will thus enable the establishment of relationships between dendrimer features and cell transfection efficiency for the design of new efficient gene delivery system.

4.4 Material and method

4.4.1 Langmuir and Langmuir-Blodgett Films preparation

Uvasol chloroform, methanol and acid were purchased from Merck (Darmstadt, Germany).

Mica V1-slabs (15x15 mm) were purchased from SPI supplies (West Chester, USA). Si (100) wafers were purchased from Si-Mat (Germany). Ultrapure water was prepared by a MilliQ system (ρ=18.2 MΩ.cm, Millipore, Molsheim, France). Compounds 1 and 2 were prepared as described elsewhere. Purified plasmid (encoding for the green fluorescent protein pGFP) (4915 bp) were kindly provided by H.P. Merkle, E.Walter and K. Weller (Institut für Pharmazeutische Wissenschaften, ETHZ, Switzerland).

Langmuir pressure-area (π-A) isotherms were recorded on an RK-2 trough (150 cm^2, Riegler & Kirsten GmBH, Wiesbaden, Germany) equipped with a Wilhelmy film balance at a temperature T = 293.2 K and a relative humidity of about 50%. Water (pH = 5.8 - 6) or trifluoroacetic acid (pH = 3) or water Millipore containing plasmid DNA (pUC18-4915bp) at the concentration 0.6mg/L were used as subphase.

Solutions of the amphiphiles TG1G1 and TG2G1 (1 $mg.mL^{-1}$, $6.75 \cdot 10^{-4}$ $molL^{-1}$ and $3.73 \cdot 10^{-4}$ mol L^{-1}) were prepared in chloroform TG1G1 or a 9:1 mixture of chloroform and methanol TG2G1. Volumes of 15 - 20 μL of these solutions were spread on the subphase using a Hamilton microsyringe, with the trough barriers fully extended. The solvent was allowed to evaporate and the system left to equilibrate for 30 min. To

determine collapse pressure, monolayers were compressed at a constant barrier speed (7mm·min^{-1}) to collapse pressure. Reversibility and hysteresis of compression were generally investigated by 5 cycles of compression up to 35 mN·m^{-1}. Minimal molecular areas (A_0) were determined by extrapolation of the linear part of the isotherm to π = 0mN.m^{-1}.

Mica supports for Langmuir-Blodgett monolayers were freshly cleaved before the transfer. Alternatively, for transfer to the (100) face of Silicon, Si wafers were cut and cleaned with Piranha solution (H_2S0_4: H_2O_2 (V/V) 2: 1 at 120°C during 10 minutes) and rinsed afterwards with Millipore water. The support was rapidly lowered into the trough. It was then withdrawn slowly (2.4 mm.min^{-1}), at constant surface pressure as indicated in the figure captions. Transfer ratios were determined and are given in the respective figure caption.

4.4.2 Brewster Angle Microscopy (BAM) Images

Brewster Angle Microscopy (BAM) was performed employing a BAM2plus microscope setup (Nanofilm Technologies GmbH, Germany) equipped with an argon laser λ = 532 nm as illumination source; images were recorded on a CCD camera. The field is 620 μm x 500 μm.

4.4.3 X-Ray diffraction measurements

The grazing incidence X-ray studies of LB film were performed on a device equipped with a programmable divergence slit (1/32°), a Soller slit collimator, a flat Ge monochromator, and a proportional Xe detector. Nickel-filtered Cu Ka line (wavelength 0.1542 nm) was used. Measurements were recorded immediately after the LB transfer.

4.4.4 AFM characterization

Atomic force microscopy (AFM) measurements were performed on a Dimension 3100 scanning probe microscope equipped with a Nanoscope III controller (Digital Instruments, Santa Barbara, CA) operated in non-contact (tapping) mode using NSG01 probes (NT-MDT, Moscow, spring constant: 2.5 -10 $N \cdot m^{-1}$, resonance frequency 120 - 150 kHz). Measurements were carried out at ambient conditions (T = 293.2 K, about 50%). Image analysis and image processing was performed with the Nanoscope Control Software (Digital Instruments, Santa Barbara, CA).

DNA sample and substrate preparation for AFM experiments:

For drop casting of complexes of plasmid DNA and dendrimer 1, 10 μL of a solution of pGFP (0.2 ng μL^{-1}) in water were mixed with 2 μL of a solution of 1 in water (8 ng μL^{-1}). The resulting solution contained DNA and dendrimer in a charge ratio of 1:6. The mixture was allowed to equilibrate for 30 min. A volume of 5 μL of the solution was then deposited onto freshly cleaved mica by drop casting. The water was allowed to evaporate (30 min at 20°C, 40-50% of humidity) and AFM imaging was performed immediately afterwards

4.4.5 Cryo-TEM characterization

Amphiphilic dendrimers TG1G1 and TG2G1 were dissolved into TE buffer at concentrations between: 1mg.mL^{-1} to 20 mg.mL^{-1}. The Tris/EDTA buffer (TE buffer) is prepared as a mixture of Tris =10mM solution and for EDTA= 1mM in water Millipore, then the pH is adjusted at 7.6.

Respectively, Tris, molecular biology grade, was purchased from Juro (Luzern, Switzerland) and Triplex II (EDTA) was purchased from Merck (Darmstadt, Germany).

In all case, solutions were prepared and sonicated at room temperature into an ultrasound bath during 45 minutes. Uranyl acetate used for negative staining samples

was purchased from Merck (Darmstadt, Germany) and is used at pH=6 at a concentration of 2% in weight. Plasmid DNA used for polyplexe experiments formation is pBR322 (concentration: 0.01mg.ml^{-1}).This plasmid was purchased from Fermentas (Nunningen, Switzerland), it is the most commonly used E.Coli cloning vectors with 4361base pairs in length. Copper 300Mesh TEM grid cover by amorphous carbon thin film were purchased from Plano (Wetzlar, Germany), a structured polymer is deposited on the top, followed by evaporation of carbon and gold. At the end the polymer is removed. The sample preparations were done onto these prepared holey carbon grids. They were transferred to a Gatan cryo-holder (Gatan,Warrendale, Pennsylvania) at T°C <180°C and inserted into a PhillipsCM12 cryo-electron microscope (Philips, Eindhoven, the Netherlands). The accelerating voltage was 80 kV. Images were recorded digitally with the use of a Gatan CCD camera (Gatan). Images analyses were performed with Gatan DigitalMicrograph software.

4.5 References

[1] N. Somia and I. M. Verma, *Nature Rev. Genetics*, **2000**, 1, 91

[2] D. Luo and W. M. Saltzman, *Nature Biotechnol.*, **2000**, 18, 33

[3] U. Boas and P. M. H. Heegaard, *Chem. Soc. Rev.*, **2004**, 33, 43

[4] E. Marshall, *Science*, **2001**, 294, 1640

[5] I. M. Verma and N. Somia, *Nature*, **1997**, 389, 239

[6] D. Luo, *Trends in Biotechnol.*, **2004**, 22, 101

[7] C. L. Gebhart and A. V. Kabanov, *J. Control. Release*, **2001**, 73, 401

[8] T. Merdan, J. Kopecek, and T. Kissel, *Adv. Drug Deliv. Rev.* **2002**, 54, 715

[9] S. Park and K. E. Healy, *Bioconjugate Chem.*, **2003**, 14, 311

[10] F. D. Ledley, *Pharm. Res.*, **1996**, 13, 1595

[11] D. Lechardeur, K. J. Sohn, M. Haardt, P. B. Joshi, M. Monck, R. W. Graham, B. Beatty, J. Squire, H. O'Brodovich, and G. L. Lukacs, *Gene Therapy*, **1999**, 6, 482

[12] G. Zuber, E. Dauty, M. Nothisen, P. Belguise, and J. P. Behr, *Adv. Drug Deliv. Rev.*, **2001**, 52, 245

[13] A. W. Bosman, H. M. Janssen, and E. W. Meijer, *Chem. Rev.*, **1999**, 99, 1665

[14] S. E. Stiriba, H. Frey, and R. Haag, *Angew. Chem. Int. Ed.*, **2002**, 41, 1329

[15] J. Haensler and F. C. Szoka, *Bioconjugate Chem.*, **1993**, 4, 372

[16] J. Dennig, *Dendrimers V: Functional and Hyperbranched Building Blocks, Photophysical Properties, Applications in Materials and Life Sciences*, **2003**, 228, 227

[17] D. Joester, M. Losson, R. Pugin, H. Heinzelmann, E. Walter, H. P. Merkle, and F. Diederich, *Angew Chem. Int. Ed.*, **2003**, 42, 1486

[18] Y. Wang, *J. Opt. Soc. Am. B*, **1991**, 8, 981

[19] A. Soldera, J. F. Nicoud, A. Skoulios, Y. Galerne, and D. Guillon, *Chem. Mater.*, **1994**, 6, 625

[20] C. A. Hacker, J. D. Batteas, J. C. Garno, M. Marquez, C. A. Richter, L. J. Richter, R. D. van Zee, and C. D. Zangmeister, *Langmuir*, **2004**, 20, 6195

[21] A. Ulman "An introduction to ultra thin organic films from Langmuir-Blodgett to self-assembly" Academic Press, Inc, **1991**

[22] J. Israelachvili "Intermolecular and surfaces forces: with applications to colloidal and bilogical surafces", Academic Press, Inc, **1991**

[23] S. Simoes, J. N. Moreira, C. Fonseca, N. Duzgunes, and M. C. P. de Lima, *Adv. Drug Deliv. Rev.*, **2004**, 56, 947

[24] R. Wattiaux, N. Laurent, S. Wattiaux-De Coninck, and M. Jadot, *Adv. Drug Deliv. Rev.*, **2000**, 41, 201

[25] A. P. Maierhofer, M. Brettreich, S. Burghardt, O. Vostrowsky, A. Hirsch, S. Langridge, and T. M. Bayerl, *Langmuir*, **2000**, 16, 8884

[26] C. Symietz, M. Schneider, G. Brezesinski, and H. Mohwald, *Macromolecules*, **2004**, 37, 3865

[27] L. Sun, M. Xu, X. L. Hou, and L. X. Wu, *Mater. Lett.*, **2004**, 58, 1466

[28] M. N. Antipina, R. V. Gainutdinov, A. A. Rachnyanskaya, A. L. Tolstikhina, T. V. Yurova, and G. B. Khomutov, *Surf. Sci.*, **2003**, 532, 1025

[29] D. McLoughlin, R. Dias, B. Lindman, M. Cardenas, T. Nylander, K. Dawson, M. Miguel, and D. Langevin, *Langmuir*, **2005**, 21, 1900

[30] D. Fotiadis, S. Scheuring, S. A. Muller, A. Engel, and D. J. Muller, *Micron*, **2002**, 33, 385

[31] S. Scheuring, D. Fotiadis, C. Moller, S. A. Muller, A. Engel, and D. J. Muller, *Single Mol.*, **2001**, 2, 59

[32] A. G. Wu, L. H. Yu, Z. A. Li, H. M. Yang, and E. K. Wang, *Analytical Biochem.*, **2004**, 325, 293

[33] L. S. Shlyakhtenko, L. Miloseska, V. N. Potaman, R. R. Sinden, and Y. L. Lyubchenko, *Ultramicroscopy*, **2003**, 97, 263

[34] C. C. Gradinaru, P. Martinsson, T. J. Aartsma, and T. Schmidt, *Ultramicroscopy*, **2004**, 99, 235

[35] D. Klein, H. Jensenius, J. Kijne, K. S. Bol, G. van der Marel, J. Frenken, and T. Oosterkamp, *Single Mol.*, **2002**, 3, 160

[36] C. Albrecht, K. Blank, M. Lalic-Multhaler, S. Hirler, T. Mai, I. Gilbert, S. Schiffmann, T. Bayer, H. Clausen-Schaumann, and H. E. Gaub, *Science*, **2003**, 301, 367

[37] H. Clausen-Schaumann, M. Seitz, R. Krautbauer, and H. E. Gaub, *Curr. Opin. Chem. Biol.*, **2000**, 4, 524

[38] J. S. Choi, D. K. Joo, C. H. Kim, K. Kim, and J. S. Park, *J. Am. Chem. Soc.*, **2000**, 122, 474

[39] R. Golan, L. I. Pietrasanta, W. Hsieh, and H. G. Hansma, *Biochem.*, **1999**, 38, 14069

[40] I. Gossl, L. J. Shu, A. D. Schluter, and J. P. Rabe, *J. Am. Chem. Soc.*, **2002**, 124, 6860

[41] D.F. Evans, H. Wennerström "the Colloidal Domain. Where Physic, Chemistry and Biology meet" 2nd Ed., Wiley V-CH, **1999**

[42] S. Huebner, B. J. Battersby, R. Grimm, and G. Cevc, *Biophys. J.* **1999**, 76, 3158

[43] R. S. Dias, B. Lindman, and M. G. Miguel, *J. Phys. Chem. B*, **2002**, 106, 12600

[44] R. S. Dias, B. Lindman, and M. G. Miguel, *J. Phys. Chem. B*, **2002**, 106, 12608

[45] I. Koltover, T. Salditt, J. O. Radler, and C. R. Safinya, *Science*, **1998**, 281(5373), 78

[46] J. O. Radler, I. Koltover, A. Jamieson, T. Salditt, and C. R. Safinya, *Langmuir*, **1998**, 14, 4272

[47] S. Huebner, B. J. Battersby, R. Grimm, and G. Cevc, *Biophys. J.*, **1999**, 76, 3158

Chapter 5

General Conclusion and Outlook

In early stage of dendrimer chemistry, many efforts have been focused on the different synthetic approaches for the design of new class of hyperbranched and well defined macromolecules. By convergent or divergent synthesis, chemist achieved the formation of dendritic molecules, highly monodisperse, flexible or stiff depending on the generation with almost infinite possibilities of external functionalisation and internal cavity modification.

In nanotechnology, with the aim to fabricate microdevices via the bottom-up approach, an increasing interest is emerging for dendrimers as new building blocks with tunable self-assembling properties.

In chapter 3, the use of self-assembled PAMAM monolayer as template for the molecular organization of cyanine monomer into well-defined J-aggregates is reported. Thus and exclusively based on self-assembly processes, J-aggregation occurs within a few seconds or minutes and leads to highly ordered cyanine monolayers with excellent optical properties and good thermal stability.

The influence of PAMAM generation on the nucleation and growth aggregation process was evaluated: J aggregation is promoted with high generation dendrimers which present a more globular shape and higher density of functional groups on their periphery.

In contrast, J-aggregation could not be successfully achieved on surfaces functionalised with polymers (e.g. poly-lysine and poly-ethylenimine coated substrates). Indeed, the polydispersity, random coiled structure as well as the poorly controlled density of functional groups of the polymeric matrix do not allow us to control the J aggregation process at the nanometer scale for the preparation of highly ordered cyanine architectures.

By measuring the quenching of J-aggregates fluorescence, the detection of acceptor molecules (e.g. paraquat) at ppm level using J-aggregates film as highly sensitive interface is demonstrated. In order to detect lower concentration (below 1ppm) additional experiments are necessary with improved set-up providing narrow light band source and more sensitive detection scheme.

Tuning the dendrimer nature and structure, this method for the preparation of highly defined J-aggregates is very versatile and the potential of such systems in field of applications such as light harvesting devices, photovoltaic cells, organic light emitting diodes and integrated secondary light source is currently investigated.

In the second part, chapter 4, it has been described the design as well as the self-assembling properties of new class of amphiphilic dendrimers as vector for non-viral gene-therapy. While the high cationic charge density at the dendrimer surface was designed to favour both DNA binding and endosomal escape, the lipophilic side enables tuning both self-assembly properties and the DNA /dendrimer polyplex stability. The self-assembly properties of the two most efficient amphiphilic dendrimers (TG1G1 and TG1G2) have been, here, investigated at the air-water interface using Langmuir–Blodgett (LB) techniques and Brewster Angle Microscopy (BAM). The influence of pH on the configuration of the two dendrimers as well as the electrostatic dendrimer/DNA interactions could be qualitatively observed. Moreover, Atomic Force microscopy (AFM) investigations confirmed the capacity of these dendrimers to strongly condense DNA into a well defined polyplexe.

In order to study the formation and structure of the DNA/dendrimer polyplexes, cryogenic Transmission Electron Microscopy (cryo-TEM) studies were performed. In vitrified solutions of the pure dendrimers TG1G1 and TG1G2, individual vesicles could be respectively characterized. The vesicles membrane thickness was determined to be 6-8 nm (± 1nm). This thickness corresponds to twice the theoretical length of a single amphiphilic dendrimer molecule demonstrates therefore the bilayer character of TG1G1 vesicles. In the presence of DNA, individual TG1G1 vesicles could no longer be observed and the sample consisted of spontaneously formed multi-lamellar DNA/dendrimer aggregates. As already reported for cationic lipids/DNA polyplexes, such aggregates are formed by fused vesicles in which the negatively-charged DNA molecules are intercalated between two positive lipid bilayers. When combined with cell transfection experiments, the imaging of DNA/dendrimer polyplexes using

cryo-TEM gives valuable insights into the fundamental mechanisms that play a role in DNA/dendrimer complex formation.

In Nanoscience, the development of enabling technologies strongly depends on the control of self-assembly process at the nanometer scale. The exquisite degree of control and tunability available from dendrimers makes them uniquely suited for the role of nanoscale building blocks that will be required in a multitude of applications in coming years.

Chapter 6

Annexes

Annexe 1: AFM image of PAMAMG4 on glass substrate

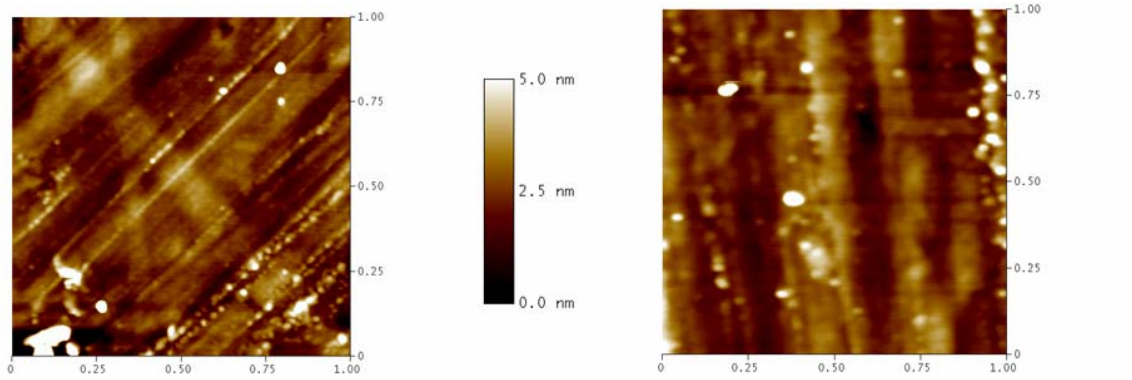

Glass substrate

Glass substrate and PAMAM G4
Some dendrimers aggregated (brigth spots)

Annexe 2: AFM image in tapping mode of poly-lysine on glass substrate

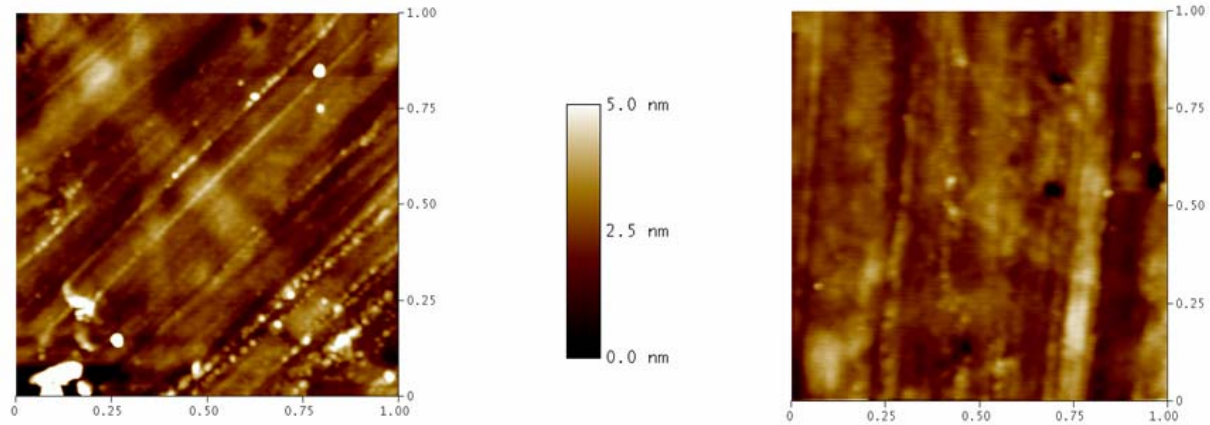

Glass substrate

Glass substrate and
polylysine coating
(MW= 9000 g.mol-1)

Annexe 3: DLS in HEPES buffer

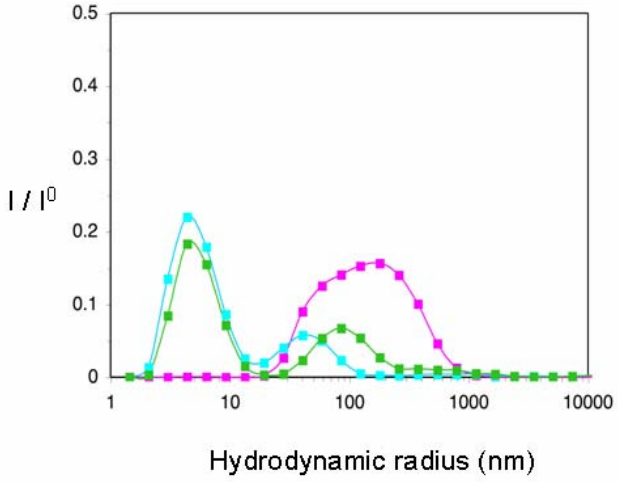

	Mw [g/mol]	Nominal charge	Nb. of C12 chains
TG1G0	918	3+	1
TG1G1	1482	3+	3
TG1G2	2680	9+	9
TG2G2	4371	9+	9

Characterization of hydrodynamic radius of amphiphilic dendrimers by Dynamic Light Scattering (90°) solubilized in HEPES buffer (20mM)

Chapter 7

List of scientific contributions

Conferences

NCCR nanoscale science workshop review panel

September 3rd-6th 2002, Pontresina

- **Poster** "Self-Assembly for Micro- and Nanostructured Materials"
- **Talk** " Presentation of activities in sector Nano at CSEM, Neuchatel"

3rd International Dendrimer Symposium

September 17th-20th 2003, Berlin

- **Poster** " Polycationic amphiphilic dendrimers: from scanning probe microscopy to gene transfection vectors" (Award)

BioSurf V

September 25th-26th 2003, Zurich

- **Poster** "Amphiphilic dendrimers/plasmid DNA assemblies for cell transfection. A scanning probe microscopy study"

22eme Journées des matériaux

October 16th-17th 2003, Lausanne

- **Invited talk** "Amphiphilic dendrimers for gene transfection"

NCCR Nanosacle Science Annual Meeting

October 6th-7th 2005, Gwatt

- **Poster** "Amphiphilic dendrimers designed for non-viral gene therapy: Self-assembly and DNA binding studied by Cryogenic Transmission Electron Microscopy (cryo-TEM)"

Publications

- **“Amphiphilic dendrimers: novel self-assembling vectors for efficient gene delivery”** D.Joester, *et al.* **,** Angew.Chem. Int. Ed, 2003**, *42*,** 1486-1490
- **“ Nano-Structuring by molecular self-assembly”** C. Minelli, *et al.***,** Chimia, 2003**, *57*,** 646-650
- **“ Self-assembly properties of tolane core based amphiphilic dendrimers as new promising vectors for efficient cell transfection”** M.Losson, *et al.*, *Langmuir in prep*
- **“Dendrimers monolayers as templates for the self-assembly of cyanine J-aggregates”,** *publication and patent in prep.*